DISSERTATION

submitted to the

Combined Faculties for the Natural Sciences

and for Mathematics

of the

Ruperto-Carola University of

Heidelberg, Germany

for the degree of

Doctor of Natural Sciences

presented by:

Christoph Körber, M.Sc. in Biochemistry

born in: Bergisch Gladbach

Oral-examination:: .....

Functional characterization of the vertebrate-specific presynaptic protein Mover in the calyx of Held

Referees: Prof. Dr. Thomas Kuner

Prof. Dr. Stephan Frings

Summary

Signal transduction at chemical synapses in the central nervous system relies on the tightly regulated release of neurotransmitter from the active zone of the presynaptic compartment. Although key components of the machinery responsible for transport, docking, priming and fusion of synaptic vesicles have been identified, our understanding of the regulation of this complex process is still incomplete. This is especially true for the probability of release, which determines whether or not one or more synaptic vesicles get released upon arrival of an action potential at the active zone. Albeit the probabilistic nature of neurotransmitter release is one of the key features underlying higher order brain functions such as learning and memory, the mechanisms that regulate this process remain largely elusive.

In the present study, we examined the functional properties of the recently identified presynaptic vertebrate-specific protein Mover. Therefore, we generated an *in vivo* knock-down of Mover using adeno-associated virus mediated shRNA expression in the globular bushy cells of the ventral cochlear nucleus, the projection neurons forming the calyx of Held. 3D immunohistochemistry 10 days after virus injection at postnatal day 2, revealed a strong reduction of Mover expression in identified single calyces expressing mOrange in cis with the shRNA. Electrophysiological characterization of Mover knock-down synapses at postnatal days 12 and 13 revealed increased EPSC amplitudes, increased and accelerated short-term depression and increased recovery from depression as compared to controls. Contrarily, spontaneous release properties, EPSC kinetics, readily-releasable pool size and synaptic vesicle mobilization were not affected by Mover knock-down. These findings are in line with an increased probability of release after Mover knock-down. The increase in release probability was confirmed by presynaptic capacitance recordings in which near-maximal release in Mover knock-down calyces was achieved with shorter depolarization steps as compared to controls. Presynaptic calcium currents were not affected by Mover, assuring that the increase in release probability was not due to alterations in calcium influx. Thus, we examined the calcium sensitivity of release in Mover knock-down synapses by monitoring the EPSC amplitude in different extracellular calcium concentrations. In these experiments, we found EPSC amplitudes in 1.5 mM extracellular calcium significantly increased upon knock-down of Mover suggesting that Mover indeed decreased the calcium sensitivity of release.

In summary, our findings show that Mover acts as a negative regulator of release probability, most likely by reducing the calcium sensitivity of release. Taking the previously shown expression pattern of Mover in certain subsets of synapses into account, Mover may constitute a novel mechanism to tune synaptic transmission.

Zusammenfassung

Die Signalübertragung an chemischen Synapsen im zentralen Nervensystem beruht auf der regulierten Freisetzung von Botenstoffen, so genannten Neurotransmittern, an spezialisierten „aktiven Zonen“ innerhalb der präsynaptischen Plasmamembran. Obwohl große Teile der zur Vesikelfreisetzung führenden Proteinmaschinerie bekannt sind, ist die Regulation dieses komplexen Prozesses nur unvollständig verstanden. Im Besonderen gilt dies für die Regulation der Freisetzungswahrscheinlichkeit die bestimmt, ob ein oder mehrere synaptische Vesikel mit der Plasmamembran fusionieren und somit Neurotransmitter freisetzen, wenn ein Aktionspotential die aktive Zone erreicht. Der probabilistische Prozess der Vesikelfreisetzung ist der eine der Grundlagen höherer Hirnfunktionen wie Lernen und Gedächtnis. Trotzdem sind seine regulativen Mechanismen bis heute nur in Ansätzen verstanden.

In der vorliegenden Arbeit wurden die funktionellen Eigenschaften des vor kurzem identifizierten Protein Mover untersucht. Mover wird in der Präsynapse definierter Synapsenpopulationen exprimiert und ist spezifisch für Vertebraten. Um Einblicke in die bislang unbekannte Funktion von Mover zu erhalten generierten wir einen zellspezifischen *in vivo knock-down* von Mover in den *globular bushy cells* des Nucleus cochlearis ventralis. Diese Projektionsneurone bilden den Held’schen Calyx, eine Riesensynapse im medialen Kern des Trapezkörpers im auditorischen Hirnstamm, aus. Hierzu wurden adeno-assoziiert Vieren die für eine gegen die mRNA von Mover gerichtete shRNA sowie das fluoreszierende Reporterprotein mOrange kodierten in den Nucleus cochlearis ventralis zwei Tage alter Ratten injiziert. Die Expression von Mover war zehn Tage nach der Injektion der Vieren stark reduziert, wie eine immunhistochemische Kontrolle des *knock-down* ergab. Dabei wurden shRNA exprimierende Calyces an Hand der Expression von mOrange identifiziert.

Die elektrophysiologische Charakterisierung von *knock-down* Calyces ergab, dass die Reduktion von Mover zu einer Erhöhung der postsynaptischen Stromamplitude, einer schnelleren und vollständigeren Kurzzeitermüdung sowie einer schnelleren Erholung von dieser Ermüdung führte. Die Eigenschaften der spontanen Vesikelfreisetzung, die Kinetiken der postsynaptischen Ströme, die Anzahl der sofort freisetzbaren Vesikel und die Mobilisierung der Vesikel dagegen waren unabhängig von Mover. Diese Ergebnisse legen nahe, dass Mover eine Reduzierung der Freisetzungswahrscheinlichkeit bewirkt. Messungen der Kapazität der präsynaptischen Membran bestätigten diesen Befund, da in *knock-down* Synapsen bereits kurze Depolarizationen ausreichten um eine nahezu maximale Freisetzung von Vesikeln zu erreichen. Dieser Effekt wurde nicht durch einen größeren Kalziumeinstrom in Mover *knock-down* Synapsen verursacht, da die präsynaptischen Kalziumströme durch Mover nicht beeinflusst wurden. Wir untersuchten daher die Kalziumsensitivität der Freisetzung, da eine Erhöhung der Kalziumsensitivität die höhere Freisetzungswahrscheinlichkeit in Mover *knock-down* Synapsen erklären könnte. Dazu wurde die postsynaptisch Stromamplitude bei unterschiedlichen extrazellulären Kalziumkonzentrationen untersucht. Wir fanden eine Erhöhung der postsynaptischen Stromantworten bei 1,5 mM extrazellulärem Kalzium in

knock-down Synapsen, was darauf hindeutet, dass Mover in der Tat die Kalziumsensitivität der Freisetzung herabsetzt.

Zusammenfassend zeigen die hier präsentierten Ergebnisse, dass Mover, vermutlich durch die Herabsetzung der Kalziumsensitivität der Freisetzung, die Freisetzungswahrscheinlichkeit synaptischer Vesikel verringert. Zusammen mit dem bereits publizierten Expressionsmuster von Mover in spezifischen Populationen von Synapsen, lassen unsere Ergebnisse vermuten, dass Mover Teil eines neuen Mechanismus zur Feineinstellung der Effizienz der synaptischen Transmission ist.

Table of Contents

1 Introduction

The mammalian brain is one of the most complex structures known in nature. It consists of approximately 100 billion neurons that are interconnected by 100 trillion synapses, leading to an average of 1000 synapses that converge on a single neuron. However, the number of inputs received by a neuron greatly differs between neuronal subtypes, giving raise to one of the great questions in neuroscience; the connectivity. Not only is the number of synapses that are formed by a given neuron on its target cells highly variable depending on both, the cell sending the axon and the receiving cell, but, importantly, the number of synapses between two neurons critically determines the reliability and strength of the connection and thereby the properties of the underlying neuronal circuit (reviewed by Atwood and Karunanithi, 2002). It is thus important to understand how neurons find their target cells and how they determine the number of synapses that have to be established in the target region of the receiving cell. This connectivity problem is still incompletely understood, despite the progress made in recent years (for review see e.g. Ziv and Garner, 2004). However, despite connectivity, neuronal signal transmission also critically depends on the highly probabilistic process of neurotransmitter release from the presynaptic compartment. The probability that neurotransmitter gets released upon arrival of an action potential at the presynapse, the so called probability of release (P_r), is highly variable both, among types of synapses and physiological states (Atwood and Karunanithi, 2002). Nevertheless, the precise mechanisms underlying P_r determination are largely unknown as they are determined by a complex and not well understood system of protein interactions.

Thus, the probabilistic nature of signal transduction and its tunability during synaptic plasticity are another fundamental problem in neuroscience. Although enormous progress has been made in the understanding of these phenomena, the precise underlying mechanisms are still not well understood. Moreover, connectivity and synaptic transmission are interconnected since the precise location as well as the temporal sequence of activation of synaptic inputs critically determines signal integration in the target cell and thereby the probability that the target cell will relay the information (Branco et al., 2010). Hence, axon sending neurons not only have to find the right target cells but also the right regions on these target cells. A lot of research has been performed regarding the release of neurotransmitter in response to an action potential (AP) since the electrical properties of the AP and the quantal nature of neurotransmitter release were first described several decades ago (Hodgkin and Huxley, 1952; del Castillo and Katz, 1954). However, it still remains elusive what actually determines the probabilistic nature of synaptic release. The probability of release upon the arrival of an AP is not only variable among populations of synapses but also between synapses that arise from the same axon. Thus both, the axon sending as well as the receiving neurons play a critical role in the determination of synaptic release probability (Atwood and Karunanithi, 2002). Till date, several mechanisms as diverse as protein phsophorylation, the number of available synaptic vesicles and presynaptic calcium dynamics have been described to be involved in the regulation of the probability to release neurotransmitter and thereby to convey information (Branco and Staras, 2009). An additional layer of complexity of neurotransmitter release arises from synaptic plasticity. This

means that the release of neurotransmitter is not only probabilistic in itself, but also depends on the recent history of synaptic activity that influences the release properties of a synapse and thereby its ability to relay information on a timescale ranging from of hundreds of milliseconds to days (Zucker and Regehr, 2002; Feldman, 2009). The long lasting ones of these changes in synaptic release have been implicated to underlie such complex and important processes as learning and memory formation. Thus, further elucidating the mechanisms that influence the probability of synaptic release will lead to a better understanding of the complex functions of the mammalian brain.

1.1 Synapses

Signal propagation between neurons requires synapses, which can be divided into electrical and chemical synapses, as specialized contact sites. Electrical synapses are formed by two hemichannels, so called connexons, each of which consists of six connexins. The line-up of the two connexons shortens the distance between the two connected neurons from ~20 nm to ~4 nm thereby forming a gap junction. Gap junctions provide a direct conductive connection of ~1.2 nm diameter between the two neurons, allowing not only ions but also small molecules to pass through. This direct connection results in an extremely fast propagation of signals such as membrane depolarisations and enables gap junctions to play a fundamental role in the synchronization of neuronal network activity (e.g. Draguhn et al., 1998; for review on gap junctions see Bennett and Zukin, 2004).

Unlike electrical synapses, chemical synapses do not form a direct conductive connection between two neurons, but rely on the release of neurotransmitter from the presynaptic neuron, the sensation of this release and the following convergence into an electrical signal by the postsynaptic cell. For this purpose, chemical synapses are composed of two opposed membrane specializations in the pre- and postsynaptic neurons, the active zone (AZ) and the postsynaptic density (PSD), respectively that are separated by the synaptic cleft. Chemical synapses, contrary to electrical ones, allow the transmission of signals over long distances, since every chemical synapse acts as an amplifier thereby preventing the neuronal signal from fading. Additionally, chemical synapses are easily tuneable allowing rapid adjustment of synapse function to the current needs of the nervous system.

The neurotransmitter that conveys the signal from the pre- to the postsynaptic neuron is stored in small round membrane compartments called synaptic vesicles (SVs) in the presynaptic compartment and only SVs that have been prepared for fusion with the presynaptic plasma membrane by a complex process (see below) are able to participate in signal transduction.

Upon the arrival of an AP, the presynaptic plasma membrane gets depolarized and voltage gated calcium channels open. This leads to the influx of calcium ions and a transient increase in the local calcium concentration in the presynaptic compartment. Binding of the calcium ions to the calcium sensor located on the SV then triggers the fusion of SVs with the plasma membrane, thereby releasing the stored neurotransmitter into the synaptic cleft. After exocytosis, the added membranes and SV-specific proteins are retrieved and recycled via endocytosis (for review see e.g. Wu et al., 2007), while the neurotransmitter diffuses through the synaptic cleft and binds to specialized neurotransmitter receptors in the opposing PSD. These neurotransmitter receptors are in most cases ligand-gated ion channels that open upon binding of neurotransmitter, leading to an ion flux thereby generating an electrical signal in the postsynpatic cell (Fig. 1.1) (Lisman et al., 2007).

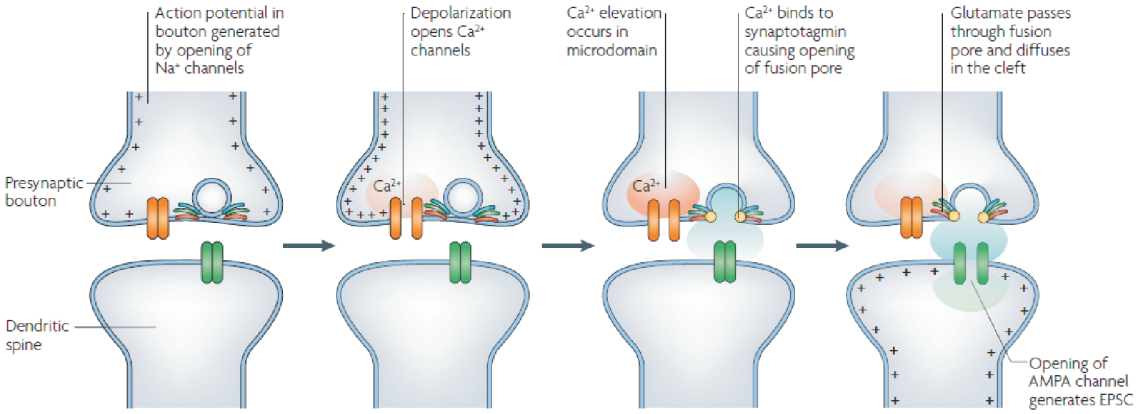

Figure 1.1: Sequence of events responsible for signal transmission at a glutamatergic bouton type synapse. Schematic representation of presynaptic SV release and generation of the postsynaptic EPSC (from Lisman et al., 2007).

In electron micrographs a chemical synapse is characterized by two opposed electron dense membrane specializations and the presence of SVs on the presynaptic site. Depending on the relative thickness of the PSD, synapses are classified as either symmetric or asymmetric (Gray type I and Gray type II, respectively, Fig. 1.2). Symmetric synapses use γ-amino-butyric acid (GABA) or glycine as neurotransmitter and are, in general, inhibitory whereas asymmetric synapses are excitatory and utilize glutamate as principle neurotransmitter.

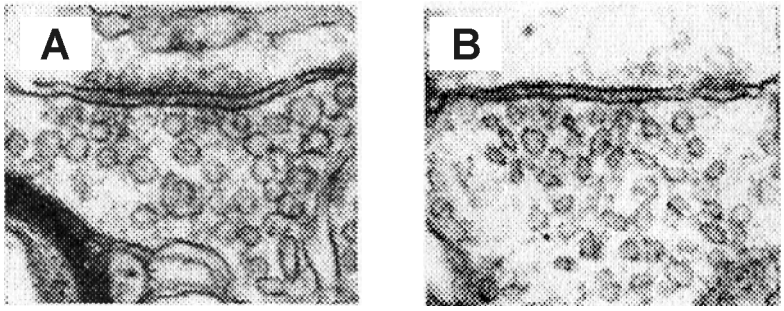

Figure 1.2: Electron micrographs of central bouton type synapses.
A: Electron micrograph of an asymmetric, excitatory synapse. **B:** Electron micrograph of a symmetric, inhibitory synapse (modified from Colonnier, 1968).

The PSD is a highly dynamic protein network that harbours the neurotransmitter receptors as well as cell adhesion molecules that span the synaptic cleft and are essential for establishment and maintenance of the synapse (Ziv and Garner, 2004) as well as diverse proteins involved in intracellular signalling cascades and signal processing. Both, neurotransmitter receptors and cell adhesion molecules are anchored to the cytosceleton by scaffold and adaptor proteins, and their number as well as their functional state (e.g. phosphorylation state) is modulated by proteins residing within the PSD (Chua et al., 2010). Although this generally applies to all synapses, distinct populations of excitatory synapses are thought to have especially dynamic PSDs, since they are modulated during postsynaptic forms of long-term synaptic plasticity. This involves the insertion of AMPA receptors into the PSD during long-term potentiation (LTP) and their removal during long-term depression (LTD) (Bredt and Nicoll, 2003; Chua et al., 2010).

In contrary to the PSDs that are highly diverse in ultrastructure as well as in protein content between excitatory and inhibitory synapses, the presynaptic compartments are structurally similar and only very few proteins are specific for either type of synapse (Grønborg et al., 2010). Structurally, the presynapse consists of two major elements, the dense protein network that defines the AZ and the SVs. The dense protein network contains, among others, three especially important groups of proteins: voltage gated calcium channels that induce SV

release, SNARE proteins that are crucial for SV fusion with the plasma membrane (Rizo and Rosenmund, 2008; Südhof and Rothman, 2009) and scaffolding proteins of the cytomatrix of the active zone (CAZ) that assist in fusion while simultaneously restricting it to the AZ (Schoch and Gundelfinger, 2006). The lumen of the presynaptic compartment is filled with SVs that can be divided into three distinct pools of vesicles based on their capacity to undergo exocytosis (Fig. 1.3). The readily releasable pool (RRP) consists of ~1% of SVs which are prepared for immediate fusion and are thus in contact with the plasma membrane of the AZ. The recycling pool makes up 5-20% of the SVs which are fusing during ongoing moderate synaptic activity once the RRP is depleted and is continuously refilled with newly endocytosed SVs. The third pool, which makes up ~ 80% of all SVs, is the reserve pool that provides a storage from which SVs only get released during intense ongoing stimulation, possibly under the control of cycline-dependent kinase 5 (CDK5, Kim and Ryan, 2010). The SVs of the three pools are morphologically similar and, apart from the SVs of the RRP that are docked to the plasma membrane, not spatially separated in the presynaptic compartment (Rizzoli and Betz, 2005).

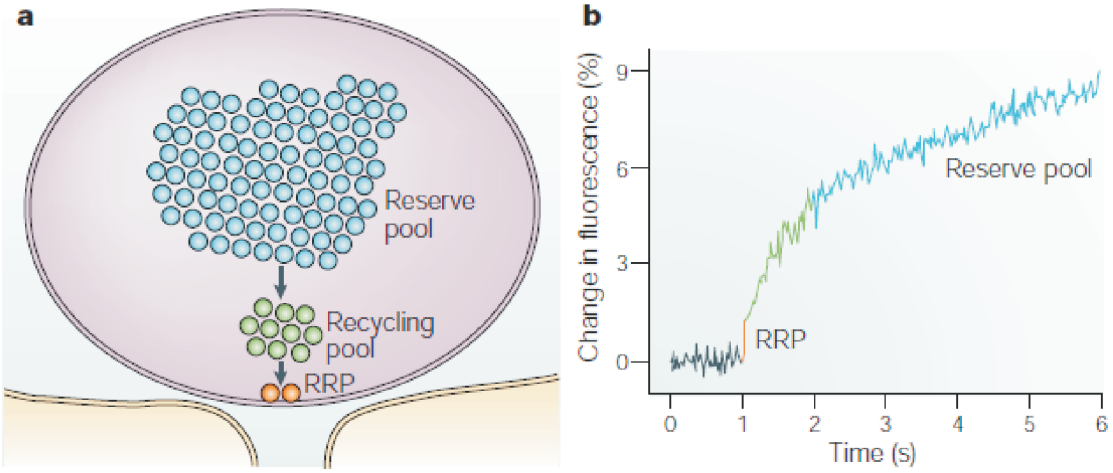

Figure 1.3: Distinct SV pools and their sequence of release.
a: Relative sizes of the RRP (~1%), the recycling pool (10-15%) and the reserve pool (~80%). **b:** Release kinetics of the distinct pools at the neuromuscular junc-tion (from Rizzoli and Betz, 2005).

1.2 Neurotransmitter release

Release of neurotransmitter at the AZ can occur in two modes: spontaneously and evoked. Evoked release is triggered by an AP-induced rise in intracellular calcium while spontaneous release, although often calcium dependent (e.g. Llano et al., 2000; Collin et al., 2005b), takes place in the absence of APs. The mechanistical differences between the two modes have been debated for a long time, but recently Doc2b, an analogue of the principle calcium sensor synaptotagmin but with a much higher calcium affinity, has been identified as the calcium sensor responsible for most of the spontaneous release events (Groffen et al., 2010). The high calcium affinity allows Doc2b to trigger SV release in response to very small changes in the intracellular calcium concentration as they may arise from stochastical opening of calcium channels or release from internal calcium stores. Moreover, Doc2b competes with synaptotagmin for the same binding site on the SNARE complex and since the binding affinity of synaptotagmin is much higher, it prevents Doc2b from extensively triggering spontaneous release thereby ensuring the availability of fusion competent SVs for AP-induced release (Groffen et al., 2010). The loss of this competitive binding to the SNARE complex upon knock-out of synaptotagmin

could explain the observed increase in spontaneous release in synaptotagmin deficient neurons (Sun et al., 2007, Pang et al. 2006). However, knock-out of Doc2b does not completely abolish spontaneous release, suggesting the existence of truly calcium-independent spontaneous release (Groffen et al., 2010; Maximov et al., 2007).

The identity of the SVs involved in spontaneous release has been a matter of debate over the last years. Based on FM-dye destaining experiments, it had been proposed that distinct populations of SVs exist that are exclusively released either during spontaneous or evoked synaptic transmission and that have little exchange with each other (Sara et al., 2005). Moreover, activation of Munc-13 by β-phorbol esters has been proposed to shift SVs from the population used for evoked synaptic release to the spontaneously releasing population, thereby increasing the rate of spontaneous release (Virmani et al., 2005). However, recent studies using several independent approaches in rat hippocampal neurons and in the neuromuscular junction strongly argue against this model of distinct SV populations for different modes of synaptic release (Hua et al., 2010; Wilhelm et al., 2010). A uniform population of SVs would be in line with two distinct calcium sensors being responsible for the two modes of release.

The second mode of SV release, phasic, synchronous release in response to an AP-induced elevation in the intracellular calcium concentration, is a complex process that involves transport of the SV to the plasma membrane, priming for release and the calcium triggered fusion (for review see Rizo and Rosenmund, 2008; Südhof and Rothman, 2009). The first step of this process, the transport of SVs to the plasma membrane is only poorly understood, although a recent study reported a strong reduction of SVs in the vicinity of the plasma membrane in synapses of RIM1/2 knock-out mice (Han et al., 2011; Deng et al., 2011). RIM proteins are well suited for involvement in SV transport to the AZ, since they have been discovered as interaction partners of the SV resident protein Rab3 (Wang et al., 1997; Wang and Südhof, 2003) and thus link SVs to the presynaptic scaffold. Interestingly, RIM, Rab3 and Munc-13, another protein thought to be involved in transport and priming of SVs, form a tripartite complex (Dulubova et al., 2005) and overexpression of Munc-13 can rescue the priming deficits of RIM1/2 knock-out synapses (Deng et al., 2011). Once SVs have reached the plasma membrane, they are docked and primed for release. This involves the formation of a protein bridge between the two membranous compartments by the assembly of the SNARE complex. The SNARE complex consists of the plasma membrane residing proteins syntaxin and SNAP25 and the SV-protein synaptobrevin (VAMP2) (Rizo and Rosenmund, 2008). Interaction of the central SNARE motives of these three proteins results in the formation of the so called four-helix-bundle. However, syntaxin can only participate in the SNARE complex when it is in its open conformation into which it is transferred by Munc-13 (Richmond et al., 2001). The four helix bundle is a stable structure whose zippering is thermodynamically favoured and provides the energy necessary for the fusion of the two lipid bilayers (Pobbati et al., 2006). But since SV release is tightly regulated, the zippering of the SNARE complex needs to be arrested at some point. This is achieved by the binding of the fusion clamp complexin to the four-helix bundle (Giraudo et al., 2006). Upon calcium influx into the presynaptic compartment the principle calcium sensor synaptotagmin (Chapman, 2008) gets activated and replaces complexin at the SNARE complex, thereby relieving the SNARE complex from the fusion clamp (Schaub et al., 2006). Additionally, synaptotagmin, in its calcium bound state, interacts with phospholipids. This brings the SV and plasma membrane in even closer proximity and supports membrane fusion (Araç et al., 2006). The energy provided by the zippering of a single SNARE complex (~35k_BT) (Li et al., 2007)

is not sufficient to reach the activation energy for lipid bilayer fusion (50-100 k_BT) (Cohen and Melikyan, 2004). Thus, SV release requires the simultaneous activation of 2-3 SNARE complexes, by synaptotagmin mediated unbinding of complexin. This has been shown recently for vesicle fusion in chromaffin cells (Mohrmann et al., 2010).

Although this mechanism of SNARE complex assembly and calcium induced fusion is generally accepted (Rizo and Rosenmund, 2008; Südhof and Rothman, 2009) our understanding of this delicate machinery is still growing as e.g. a recent study reported the involvement of the SV protein α-synuclein in SNARE complex assembly (Burré et al., 2010). Moreover, the precise role of Munc-18, which is essential for all modes of SV release (Verhage et al., 2000), is not entirely clear yet, although it has been suggested that Munc-18 may promote SNARE complex formation by binding to the four-helix-bundle (Shen et al., 2007; Dulubova et al., 2007). Even though it is still not completely known how proteins like Munc-13, Munc-18 and complexin interact with the SNARE complex Figure 1.4 depicts a possible arrangement of the fusion machinery.

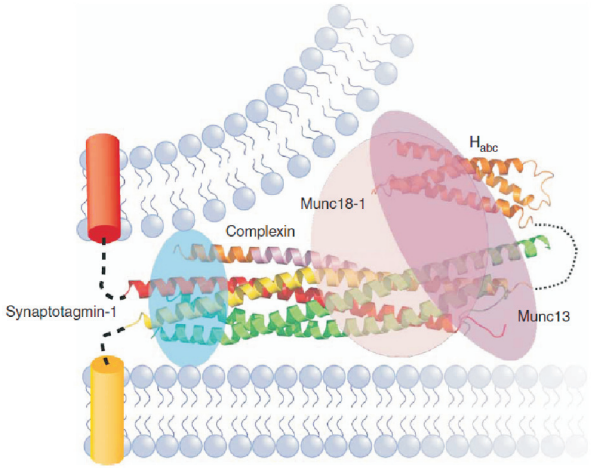

Figure 1.4: The SV release machinery.
A possible spatial arrangement of the primed SNARE complex and its effectors Munc-13, Munc-18, complexin and synaptotagmin is depicted (from Rizo and Rosenmund, 2008).

In summary, SVs that are utilized during synaptic activity undergo the SV cycle consisting of docking to the plasma membrane, priming for release, the actual fusion event, reuptake of the SV components via endocytosis, reformation of the SV and refilling with neurotransmitter (Südhof, 2004). All of these steps have to be precisely orchestrated since alterations at any step lead to distinct defects in synaptic function; modifications of the SV fusion process, for example, result in asynchronous release, whereas alterations in docking and priming have a severe impact on the RRP size and thereby EPSC amplitudes and short-term plasticity (Südhof, 2004).

1.3 The cytomatrix of the active zone (CAZ)

The release of SV takes place at the AZ, which is defined by the presence of an electron dense membrane specialization made up by the so-called cytomatrix of the active zone (CAZ, Schoch and Gundelfinger, 2006). The CAZ is a network of scaffold proteins that serves functions as diverse as the anchoring of presynaptic cell adhesion molecules (e.g. neurexins) thereby assuring the precise alignment with the PSD (Ziv and Garner, 2004; Dean and Dresbach, 2006), assisting in SV transport to the plasma membrane and restricting SV release to the AZ (reviewed in Schoch and Gundelfinger, 2006). Among the proteins present at the presynaptic compartment,

five protein families have been shown to be particularly enriched in the CAZ: Munc-13s, RIMs, ELKSs (ERC/CAST), leprins-αs and piccolo and bassoon (Schoch and Gundelfinger, 2006). With the exception of leprins-α, all these proteins are forming an interaction node at the N-terminal domain of Munc-13 (Wang et al., 2009). However, beside the interactions with each other, proteins of CAZ enriched families interact with numerous other proteins of the presynaptic compartment (Fig. 1.5).

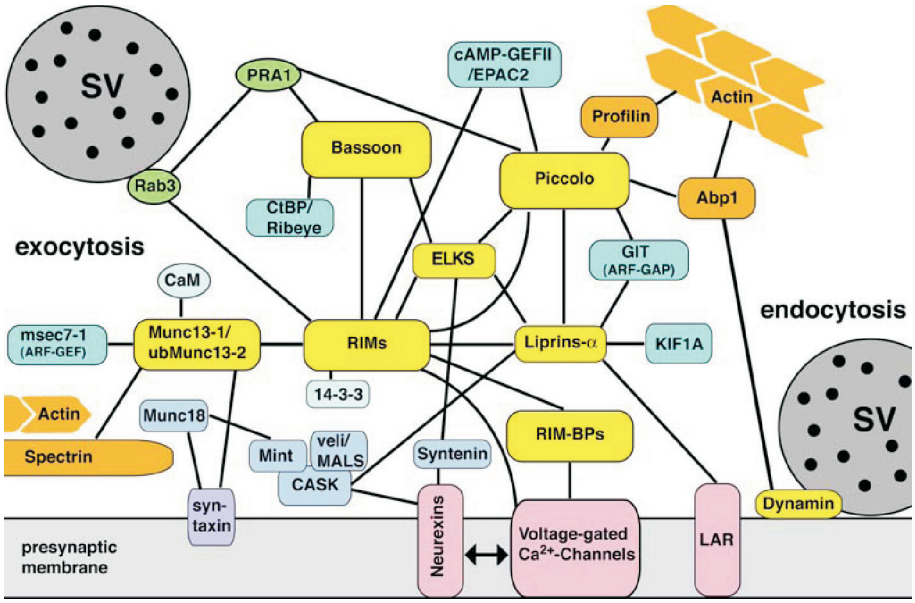

Figure 1.5: Molecular interactions within the cytomatrix of the active zone.
Schematic representation of CAZ protein interactions with various proteins of the presynaptic compartment (from Schoch and Gundelfinger, 2006).

Although the afore mentioned CAZ enriched proteins serve mostly structural purposes, they are also involved in various dynamic processes such as SV transport, priming and SV release. This is especially true for Minc-13s that are required for the formation of the RRP of SVs at the AZ (Augustin et al., 1999; Varoqueaux, et al., 2002) as well as for transformation of synataxin to the open conformation, which allows the formation of the SNARE complex (Richmond et al., 2001). Additionally, Munc-13s are the targets of intracellular signalling cascades since they bind directly to diacyglycerol, β-phorbol esters and calmodulin (Betz et al., 1998; Junge et al., 2004), and have been implicated in short-term plasticity (Rosenmund et al., 2002; Junge et al., 2004). A recent study reported Munc-13 to be involved in lowering the energy barrier for SV fusion, thereby expanding the functional role of Munc-13 from SV transport and priming to release (Basu et al., 2007).

The RIM family of CAZ multidomain scaffolding proteins consists of four genes which encode six isoforms (Wang and Südhof, 2003). Conditional double knock-out of RIM1 and RIM2 results in deficits in SV docking and priming as well as in diminished calcium channel clustering at the AZ (Han et al., 2011). The defects in SV docking and priming are explained by homodimerization and therefore inactivation of Munc-13 in the absence of RIM (Deng et al., 2011), whereas calcium channel clustering requires direct interaction of the channel with the PDZ domain of RIM (Kaeser et al., 2011).

Another family of CAZ scaffolding proteins are ELKS/CAST/ERC proteins that contain three different proteins (Wang et al., 2002; Ohtsuka et al., 2002). ELKS1B and ELKS2 are expressed in the brain (Wang et al., 2002) and bind to RIMs, liprin-αs, piccolo and bassoon, thereby forming an extensive scaffolding network (Wang et al., 2002; Ohtsuka et al., 2002; Ko et al., 2003; Takao-Rikitsu et al., 2004). Besides these structural functions, ELKS proteins are

linked to SV release by the interaction with Munc-13 (Wang et al., 2009).

The least well understood protein family of CAZ proteins are the leprin-αs, that consist of four proteins and have been reported to interact with the CAZ proteins RIM, ELKS and CASK (Schoch et al., 2002; Ko et al., 2003; Olsen et al., 2005). Deletion of the *C. elegans* homolog syd-2 leads to an increase in number and length of AZs, pointing towards a role for liprin-αs in confining the active zone area (Zhen and Jin, 1999). Interestingly, liprin-αs have also been implicated in anchoring of postsynaptic neurotransmitter receptors (Wyszynski et al., 2002).

The fifth family of CAZ proteins contains the two largest proteins described at the AZ thus far: the closely related vertebrate-specific proteins bassoon and piccolo (tom Dieck et al., 1998; Cases-Langhoff et al., 1996). Both proteins contain ten so called piccolo-bassoon homology domains throughout their sequence and interact with ELKSs, Munc-13 and ribeye, the main component of the ribbon in ribbon-type synapses (Takao-Rikitsu et al., 2004; Wang et al., 2009; tom Dieck et al., 2005).

Piccolo contains, in contrast to bassoon, an N-terminal proline rich Q-domain and, at the C-terminus, a PDZ and two C2 domains through which it interacts with multiple proteins of the CAZ and with actin interacting proteins (Schoch and Gundelfinger, 2006). Thus, piccolo mainly seems to play a role as a scaffold and in connecting the CAZ to the cytoskeleton, although a link to SVs is established by the interaction with Pra1 that in turn binds to Rab3 and synaptobrevin (Fenster et al., 2000).

In contrast to piccolo, bassoon gets myristosylated at the N-terminus which suggests plasma membrane localization (Dresbach et al., 2003). Besides the protein interactions common for bassoon and piccolo, only the novel protein Mover has been suggested to bind to bassoon specifically (Kremer et al., 2007, see below). The functional properties of bassoon have been investigated using either knock-out mice (Frank et al., 2010; Hallermann et al., 2010) or mice that express a truncated form of bassoon which is not localized to the CAZ (Altrock et al., 2003). The truncation and mislocalization of bassoon leads to the development of epileptic seizures and the silencing of a fraction of glutamatergic hippocampal synapses, but has no effect on synapse morphology or the equipment of central synapses with SVs (Altrock et al., 2003). However, piccolo may compensate for bassoon since it is upregulated in mice expressing the truncated form of bassoon (Altrock et al., 2003).

At the ribbon synapses of photoreceptors and the inner hair cells, truncation of bassoon leads to the detachment of the ribbon from the AZ which results in impairment of synaptic transmission at these synapses (Dick et al., 2003; tom Dieck et al., 2005; Khimich et al., 2005). However, the strong effect of bassoon truncation on synaptic transmission in ribbon synapses might be rather due to the inability of the truncated bassoon to anchor the ribbon to the AZ than to a direct interference of bassoon with synaptic release. In line with this model are results obtained from the inner hair cell synapse of bassoon knock-out mice, which display altered positioning of calcium channels, RRP size and occupancy of release sites and in which the severeness of the effects correlates with the attachment of the ribbon to the AZ (Frank et al., 2010). Nevertheless, the reduced occupancy of release sites could be a direct consequence of the loss of bassoon, since bassoon knock-out mice also show defects in the fast replenishment of SVs at the cerebellar mossy-fibre to granule cell synapse (Hallermann et al., 2010). Interestingly, the concomitant loss of bassoon and piccolo does not result in an electrophysiological phenotype in cultured hippocampal neurons, although ultrastructual examination revealed a strong reduction in the

number of SVs in the presynaptic compartment (Mukherjee et al., 2010). This suggests that bassoon and piccolo are not required for basal synaptic transmission, but may serve modulatory roles.

1.4 Mover

Mover is a novel presynaptic, vertebrate specific protein of 266 amino acids (30 kDa) that was identified as an interaction partner of bassoon in yeast-two-hybrid screen (Pubmed accession number: NP_080664) (Kremer et al., 2007). The cDNA is highly expressed in all regions of the hippocampus, in cerebellar purkinje neurons, in the superficial layers of neocortex and in distinct areas of the striatum while the expression levels in the rest of the brain are rather low (Allen Mouse Brain Atlas, available from: http://mouse.brain-map.org). On the protein level, Mover is dispersedly expressed in excitatory and inhibitory synapses throughout the central nervous system including hippocampus, cortex, cerebellum, brain stem and spinal cord (Kremer et al., 2007; Kremer, 2008). Mover has also been identified as SVAP30 in an analysis of the SV proteome (Burré et al., 2006; but see Takamori et al., 2006) and as Tprgl in a gene expression study of brain and various other tissues (Antonini et al., 2008). The identification of Mover in the SV proteome is consistent with subcelluar fractionation experiments showing a close association of Mover with SVs (Kremer et al., 2007).

Structurally, nothing is known about Mover. Bioinformatical analysis only predicts a hSac2, pfam12456 phosphoinositol phosphatase domain but that domain apparently lacks the catalytic amino acid residues (Thomas Dresbach, personal communication). Moreover, a phosphorylation at threonine residue 13 has been detected by mass spectrometry (Munton et al., 2007) but the responsible kinase remained unknown.

Knock-down of Mover in hippocampal cultured neurons did neither alter the number of functional synapses nor FM-dye destaining kinetics (Kremer, 2008), leaving Mover as a SV-associated bassoon interacting protein of unknown function.

1.5 The calyx of Held as a model synapse

The calyx of Held, named after its discoverer Hans Held, is a giant excitatory synaptic terminal in the medial nucleus of the trapezoid body (MNTB) of the auditory brainstem (Held, 1893). It is the third synapse in the auditory pathway responsible for sound source localization (Fig. 1.6) and arises from the globular bushy cells in the ventral choclear nucleus (VCN) of the contralateral side (Kuwabara et al., 1991). The calyx is an axo-somatic synapse and each MNTB principal neuron receives input from only a single calyx (Hoffpauir et al., 2006). Each calyx synapse contains, depending on the maturational state, ~300-700 AZs (Sätzler et al., 2002; Taschenberger et al., 2002; Donzillo et al., 2010) that operate independently, ensuring high-fidelity signal transmission (reviewed in von Gersdorff and Borst, 2002; Schneggenburger and Forsythe, 2006).

During synaptic maturation, especially around the onset of hearing at P11 (in rats, Blatchley et al., 1987), the calyx of Held undergoes pronounced morphological and functional changes including fenestration of the originally cup-shaped calyx terminal (Kandler and Friauf, 1993), shortening of the presynaptic AP, decreased synaptic delay, reduced probability of release, faster EPSC kinetics, less pronounced short-term depression and tighter coupling between SVs and calcium channels (Taschenberger and von Gersdorff, 2000; Taschenberger et al., 2002;

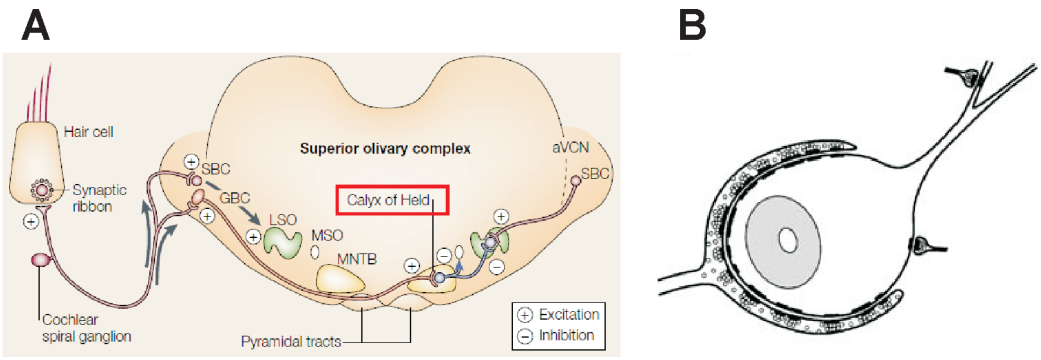

Figure 1.6: The calyx of Held model synapse.
A: Position of the calyx of Held in the auditory brainstem circuitry (modified from von Gersdorff and Borst, 2002).
B: Schematic drawing of a calyx of Held synapse contact-ing a MNTB principle neuron (from Schneggenburger and Forsythe, 2006).

Fedchyshyn and Wang, 2005; Kochubey et al., 2009). Moreover, the number of AZ increases on the expense of AZ length as well as the number of SVs increases (Taschenberger et al., 2002). All these morphological and functional adjustments assure high-fidelity transmission during sustained synaptic activity (Taschenberger and von Gersdorff, 2000).

The calyx of Held is one of the very few central synapses that are accessible for direct presynaptic patch-clamp recordings (Borst et al., 1995). Therefore, it is an ideal model synapse for the examination of presynaptic mechanisms and has been used for investigations of e.g. SV pool dynamics, coupling of intracellular calcium concentration and SV release, the spatio-temporal dynamics of calcium microdomains and synaptic endocytosis (reviewed in von Gersdorff and Borst, 2002; Schneggenburger and Forthyse, 2006). Moreover, the calyx has also been used, to investigate properties of presynaptic proteins by virus mediated overexpression approaches (Wimmer et al., 2004; Young and Neher, 2009; Schwenger and Kuner, 2010). A recent study used the Krox20-Cre-driver mouse line to conditionally knock-out floxed allels of RIM in the auditory brainstem (Han et al., 2011). This strategy, although promising, has the disadvantage that Cre-recombinase is also expressed in the postsynaptic MNTB neurons, which may cause problems if proteins are examined that have functions in both, the pre- and the postsynaptic compartment.

Hence, this model system provides the rare opportunity to study synaptic mechanisms at a defined monosynaptic connection and the combination of genetic tools with electrophysiological recording techniques allows unique insides into presynaptic function.

1.6 Aim of the study

The aim of this study was to elucidate the functional role(s) of the vertebrate-specific protein Mover. Vertebrate specific proteins are of special interest, since only very few of them have been identified in brain thus far albeit the structural and functional complexity increased enormously during evolution. In stead of *de novo* conception, invertebrate proteins often evolved into distinct isoforms in vertebrates. Thus, truly vertebrate-specific proteins are likely to have modulatory roles during complex synaptic processes such as synaptic plasticity rather than being essential for basic synaptic transmission.

We sought out to assess the functional role of Mover by establishing a synapse specific shRNA mediated knock-down of Mover in the calyx of Held *in vivo* and characterizing the

resulting changes in synaptic transmission. Since preliminary data obtained from hippocampal cultured neurons devoid of Mover were available but inconclusive (Kremer, 2008), we additionally investigated the effects of Mover on quantal release in this experimental system. Hippocampal cultures provide the opportunity to separately examine excitatory and inhibitory synapses making it possible to detect effects of Mover specific for either type of synapse. In a second step, we aimed to reveal the mechanism(s) by which, if at all, Mover may affect synaptic function.

2 Materials and Methods

2.1 Plasmids

pFUGW_sh007G	kind gift of Dr. Thomas Kremer
pFUGW_sh007MM	kind gift of Dr. Thomas Kremer
pVSVg	kind gift of Prof. Dr. Jochen Kuhse
pΔ8.9	kind gift of Prof. Dr. Jochen Kuhse
pAM-mOrange_sh007G	kind gift of Dr. Thomas Kremer
pAM-mOrange_sh007MM	kind gift of Dr. Thomas Kremer
pAM-mGFP	kindly provided by Michaela Kaiser
pDP1rs	PlasmidFactory, Bielefeld, Germany
pDP2rs	PlasmidFactory, Bielefeld, Germany

2.2 shRNA sequences

sh007G (Mover knock-down):
AATTCCAGTTTCCTCCAAAGT
sh007MM (Mover knock-down, mismatched control):
AGTTTCAATTTCCACCTAAAT

2.3 Antibodies

Table 2.1: List of primary antibodies used in this study.

Primary Antibodies			
antigen	developed in	clone	source (Cat. no.)
Mover	rabbit	polyclonal	kind gift of Dr. T. Kremer
VGLUT1	guinea pig	polyclonal	Millipore (AB5905)
bassoon	mouse	SAP7F407	Stressgen (VAM-PS003)
β-actin	mouse	AC-15	Sigma (A3854)

Table 2.2: List of secondary antibodies used in this study.

Secondary Antibodies			
against	developed in	coupled to	source (Cat.no.)
rabbit	goat	Alexa633	Invitrogen (A21070)
mouse	goat	Alexa546	Invitrogen (A11003)
guinea pig	goat	Alexa546	Invitrogen (A11074)
rabbit	goat	peroxidase	Millipore (AP132P)
mouse	rabbit	-	Vector Labs

2.4 Virus production

2.4.1 Lenti virus production

HEK293LTV cells (Cell Biolabs, San Diego, CA) were grown to 70-80% confluency in DMEM (Gibco) supplemented with 10% FCS, 0.2 mM non-essential amino acids, 2 mM sodium pyruvate, 1% penicillin/strptomycin in 10 cm cell culture dishes. Cells were transfected with equimolar amounts of pFUGW, pΔ8.9 and pVSVg (10 µg/dish, 7.5 µg/dish and 5 µg/dish, respectively) using PEI (67.5 µl/dish, Sigma) diluted in OptiMEM (1ml/dish, Invitrogen). Transfection mixtures were incubated for 30-45 min at room temperature before applying them drop wise to the HEK293LTV cells. Medium was exchanged after 4 hours to stop the transfection. Virus particles were harvested two days after transfection by collecting and filtering (0.45 µm pore diameter) the cell culture supernatant. To concentrate the virus particles, the filtered supernatant was subjected to ultracentrifugation (90 min, 25000 rpm, SW32Ti rotor). The resulting pellet was dried and gently resuspended by incubation in PBS supplemented with 20 mM HEPES-Tris pH 7.4 at 4 °C for 120 min. Virus containing solution was aliquoted, shock frozen in liquid nitrogen and stored at -80 °C for further use.

2.4.2 Adeno-associated virus production

Adeno-associated virus particles were produced as chimeras of the serotypes 1 and 2. Therefore, $4x10^6$ HEK293 cells (293AAV, Cell Biolabs, San Diego, CA) were seeded in DMEM (supplements see above) on 14 cm cell culture dishes. Cells were transfected after 24 h with equimolar amounts of pAM, pDP1rs and pDP2rs using the calcium phosphate method. Threefore transfection mixture (2 ml/dish, 125 mM $CaCl_2$, HBS (140 mM NaCl, 25 mM HEPES, 0.7 mM Na_2HPO_4, pH 7.05)) containing 37.5 µg DNA was applied drop wise to the cells. After 24 h, the medium was exchanged to stop transfection. Three days after transfection chimeric virus particles were harvested and purified. Therefore, cells were removed from the dish, pelleted (200g, 10 min), resuspended in lysis buffer (150 mM NaCl, 50 mM Tris-HCl pH 8.5) and lysed via three freeze/thaw cycles. Genomic DNA was removed by digestion with 500 U of benzonase endonuclease (Sigma) for 2 h at 37 °C. Cell debris was pelleted and the supernatant containing the viral particles was filtered (0.45 µm pore diameter) to obtain the crude lysate. AAV particles were purified from the crude lysate via heparin-agarose columns. Columns (Biorad, Cat.no.: 7321010) were washed with 10 ml of equilibrium buffer (1 mM $MgCl_2$, 2.5 mM KCl in PBS pH 7.2) and filled with 5 ml heparin-agarose (Sigma, Cat.no.: H6508) and 10 ml equilibration buffer. Equilibration buffer was drained from the column once the heparin-agarose had settled. The crude lysate was added to the column and incubated for 2 h at 4 °C on a shaker. Crude lysate was let off and the column washed with 20 ml equilibration buffer, before the purified virus particles were eluted with 15 ml elution buffer (500 mM NaCl, 50 mM Tris-HCl, pH 7.2) into a filter tube (Amicon Ultra Filter, Milliore, Cat.no.: UFC9 100 24). The eluate was concentrated by centrifugation (4500 rpm) until less than 1 ml was left in the tube. To remove the high salt concentration, the filter tube was refilled twice with 15 ml PBS and centrifugation was repeated. The last centrifugation was run until less than 200 µl of virus stock were left. The virus solution was then filtered (0.22 µm pore diameter), aliquoted and stored at +4 or -80 °C for further use.

2.5 Primary hippocampal neuronal culture

Primary cultures of rat hippocampal neurones were prepared and from E19 embryos and maintained as described previously (Dresbach et al., 2003; Kremer, 2008). Hippocampal cultured neurons were kindly provided by Dr. Thomas Kremer, Dr. Nina Wittenmayer and Andrea Schlicksupp.

2.6 Western Blotting

Cultured hippocampal neurons transduced at DIV 5 were lysed at DIV 14 in 80 µl RIPA buffer (50 mM Tris HCl pH 7.5, 150 mM NaCl, 1% Nonidet P40, 0.5% sodium desoxycholate, protease inhibitors "complete mini" (Roche))and boiled (5 min, 95 °C). The membranes were pelleted and the protein concentration in the supernatant was determined using the BCA Protein Assay Kit (Pierce). Samples containing 20 µg of protein were mixed with sample buffer (125 mM Tris-HCl pH 6.6, 10% glycerol, 4% SDS, 5% β-mercaptoethanol, 0.5% bromphenolblue in H_2O), boiled for 5 min and subjected to SDS-PAGE (4-16% gradient gels purchased from Biorad) at 80 V for ~90 min (Running buffer: 25 mM Tris base, 192 mM glycine, 0.1% SDS). After separation by SDS-PAGE, proteins were transferred to PVDF membranes (Millipore) by semi-dry Western blotting. Therefore, gel and PVDF membrane were sandwiched between Watman papers soaked in transfer buffer (30 mM Tris base, 20% methanol). The transfer was performed at 150 mA for 60 min using a Trans-blot semi-dry system (Biorad). After transfer, membranes were blocked (60 min, room temperature, PBS supplemented with 0.5% Tween20 and 10% FCS). Proteins were probed by incubating the membranes for either 1 h at room temperature or at 4 °C over night with primary antibodies diluted to the appropriate concentration (1:1000 in blocking solution). Thereafter, membranes were washed (3x, 10 min each, PBS containing 0.5% Tween20) and incubated with secondary antibodies conjugated to horseradish peroxidase (1:10000 in PBS containing 0.5% Tween20, 45 min, room temperature). Membranes were washed three times for 10 min with PBS containing 0.5% Tween20 and protein signal was detected on photofilm (Amersham), using the SuperSignal West Pico Trial Kit (Pierce).

Equal amount of protein in all samples was assured by probing β-actin as a loading control. Membranes already probed for the protein of interest were incubated for 20 min at room temperature in methanol to remove bound antibodies. Thereafter, membranes were blocked (5% milk powder, 0.5% Tween20 in PBS, 60 min, room temperature) and the primary antibody was incubated (1:25000, 30 min, room temperature) in blocking solution. Since the primary antibody was already conjugated to a peroxidase the protein signal could be detected directly after washing (3x, 10 min each, PBS containing 0.5% Tween20).

2.7 Immunocytochemistry

Cultured hippocampal neurons transduced at DIV 5 were fixed (4% PFA in PBS, 20 min) at DIV 14. The cells were blocked and permabilized (5% sucrose, 5% serum albumin, 10% FCS and 0.3% Triton X-100 in PBS, 30 min) and thereafter incubated with the primary antibody (1:1000, 90 min, room temperature) in the same solution used for blocking. After washing (3x, 10 min each, PBS), the cells were incubated with appropriate secondary antibodies conjugated to Alexa dyes (1:1000 in PBS containing 5% sucrose and 0.3% Triton X-100, 45 min, room temperature) in the dark. Finally, the cells were again washed (3x, 10 min each, PBS), mounded in Aqua Poly Mound (Polysciences, Warrington, PA) and subjected to fluorescence microscopy.

2.8 Stereotaxic injections

AAV particles were injected into the VCN of two day old Sprague Dawly rats. Animals were anaesthetized with 5% isoflurane (Baxter, Deerfield, IL) in oxygen for ~5 min (Vaporizer: Isotec4, Sugivet, Dublin, OH). The isoflurane concentration was lowered to ~1% and kept at this level throughout surgery. Lidocain (~30 µl) was administered subcutaneously at the position of skin opening to achieve additional local anaesthesia. Surgery was only performed if the animal was in deep anaesthesia, as tested by loss of the retraction reflex in response to pinching between toes. The skull was mounted in a stereotax (Kopf Instruments, Tujunga, CA) and the skin was opened. A craniectomy of ~2 x 3 mm was performed in occiput using a dental drill (EXL-40, Osada, Los Angeles, CA). The tissue was wetted and cleaned throughout the surgical procedure with normal rat Ringer's solution (in mM: 135 NaCl, 5.4 KCl, 5 HEPES, 1.8 $CaCl_2$, 1 $MgCl_2$). Using an electronic levelling device (eLeVeLeR, Sigmann Elektronik, Hüffenhardt, Germany), the skull was aligned in the stereotax in a way that the roof of the skull was in a plane parallel to the ground plate of the stereotax. Injection capillaries were obtained by shaping of micropipettes (Cat. no: 708707, Brand, Wertheim, Germany) on a horizontal puller (P97, Sutter Instruments, Novato, CA) and mounted on a custom-build manipulator (Wimmer et al., 2004). The capillaries were connected to a syringe via a silicon tube, and ~2.5 µl of virus solution sucked into the capillary. The tip of the capillary was positioned on bregma, and all coordinates were set to zero. The virus solution was distributed evenly to six injections sites at the following coordinated relative to bregma and midline (x, y, in mm): -6.6, 0.7; -7.0, 0.7; -7.4, 0.7; -6.8, 0.9; -7.2, 0.9; -7.6, 0.9. The z- and a-coordinated were 0.45 mm and 6.5 mm, respectively for all injection sites. After virus injection the skin opening was sutured and an ear mark was set. The animals recovered within minutes after isoflurane administration ended and were returned to their mothers.

2.9 Preparation of fixed brain slices

P12/13 rats previously injected with AAV particles were deeply anaesthetized with isoflurane and transcardially perfursed with PFA. Anaesthesia was confirmed by loss of reflexes and skin and abdomen wall were cut open in the area of the apex. The diaphragm was cut and the thorax was opened to expose the heat. A steel needle (0.6 mm diameter) was inserted into the left ventricle and the right atrium was cut widely to open the blood circulation. The blood was removed by perfusing the animal with ~15 ml PBS followed by ~20 ml of 4% PFA dissolved in PBS for fixation.

The rats were decapitated and the brains were removed and stored in 4% PFA at 4 °C for 2-3 h for post-fixation. Brains were rinsed three times with PBS to remove excess PFA and brain slices of 100 µm thickness were cut on a vibratome (Sigmann Elektronik). Slices were stored in PBS at 4 °C for further use.

2.10 Immunohistochemistry

2.10.1 Antibody staining

Antibody staining of fixed brain stem slices was performed as described by Schwenger and Kuner (2010) with all incubation steps performed on a horizontal shaker. In detail, fixed slices were permabilized and blocked in PBS containing 5% normal goat serum (NGS) (Jackson Immuno Research, West Grove, PA) and 1% Triton X-100 for 2-3 h at room temperature. Thereafter,

primary antibodies were diluted 1:1000 in PBS supplemented with 1% NGS and 0.2% Triton X-100 and applied over night at 4 °C. Brain slices were washed three times for 10 min each in PBS containing 2% NGS before appropriate secondary antibodies coupled to Alexa dyes (1:1000 dilution) were applied in PBS supplemented with 1% NGS and 0.2% Triton X-100 for 2-3 h at room temperature in the dark. Three washing steps (10 min each) with PBS containing 1% NGS were followed by three washing steps (10 min each) in pure PBS. Thereafter, brain slices were mounted on glass slides and embedded in Slow Fade Gold (Invitrogen). Spacers of appropriate thickness were used to prevent tissue squeezing by the coverslip. Mounted and embedded slices were stored at 4 °C in the dark for further use.

2.10.2 Confocal microscopy

Confocal image stacks of stained brainstem slices were acquired using a Leica TCS SP5 microscope equipped with a 63x HCX PL APO (1.45 NA) objective. The photomultiplier gain was kept constant at 900 V whereas the laser power was adjusted to account for the whole dynamic range of 8 bit TIFF images. Averages of 2-4 individual images of 512 x 512 pixels size were acquired at 400 Hz scanning speed to increase the signal to noise ratio. Images of fluorophores with overlapping or nearly overlapping spectra were acquired sequentially to avoid bleed-through effects. Typical voxel sizes were 80-100 nm in x-y direction and 150-250 nm in z-direction.

2.10.3 Image processing

3D reconstruction of calyces prelabelled with membrane-bound GFP (mGFP) and quantitative image analyses of fluorescence signals was performed using Amira 4.2 (Visage Imaging, Richmond, Australia) as described recently (Dondzillo et al., 2010; Schwenger and Kuner, 2010). mGFP and immunoreactive signals were 3D median filtered (Kernel 3) before the mGFP-signal used for 3D reconstruction was thresholded. Fluorescence signal originating from axons and neighbouring calyces was removed manually, thereby isolating the 3D structure of the calyx of interest. The mGFP-delineated calyces were then multiplied with the immunoreactive signals in the 3D immunofluorescence data stack, thereby isolating the immunoreactive signals within the reconstructed calyx. These data were again tresholded and subjected to quantitative analysis using Amira 4.2. Thresholding of immunoreactive signals was performed by two examiners independently. Image stacks used for co-localization analyses were not 3D median filtered but deconvolved using Huygens2 software (Scientific Volume Imaging, Hilversum, The Netherlands).

2.11 Pre-embedding immunoelectron microscopy

Fixed tissue slices (prepared as described above) were permeabilized with 0.5% Triton X-100 in PBS for 5 min at room temperature, washed three times (10 min each) in PBS and blocked for 20 min in 10% FCS. Primary antibodies were applied at a dilution of 1:25 in PBS supplemented with 5% FCS over night at 4 °C. Samples were washed (3x, 10 min each, PBS) and if the primary antibody was not developed in rabbit, an appropriate secondary antibody was applied at a dilution of 1:70 in PBS containing 5% FCS for 6 h at 4 °C. The Fc-fragment of the rabbit antibody (primary or secondary) was labelled with protein A gold (5 nm diameter, 1:60 dilution in PBS, Cell Microscopy Center, Department of Cell Biology, University Medical Center,

Utrecht, The Netherlands) by incubation over night at 4 °C. Slices were washed (3x, PBS) and the region of interest was excised from the slice. The excised samples were postfixed with 0.1 M cacodylate buffer, pH 7.4 and 2% $OsO_{4/}$1.5% potassium-ferry-cyanide for 1 h in the dark before they were washed for 3 h in H_2O and stained with saturated uranyl acetate (16 min) followed by lead citrate (8 min) (modified Reynold's-procedure). Samples were dehydrated using an ascending series of ethanol followed by incubation in propylene oxide. Epoxy resin was used for embedding which was polymerized at 60 °C for 36 h. All chemicals used were purchased from SERVA (Heidelberg, Germany).

Sections of 70 nm thickness were cut through the MNTB using an Ultracut S ultramicrotome (Leica) equipped with a diamond knife angled at 35° (Diatome, Biel, Switzerland) (Blumer et al., 2002) and collected on Formvar-coated copper grids (Plano, Wetzlar, Germany). Transmission electron micrographs were obtained using a LEO 906E (Zeiss).

2.12 Preparation of acute brain slices

Rats previously injected with AAV particles were rapidly decapitated at P12/13. The brains were removed in ice-cold slicing solution (in mM: 125 NaCl, 25 $NaHCO_3$, 2.5 KCl, 1.25 NaH_2PO_4, 3 myoinositol, 2 Na-pyruvate, 0.4 ascorbic acid, 0.1 $CaCl_2$, 3 $MgCl_2$, 25 glucose aerated with carbogen pH 7.3) and angled coronal brainstem slices of 200-300 µm thickness were prepared on a vibratome (VT1200S, Leica). Slices were stored in ASCF (in mM: 125 NaCl, 25 $NaHCO_3$, 2.5 KCl, 1.25 NaH_2PO_4, 2 $CaCl_2$, 1 $MgCl_2$ and 25 glucose aerated with carbogen, pH 7.3) at 37 °C for 45 min and at room temperature thereafter.

2.13 Electrophysiology

2.13.1 Recordings from MNTB principal neurons

Whole-cell patch-clamp recordings were established from principal cells of the MNTB using an EPC-9 amplifier controlled by Pulse 8.80 software (HEKA, Lambrecht, Germany) at room temperature (22 ± 1 °C). Cells were visualized by video microscopy using Dodt-contrast illumination (Luigs und Neumann, Ratingen, Germany) and CCD camera detection (Spot RT, Diagnostic Instruments, Sterling Heights, MI) on an Axioskop upright microscope (Zeiss) equipped with standard 20x, 40x and 60x objectives (Olympus). Neurons targeted by calyces expressing either knock-down or mismatched shRNAs were identified by the calyceal expression of the fluorescent reporter mOrange. Fluorescence was visualized on using a Polychrome II monochromator (Till photonics, Gräfelfing, Germany) and adequate filter sets (AHF, Tübingen, Germany). The postsynaptic cells were filled with Alexa488 dye via the patch-pipette to confirm targeting of the recorded cell by a calyx expressing either type of shRNA (Fig. 2.1A).

Recordings were performed at a holding potential of -70 mV in ACSF (in mM: 125 NaCl, 25 $NaHCO_3$, 2.5 KCl, 1.25 NaH_2PO_4, 2 $CaCl_2$, 1 $MgCl_2$ and 25 glucose aerated with carbogen, pH 7.3). Patch-pipettes were pulled from thick-walled borosilicate glass (Cat. no.: 1807515, Hilgenberg, Malsfeld, Germany) on a horizontal puller (P97, Sutter Instruments, Novato, CA), had open tip resistances of 1.8-2.5 MΩ and were filled with solution containig (in mM): 130 Cs-gluconate, 10 CsCl, 10 HEPES, 10 TEA-Cl, 5 Na_2-phosphocreatine, 5 EGTA, 4 Mg-ATP and 0.3 GTP (pH 7.2). Series resistances ranged from 3 to 6 MΩ and were compensated for by >90%. Currents were digitized at sampling rates of 10-100 kHz and Bessel-filtered at 2.9 kHz. EPSCs were elicited by afferent fiber stimulation via a parallel bipolar electrode (Cat. no PBSA0275,

FHC, Bowdoin, ME) placed close to midline (2-6 V stimuli, 100-200 µs duration). During recordings under varying extracellular Ca^{2+}-concentrations, Ca^{2+} was substituted by Mg^{2+} to keep the concentration of divalent cations constant. New Ca^{2+} equilibrium concentration was achieved within 3-4 min (perfusion rate 4.5 ml/min).

Recordings were excluded from analyses if one of the following criteria was fulfilled: R_s greater than 6 MΩ, leak current larger than 250 pA, synapse unable to follow 100 Hz trains, EPSC larger than 20 nA (amplifier saturation). Spontaneous EPSCs arising from non-calyceal inputs to the MNTB neuron were excluded from analyses based on their kinetic properties (Hamann et al., 2003).

2.13.2 Recordings from calyx terminals

Presynaptic recordings from visually identified calyces were performed with amplifier settings as described for recordings from MNTB principal neurons. The tips of the patch-pipettes were wrapped with parafilm to reduce pipette capacitance. The pipettes were filled with solution containing (in mM): 130 Cs gluconate, 15 CsCl, 10 HEPES, 20 TEA-Cl, 5 Na_2-phosphocreatine, 0.5 EGTA, 4 Mg-ATP and 1 GTP (pH 7.2). Open tip resistances ranged from 3 to 6 MΩ resulting in series resistances of 10-30 MΩ (compensated for by 30-70%). The ASCF (see above) was supplemented with 1 µM TTX (Ascent Scientific, Bristol, UK) and 20 mM TEA-Cl to isolate Ca^{2+}-currents. Stimulation of the calyx terminal was induced by step depolarizations from holding potential (-80 mV) to 0 mV of various durations. The membrane capacitance was calculated from the application of a sinusiodal stimulus wave (1000 Hz, 30 mV amplitude) on top of the DC holding potential by using the lock-in amplifier of Pulse 8.80 software. The increase in membrane capacitance was determined 250 ms after the end of the stimulus to prevent contamination of recordings with capacitance artefacts that are independent of calcium influx (Yamashita et al., 2005). Passive current transients were not determined systematically, since they have no influence on capacitance recordings (Sun et al., 2004). Recordings were excluded from analyses if R_s was above 30 MΩ or a prominent rundown in stimulus induced capacitance increase was observed over the time of the experiment. Calyces were filled with Alexa488 via the patch-pipette to ensure presynaptic localization of the recording site (Fig. 2.1B).

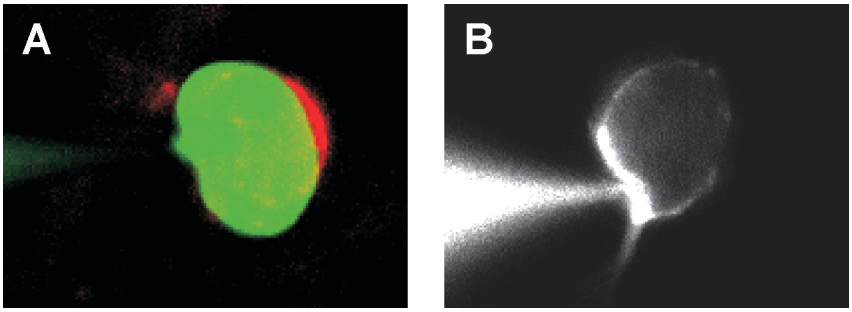

Figure 2.1: Recording configurations.
A: Whole-cell recording from a MNTB principle cell (green, filled with Alexa488 via the patch-pipette) that is contacted by a shRNA expressing calyx (red). **B:** Direct whole-cell recording from a calyx of Held terminal filled with Alexa488.

2.13.3 Recordings from cultured hippocampal neurons

Whole-cell patch clamp recordings of hippocampal cultured neurons were performed at DIV 15-17 at room temperature. The amplifier settings were as described in chapter 2.13.1. The holding potential was -70 mV. Series resistance was compensated to 70-90%. Pipettes had open tip resistances of 4-6 MΩ. The extracellular solution contained (in mM): 119 NaCl, 2,5 KCl, 2 $CaCl_2$, 2 $MgCl_2$, 25 HEPES and 30 glucose adjusted to pH 7.4 with NaOH. The pipette solution contained (in mM): 120 Cs gluconate, 10 HEPES, 10 Na gluconate, 10 Na_2-phosphocreatine, 4 NaCl, 4 Mg-ATP, 0.1 EGTA, 0.3 GTP, 0.1 spermine and 2,5 QX-314 adjusted to pH 7,2 with CsOH. mPSCs were pharmacologically isolated by addition of 1 µM TTX and either 10 µM SR95531 (gabazine) (mEPSCs) or 10µM CNQX and 50 µM APV (mIPSCs) to the extracellular solution. All drugs were purchased from Ascent Scientific (Bristol, UK)

2.13.4 Data analyses

Data was analysed using custom-written IGOR (Wavemetrics, Lake Oswego, OR) routines. Statistical significance was determined by one-way ANOVA followed by Dunnett's test using Prism 5.0 software (Graphpad software, La Jolla, CA) (* = $p < 0.05$, ** = $p < 0.01$, *** = $p < 0.001$). Data is presented as mean ± SEM.

3 Results

3.1 Lenti virus mediated knock-down of Mover in hippocampal cultured neurons

To assess the unknown function of the novel presynaptic protein Mover, we sought to first knock it down in hippocampal cultured neurons. Lenti virus (LV) particles containing the coding sequences of either a shRNA directed against Mover mRNA or a mismatched control shRNA, both under the control of the U6 promoter, were produced. The LV particles additionally expressed the fluorescent reporter EGFP under human synapsin promoter control (Kremer, 2008). High density cultures of hippocampal neurons were transduced with LV particles after 5 days in vitro (DIV). Transduction efficiency was determined as the percentage of cells expressing EGFP at DIV 14 and found to be roughly 95%. The knock-down was efficient and specific as shown by immunocytochemistry and Western bolt analyses (Kremer, 2008).

Since Mover is located in presynaptic terminals we examined whether Mover is somehow involved in SV release and therefore analysed spontaneous synaptic transmission as a read out of presynaptic activity. Pharmacologically isolated mEPSCs were recorded at DIV 14-16 from either untreated control cultures or cultures transduced with LV particles expressing knock-down or mismatched control shRNA. Only cultures that showed very high transduction efficiencies were used for recordings, thereby ensuring that virtually all terminals contacting the recorded neuron were originating from neurons expressing the shRNA. Unfortunately, no significant effect of Mover knock-down could be detected in any of the parameters analyzed (Fig. 3.1). The frequency of mEPSCs was unaltered, suggesting that the number of synapses formed on a given neuron was unchanged and that the probability of spontaneous release at these synapses was not affected. This confirmed results obtained by the stimulation dependent uptake of antibody directed against the luminal domain of synaptotagmin 1 (Kremer, 2008), which showed no change in the number of functional synapses after knock-down of Mover. The basic properties of the vesicle release machinery also seem to be unaltered since no change in mEPSC kinetics, neither in rise time nor in the time constant of decay, was observed. Finally, the amplitude of the mEPSCs remained constant after Mover knock-down, excluding effects of Mover on the vesicular neurotransmitter content and on the number of postsynaptic glutamate receptors.

Mover is expressed in both excitatory and inhibitory synapses. Hence, the properties of mIPSCs were examined to exclude a specific effect of Mover on inhibitory synapses. Pharmacologically isolated mIPSC were recorded with results similar to those obtained for mEPSCs (Fig. 3.2). None of the parameters examined (frequency, amplitude, rise time, time constant of decay) was altered after knock-down of Mover. Thus, Mover is not involved in quantal synaptic transmission neither at excitatory nor at inhibitory synapses of hippocampal cultured neurons.

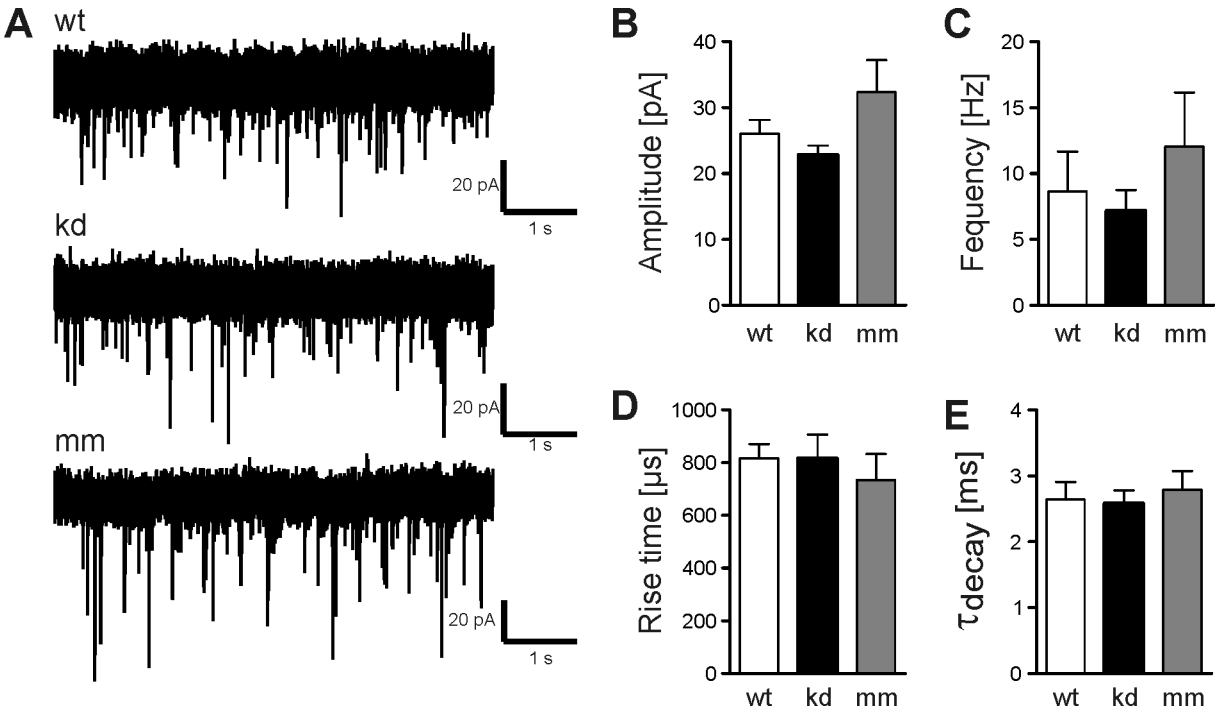

Figure 3.1: Mover has no effects on mEPSCs in hippocampal cultured neurons.
A: Representative sample current traces. **B-E:** Quantification of mEPSC parameters (n = 11-17). wt: wild type, kd: knock-down, mm: mismatched control

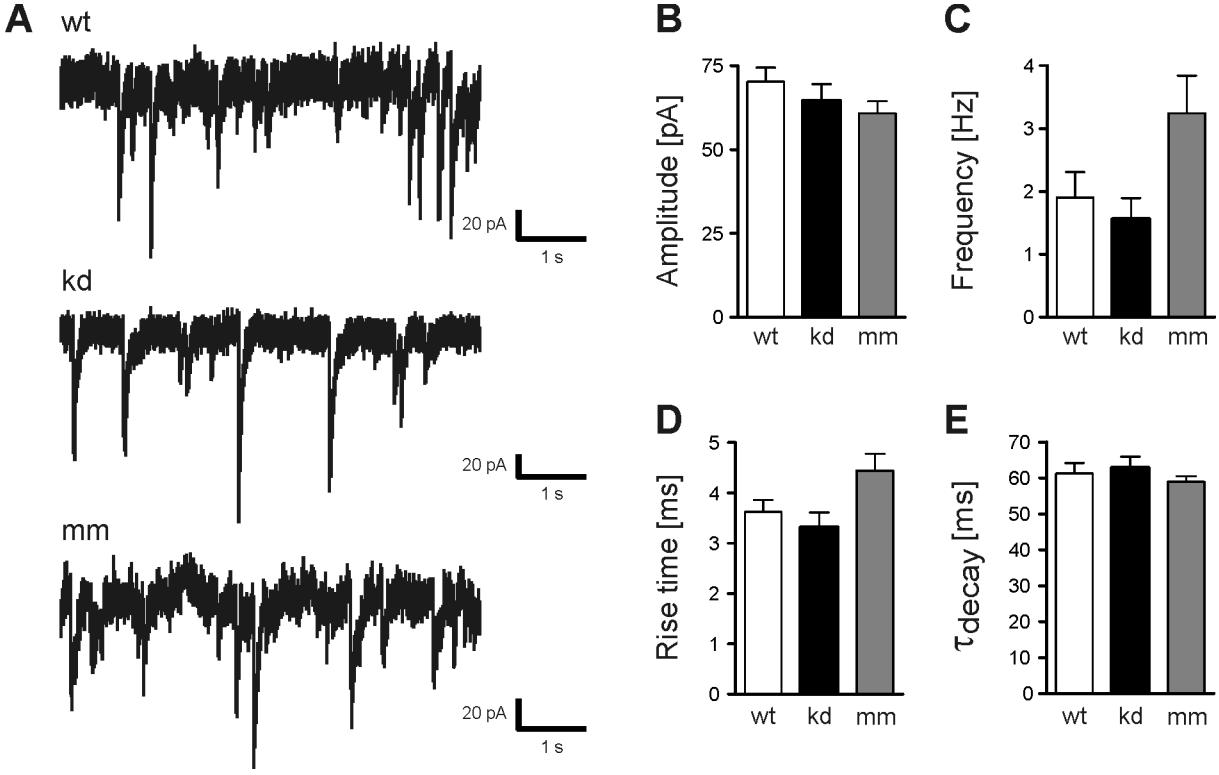

Figure 3.2: Mover has no effects on mIPSCs in hippocampal cultured neurons.
A: Representative sample current traces. **B-E:** Quantification of mIPSC parameters (n = 13-15).

3.2 AAV mediated knock-down of Mover in hippocampal cultured neurons

The results obtained in hippocampal cultured neurons so far did not yield any insights into Mover function. Thus, we sought out to assess Mover function on the level of single identified synapses instead of examining synapse populations as in hippocampal neuronal cultures. From an earlier study, we were aware of Mover being expressed in the calyx of Held, a giant synapse in the MNTB in the auditory brainstem. This synapse has some unique advantages since it is accessible to both pre- and postsynaptic recordings and has a defined input/output relation (1:1, Hoffpauir et al., 2006, Borst et al., 1995). We therefore decided to establish a shRNA mediated *in vivo* knock-down of Mover in the calyx of Held.

The LV system has two major disadvantages for the use in neuronal tissue, first it has a very limited spread, which prevents it from transducing larger neuronal populations and secondly, LV particles transduce both, neurons and glial cells. Therefore it was necessary to use a different virus system. Adeno-associated viruses (AAV) of the chimeric serotype 1/2 are far better suited for *in vivo* transduction, since they are spreading well in neuronal tissue and are selectively infecting neurons (Klugmann et al., 2005, Hauck et al., 2003). Both differences between the two virus systems, especially the spread in neuronal tissue but also the selective transduction of neurons are depicted in Figure 3.3.

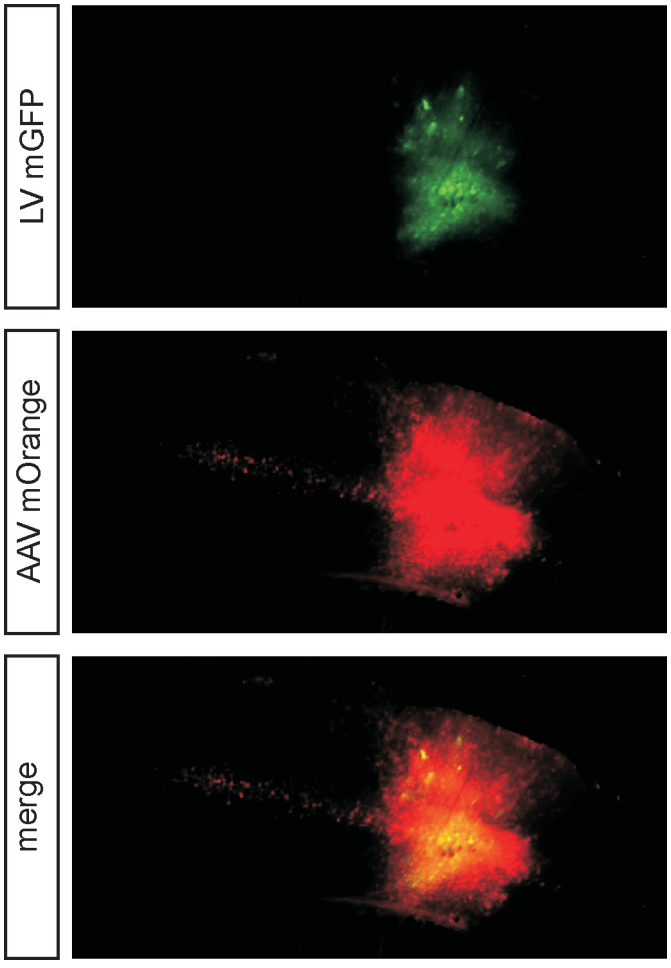

Figure 3.3: AAV particles are spreading better than LV particles and are more selective for neurons when both types of viruses are co-injected into neuronal tissue.
Top: LV mediated expression of mGFP. **Middle:** AAV mediated expression of mOrange. Note the selective expression of mOrange in layer 4 neurons far outside the injection side. **Bottom:** merge. Images kindly provided by Dr. Darius Schwenger.

Thus, we re-established the knock-down of Mover in hippocampal neurons using AAV particles for transduction. The sequences coding for either of the shRNAs were subcloned into an AAV vector in which their expression was driven by the U6 promoter. As a fluorescent reporter this vector expressed mOrange under the chicken-β-actin promoter. The expression cassette further contained the cytomegalovirus early enhancer, a woodchuck post-regulatory element and a bovine growth hormone polyA signal and was flanked by AAV serotype 2 inverted terminal repeats (Kügler et al., 2003) (Fig. 3.4).

Chimeric AAV particles of the serotypes 1 and 2 were prepared and used to transduce hippocampal cultured neurons at DIV 5. Knock-down efficiency was examined at DIV 14 by immunocytochemistry and Western Blot analyses. Neurons transduced with AAV particles expressing knock-down shRNA

Figure 3.4: Schematic drawing of the expression cassette used to produce shRNA expressing AAV particles. ITR: inverted terminal repeat, CMV: human cytomegalovirus, CBA: chicken β-actin, WPRE: woodchuck hepatitis B virus posttranscriptional element, BGH polyA: bovine growth hormone polyadenylation signal.

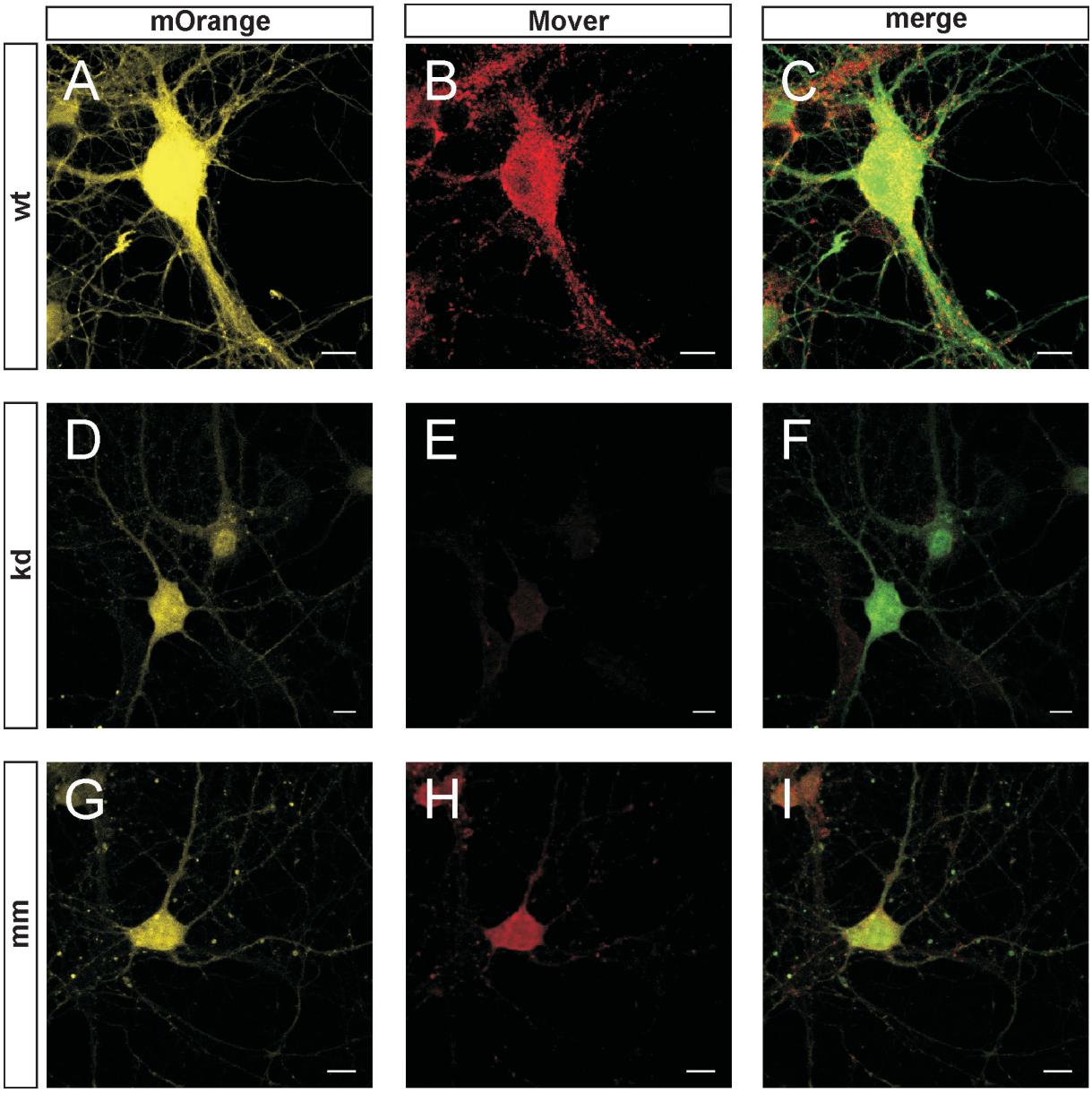

Figure 3.5: Mover is efficiently knocked-down in hippocampal cultured neurons by AAV mediated expression of shRNA.
Mover immunoreactive puncta are virtually absent in neurons expressing knock-down shRNA (D-F), whereas clustered Mover signal is readily detectable in neurons expressing either mOrange only (wild type control, A-C) or mismatched control shRNA (G-I). Scale bars represent 10 µm.

showed an almost complete loss of immunoreactive Mover puncta in immunocytochemistry experiments (Fig. 3.5D-F). In contrast, Mover immunoreactive puncta were readily detectable in neurons transduced with AAV particles expressing either only mOrange (Fig. 3.5A-C) or mismatched control shRNA (Fig. 3.5G-I).

Additionally, the amount of Mover protein after knock-down was examined. Therefore, transduced hippocampal cultured neurons were lysed at DIV14 and the lysates were subjected to Western Blot analyses. Mover signal was only barely detectable in lysates originating from cultures expressing knock-down shRNA indicating an almost complete loss of Mover upon expression of knock-down shRNA. On the contrary, the expression of the mismatched control shRNA did not lead to detectable changes in the amount of Mover protein as compared to untreated control cultures (Fig. 3.6).

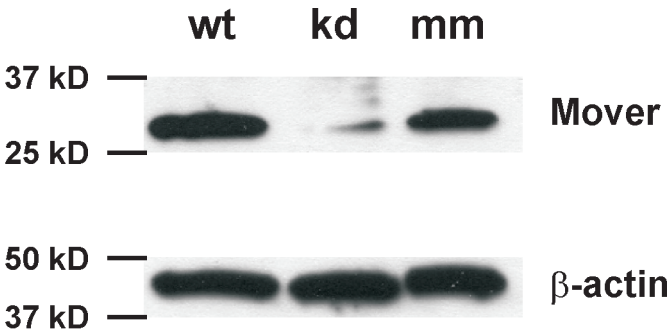

Figure 3.6: The amount of Mover protein is efficiently reduced in hippocampal cultured neurons by AAV mediated expression of knock-down shRNA.
Western blot analyses of untreated cultures (wt) and cultures transduced with AAV particles expressing either knock-down or mismatch shRNA (kd and mm, respectively). Note the strong reduction of Mover expression in knock-down cultures. β-actin was used as loading control.

3.3 AAV mediated knock-down of Mover in the calyx of Held *in vivo*

After establishing the shRNA mediated knock-down of Mover in hippocampal cultured neurons using AAV delivery, we aimed for the knock-down of Mover in the calyx of Held *in vivo*. We therefore injected AAV particles expressing either knock-down or mismatched control shRNA and mOrange as fluorescent reporter into the VCN of P2/3 rats. AAV particles expressing membrane-bound GFP (mGFP) were co-injected to allow for 3D reconstruction of individual calyces independent of the expression of a shRNA. Fixed coronal brainstem slices were prepared from transcardially perfused P12 rats and subjected to immunohistochemistry against Mover. High resolution confocal microscopy stacks were recorded from individual mGFP expressing calyces stained with an antibody directed against Mover. Calyces were 3D reconstructed from the confocal image stacks using the mGFP signal. The calyx reconstruction was then used to determine the immunoreactive Mover signal present inside the calyx of interest (Dondzillo et al., 2010). The mOrange signal identified calyces expressing one of the shRNAs.

Immunoreactive Mover signal was strongly reduced in calyces expressing knock-down shRNA (Fig. 3.7B) as compared to those expressing either mismatched control shRNA (Fig. 3.7C) or mGFP only (Fig. 3.7A). Quantification of the immunoreactive Mover signal in individual calyces revealed a ~75% reduction in the calyx volume occupied by Mover immunoreactive signal in calyces expressing knock-down shRNA (5.09 ± 0.93%) as compared to wild type calyces expressing only mGFP (14.94 ± 0.96%). Expression of the mismatched control shRNA had no effect on the volume occupied by Mover immunoreactivity (17.48 ± 1.22%) (Fig. 3.7E). Interstingly, the density of Mover immunoreactive clusters (number of clusters per volume) was not affected by the knock-down of Mover (wild type: 0.13 ± 0.02 clusters/μm^3 calyx volume, knock-down: 0.1 ± 0.01 clusters/μm^3 calyx volume, mismatch: 0.12 ± 0.01 clusters/μm^3 calyx volume) (Fig. 3.7D) which indicates a strong reduction in the size of individual Mover clusters after expression of knock-down shRNA.

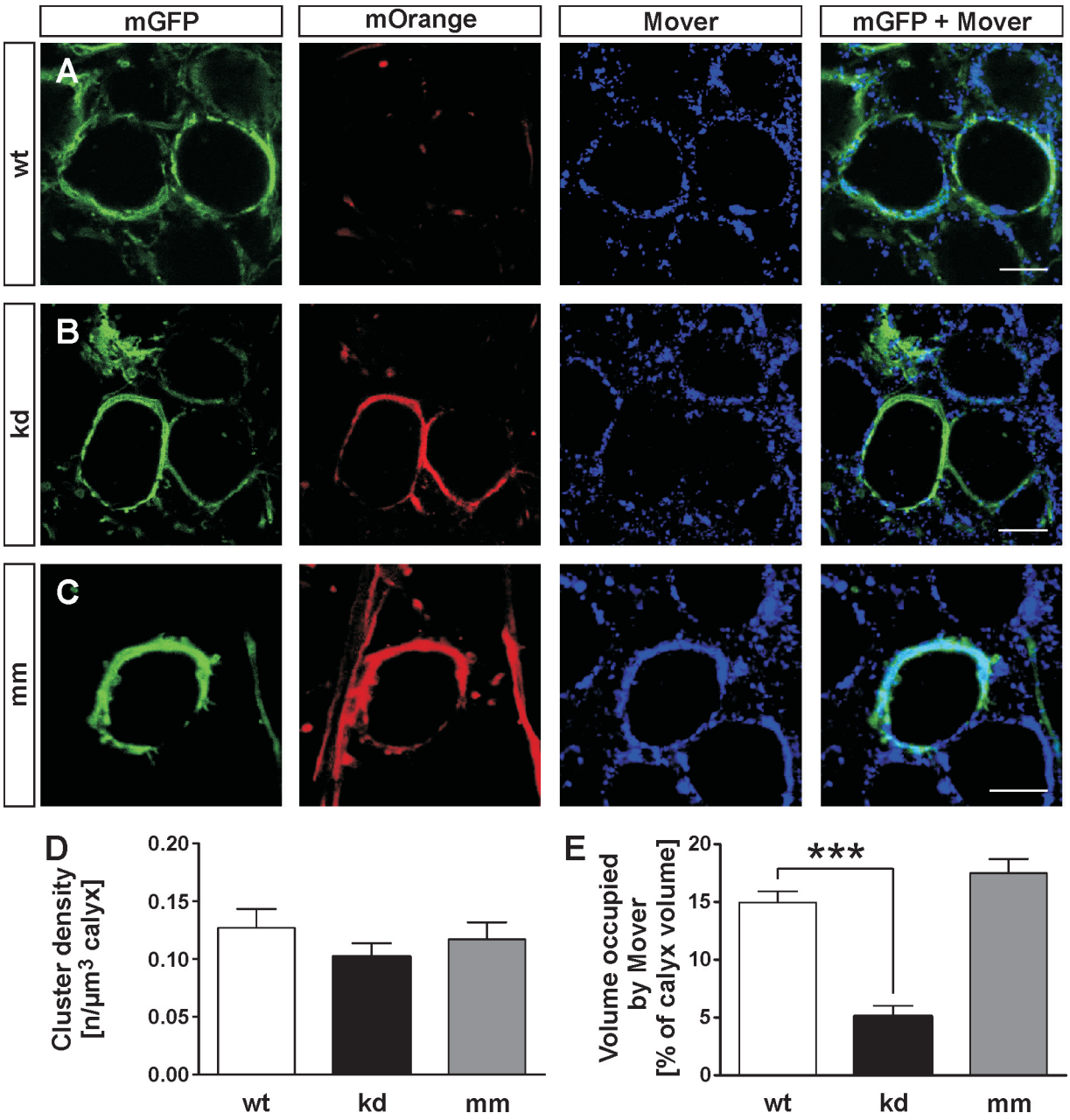

Figure 3.7: Mover is efficiently knocked-down in the calyx of Held *in vivo*.
A-C: Individual confocal sections of mGFP prelabelled calyces, Mover knock-down (kd) and mismatch (mm) shRNA reported by the expression of mOrange. Wild type (wt) cells lacking mOrange. mGFP-expressing calyces in the same brain section not expressing mOrange were used as wild type controls. Scale bars are 10 µm. **D, E:** 3D-quantification of the density of Mover clusters with in single calyces and the calyx volume occupied by Mover immunoreactive signal (n = 9-12).

3.4 Subcellelar localization of Mover

Before investigating the functional consequences of an *in vivo* knock-down of Mover, we sought out to precisely localize Mover in the calyx of Held. Although Mover was discovered as an interaction partner of Bassoon associated with SVs, most previous experiments were performed either in cultured neurons or in bouton-type synapses, in which it is, due to their small size, difficult to resolve subcellular localizations (Kremer et al., 2007, Kremer, 2008). We examined Mover localization in the calyx by employing high resolution confocal microscopy in combination with deconvolution analyses and preembedding immuno-gold labelling transmission electron microscopy.

Co-localization of Mover with the SV marker VGLUT1 was determined in mGFP prelabelled calyces (Fig. 3.8A). 3D reconstruction of individual calyces and subsequent quantification of the immunoreactive signals of Mover and VGLUT1 revealed slightly more Mover immunoreactive clusters than clusters positive for VGLUT1 (Fig. 3.8C). The discrepancy may arise from VGLUT1 clusters being highly abundant in the calyx resulting in distances between VGLUT1 clusters that are to small to be resolved by confocal microscopy. When we quantified the cluster co-localization, we found that most of the VGLUT1 clusters were co-localized with Mover (93 ± 12%). VGLUT1 clusters devoid of Mover signal might represent a population of SVs close to the release sites at which Mover was rarely detected in electron micrographs (see below). The number of Mover clusters that are co-localized with VGLUT1 was slightly lower (73 ± 9%) indicating that some Mover immunoreactive signal arises from structures not positive for VGLUT1 (Fig. 3.8D). However, the identity of these structures

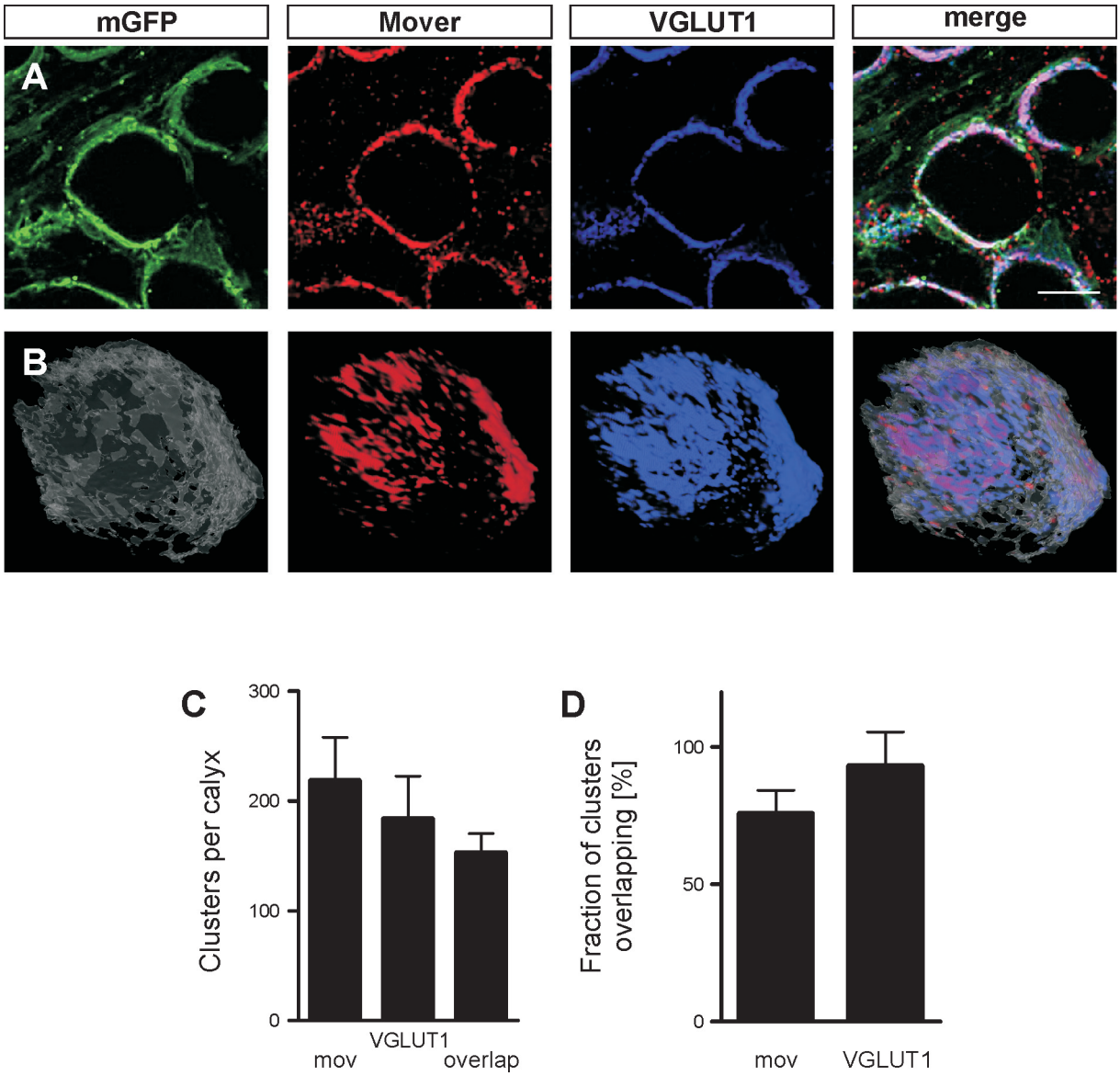

Figure 3.8: Mover is associated with SV clusters.
A: Individual confocal sections of mGFP-prelabelled calyces, Mover and SV marker VGLUT1 antibody stainings. Colours in merged panel: pink: Mover and VGLUT1 co-localization outside the mGFP labelled calyx, white: Mover and VGLUT1 co-localization inside the mGFP labelled calyx. Scale bar is 10 µm. **B:** 3D representation of a single mGFP labelled calyx stained for Mover and VGLUT1. **C, D:** Quantification of Mover (mov) and VGLUT1 cluster number and overlapping fraction (n = 6).

remained elusive, but VGLUT1 is known to be restricted to SVs much more rigorously than other SV proteins such as VAMP2 (Voglmaier et al., 2006). Nevertheless, our immunohistochemical experiments confirm that the vast majority of VGLUT1 immunoreactive signal is co-localized with Mover indicating that Mover is associated with SVs.

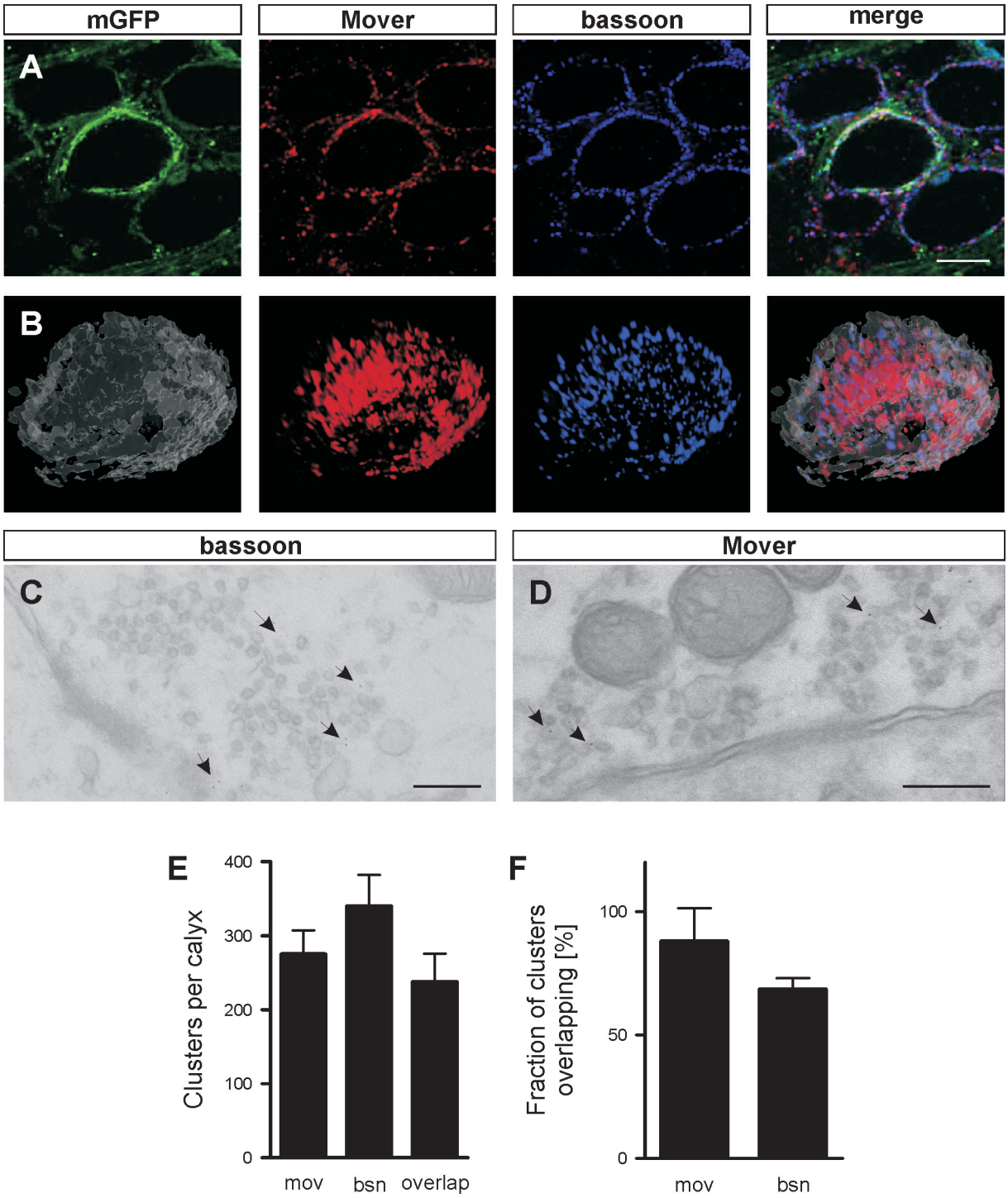

Figure 3.9: Mover is localized to the outer membranes of SVs at active zones.
A: Individual confocal sections of mGFP-prelabelled calyces, Mover, and active zone marker bassoon antibody stainings. Colours in merged panel: pink: Mover and bassoon co-localization outside the mGFP labelled calyx, white: Mover and bassoon co-localization inside the mGFP labelled calyx. Scale bar is 10 µm. **B:** 3D representation of a single mGFP labelled calyx stained for Mover and bassoon. **C, D:** Electron micrographs of immunogold-labeled Mover and bassoon. Gold particles (5 nm) labeled with arrows. Scale bars are 200 nm. Electron micrographs were kindly provided by Heinz Horstmann. **E, F:** Quantification of Mover (mov) and bassoon (bsn) cluster number and overlapping fraction (n = 6).

In the calyx of Held, two subpopulations of SVs exist; one population is located in high density clusters that localize to AZs, whereas the second one is diffusely distributed throughout the calyx (Dondzillo et al., 2010). To determine whether Mover is preferentially associated with one of the two subpopulations, we examined the co-localization of Mover with the AZ marker bassoon that strongly co-localizes with high density SVs (Dondzillo et al., 2010). Co-localization of Mover and bassoon immunoreactive signals inside mGFP labelled calyces was evident from confocal image stacks (Fig. 3.9A). Quantification of immunoreactivity after 3D reconstruction revealed a slightly higher number of clusters positive for bassoon than for Mover (Fig. 3.9E). This indicated the presence of active zones devoid of Mover and was underlined by the finding that only 68 ± 5% of the bassoon immunoreactive clusters were colocalized with Mover. On the contrary, most Mover immunoreactive clusters co-localized with bassoon (88 ± 14%) (Fig. 3.9F) pointing towards a preferential localization of Mover to SV that are close to active zones rather than to those diffusely distributed in the calyx.

Although high resolution confocal microscopy gave a good estimate of the subcellular localization of Mover, confocal microscopy suffers from the diffraction limit. To overcome this limitation we performed preembedding immuno-gold labelling with antibodies against either bassoon or Mover (5 nm gold particles) and examined the distributions of gold particles with transmission electron microscopy. In line with the results obtained by Dondzillo and colleagues (2010), we found the majority of bassoon immuno-gold signals at least 100 nm away from release sites (Fig. 3.9C) in the same region where we detected most of the Mover immuno-gold signals, too (Fig. 3.9D). The localization of the active zone marker bassoon distant from the release site seems counterintuitive but was confirmed by a recent super resolution microscopy study (Dani et al., 2010). In regard to the localization of Mover to SVs, Mover immuno-gold signals were found at the cytosolic surface of the SV membrane (Fig. 3.9D) confirming the attachment of Mover to SVs. Interestingly, we rarely found Mover immuno-gold signal to be attached to SVs that were docked to the plasma membrane (Fig. 3.9D).

3.5 Electrophysiological characterization of Mover knock-down calyces

3.5.1 Spontaneous release

After establishment of an efficient and specific knock-down of Mover in the calyx of Held, we examined the effects of Mover knock-down on synaptic transmission. Whole-cell patch-clamp recordings from MNTB principle cells, the cells postsynaptic to the calyx of Held, were established in acute brain slices of P12/13 rats. Since each MNTB principle cell receives input from only a single calyx (Hoffpauir et al., 2006) this approach allows the investigation of synaptic transmission mediated by single synapses. MNTB cells targeted by calyces expressing one of the two shRNAs were identified by the expression of mOrange in the calyx.

Consistent with the results obtained in cell culture (see above), knock-down of Mover did not affect spontaneous release of SVs in the calyx of Held (Fig. 3.10). Neither the kinetics (rise time and time constant of decay) nor amplitude of spontaneous EPSCs were altered in Mover knock-down calyces. The frequency with which spontaneous EPSC occurred was unchanged upon knock-down, too. These results indicate that, similar to synapses in hippocampal cultured neurons, Mover has no effect on the basic release machinery, the number of functional release sites, the neurotransmitter content of the SVs and the postsynaptic glutamate receptors at the calyx of Held synapse.

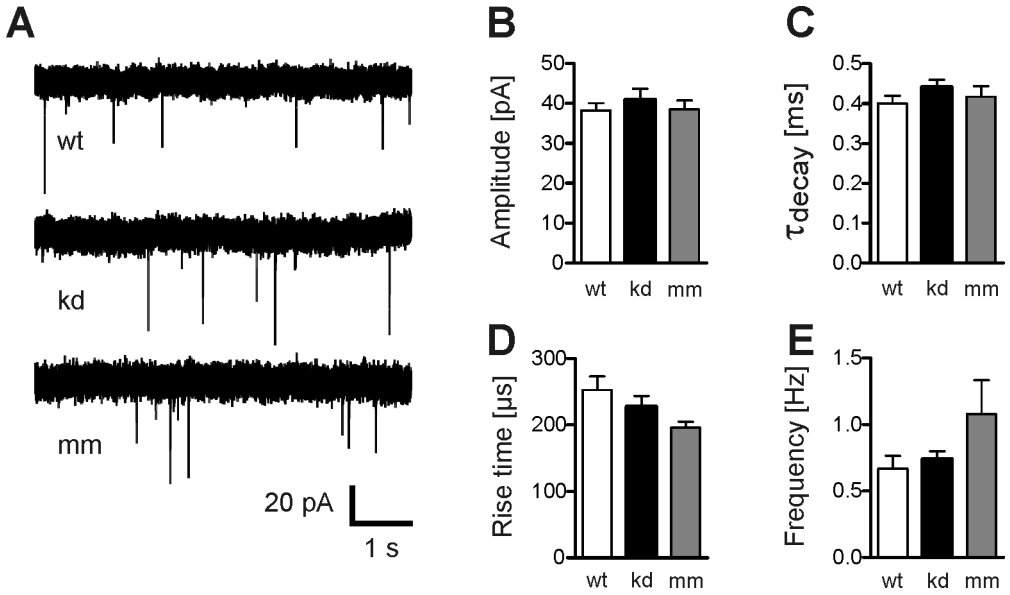

Figure 3.10: Mover knock-down does not affect spontaneous release at the calyx of Held.
A: Representative sample current traces. **B-E:** Quantification of amplitude, frequency and kinetics of spontaneous EPSCs at the calyx of Held (n = 10-15).

3.5.2 Evoked release

We next examined whether Mover has any effect on Ca^{2+} triggered, phasic release. Therefore we recorded evoked EPSC from the principle cells of the MNTB. EPSC were evoked by afferent fibre stimulation via a parallel bipolar electrode placed close to midline.

Figure 3.11A shows the increase in amplitude of evoked EPSCs recorded in Mover knock-down synapses (12.54 ± 0.94 nA) as compared to wild type or mismatched control calyces (8.04 ± 0.74 nA and 10.27 ± 1.51 nA, respectively) (Fig. 3.11E). Since the amplitude of spontaneous EPSCs were not affected by Mover knock-down (Fig. 3.10B), the increase in

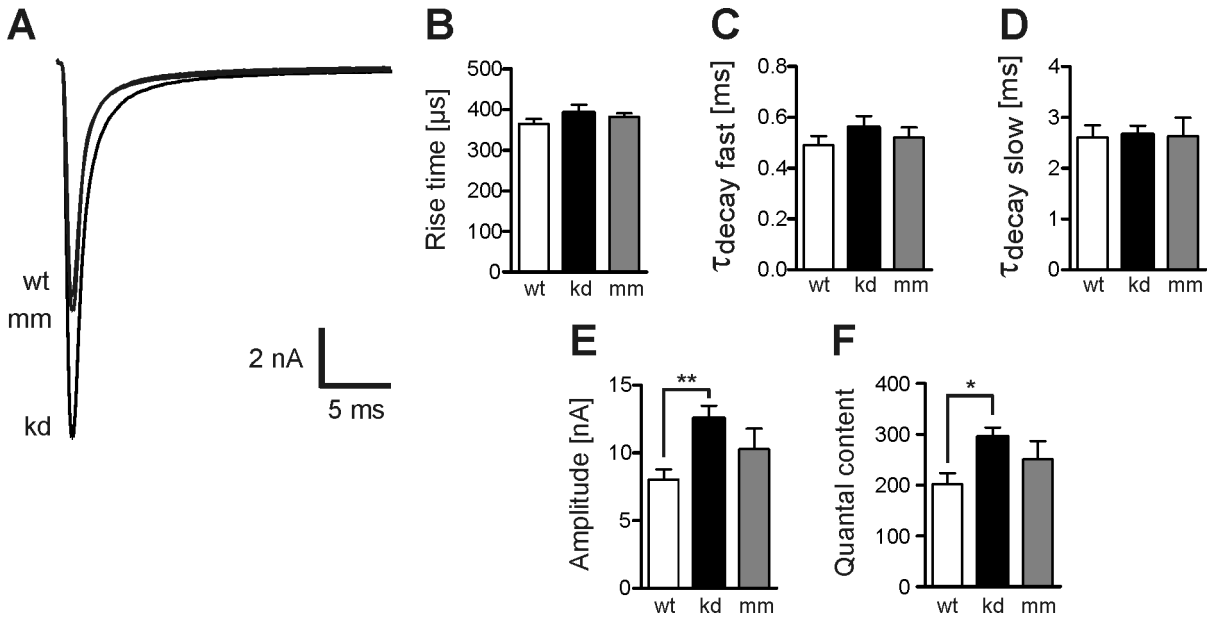

Figure 3.11: Mover knock-down increases the amplitude of evoked EPSCs.
A: Superimposed representative recordings of evoked EPSCs from wild type, knock-down and mismatch control synapses. **B-E:** Quantification of evoked EPSC parameters. The amplitude as well as the quantal content of evoked EPSCs of Mover knock-down calyces is significantly increased (E, F), whereas the kinetic properties of the EPSC remain unchanged (B-D) (n = 12-20).

EPSC amplitude resulted in an increase in the quantal content of evoked EPSCs (Fig. 3.11F). EPSC kinetics (rise time and time constants of decay) were unchanged upon knock-down of Mover (Fig. 3.11B-D) indicating that Mover does not affect the synchronicity of release.

3.5.3 Short-term depression

Since the amplitude of single evoked EPSC was increased, we next examined the impact of Mover knock-down during trains of stimuli. A prominent feature of the calyx of Held is pronounced short-term depression (STD) which, at least at high frequencies (100 Hz), reflects depletion of the readily releasable pool (RRP) of SVs (von Gersdorff and Borst, 2002).

We first examined the effects of Mover knock-during moderate stimulation by application of trains of 20 stimuli at 10 Hz. Even at this moderate stimulation frequency, STD was evident regardless whether a shRNA was expressed in the calyx investigated or not (Fig. 3.12A and A'). To quantitatively investigate STD, we normalized the EPSCs to the amplitude of the first EPSC in the train (Fig 3.12B), fitted the amplitude decay with a mono-exponential function and determined the time constant of the amplitude decay, the extent of depression and the paired-pulse ratio (PPR) between the first two EPSCs of the train. Quantification of these parameters revealed that knock-down of Mover resulted in a faster amplitude decay (Fig. 3.12A and C), a more complete depression (Fig. 3.12A and D) and a reduced PPR (Fig. 3.12A and E) whereas all three parameters were unchanged in mismatch control calyces (Fig. 3.12A', C, D and E).

Knock-down of Mover resulted in a twofold accelerated amplitude decay (wild type: 0.192 ± 0.016 s, knock-down: 0.112 ± 0.009 s, mismatched control: 0.218 ± 0.023 s, Fig.3.12C), whereas the effect of Mover knock-down on the extend of depression (determined as Y_0 of the mono-exponential fit of the amplitude decay multiplied by 100) was rather moderate (wild type: 71 ± 2%, knock-down: 78 ± 1%, mismatch: 73 ± 2%, Fig. 3.12D). The strong effect of Mover

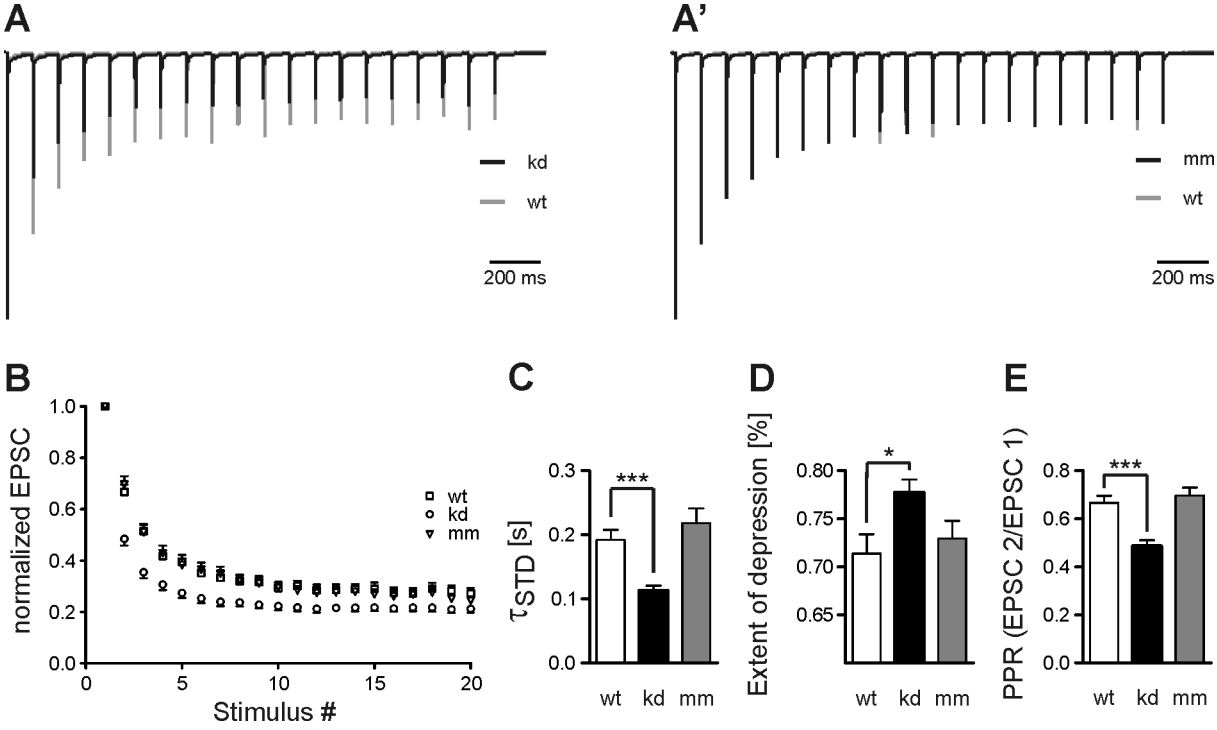

Figure 3.12: Mover knock-down increases and accelerates STD during moderate stimulation.
A, A': Superimposed scaled representative current traces recorded during 10 Hz stimulus trains (20 stimuli). **B:** Averaged normalized EPSC amplitudes during 10 Hz trains. **C-E:** Quantification of STD parameters (time constant of amplitude decay, extent of depression and PPR) during 10 Hz trains (n = 12-20).

on the PPR between the first two EPSCs (wild type: 0.67 ± 0.03, knock-down: 0.49 ± 0.03, mismatched control: 0.7 ± 0.03, Fig. 3.12E) argued against a higher number of docked SVs as source of the increase in EPSC amplitude since this would increase the amplitudes of both, the first and the second EPSC and leave the PPR unchanged.

At moderate stimulation frequencies like the 10 Hz investigated above, the dynamics of SV pools such as pool refilling could mask potential effects Mover. We therefore increased the stimulation frequency to 100 Hz and applied trains of 50 stimuli to calyces. Thereby, we examined STD under conditions, under which it is thought to reflect purely RRP depletion (von Gersdorff and Borst, 2002). Investigation of STD during high frequency stimulation yielded results similar to those obtained at moderate stimulation frequency (Fig. 3.13). As during 10 Hz stimulus trains, at 100 Hz the time constant of amplitude decay and the PPR were decreased while the extend of depression was increased (Fig. 3.13 C-E) upon knock-down of Mover. During high frequency stimulation, the EPSCs late in the train are thought to reflect the release of SVs newly recruited to the release sites (von Gersdorff and Borst, 2002). Thus, we compared the amplitudes of the last EPSCs in the train to examine a potential effect of Mover knock-down on the recruitment of SVs to release sites under ongoing activity. Interestingly, the amplitude of the 50th EPSC did not change significantly upon knock-down of Mover (Fig. 3.13F) suggesting that Mover does not interfere with SV recruitment under these conditions.

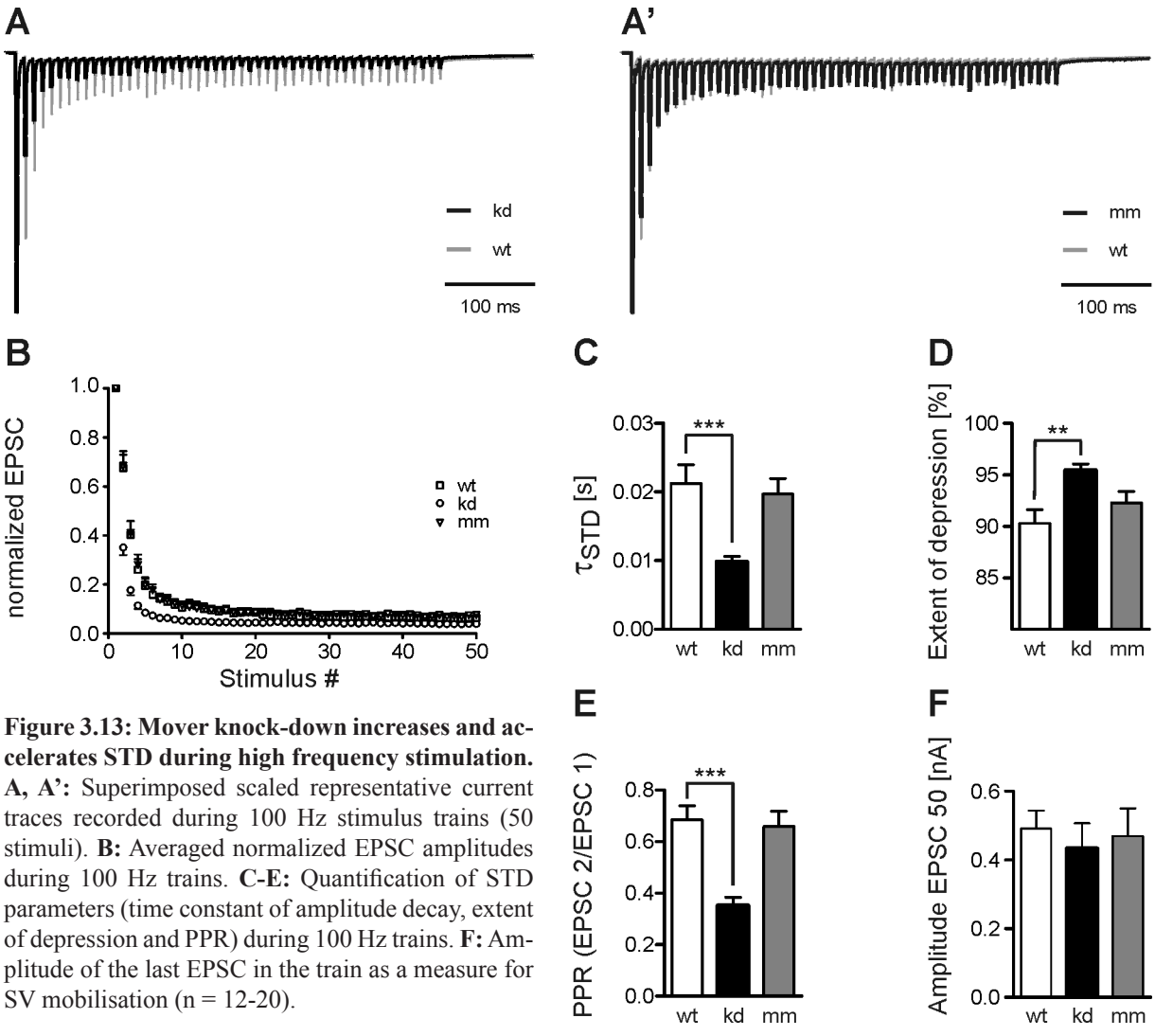

Figure 3.13: Mover knock-down increases and accelerates STD during high frequency stimulation. **A, A':** Superimposed scaled representative current traces recorded during 100 Hz stimulus trains (50 stimuli). **B:** Averaged normalized EPSC amplitudes during 100 Hz trains. **C-E:** Quantification of STD parameters (time constant of amplitude decay, extent of depression and PPR) during 100 Hz trains. **F:** Amplitude of the last EPSC in the train as a measure for SV mobilisation (n = 12-20).

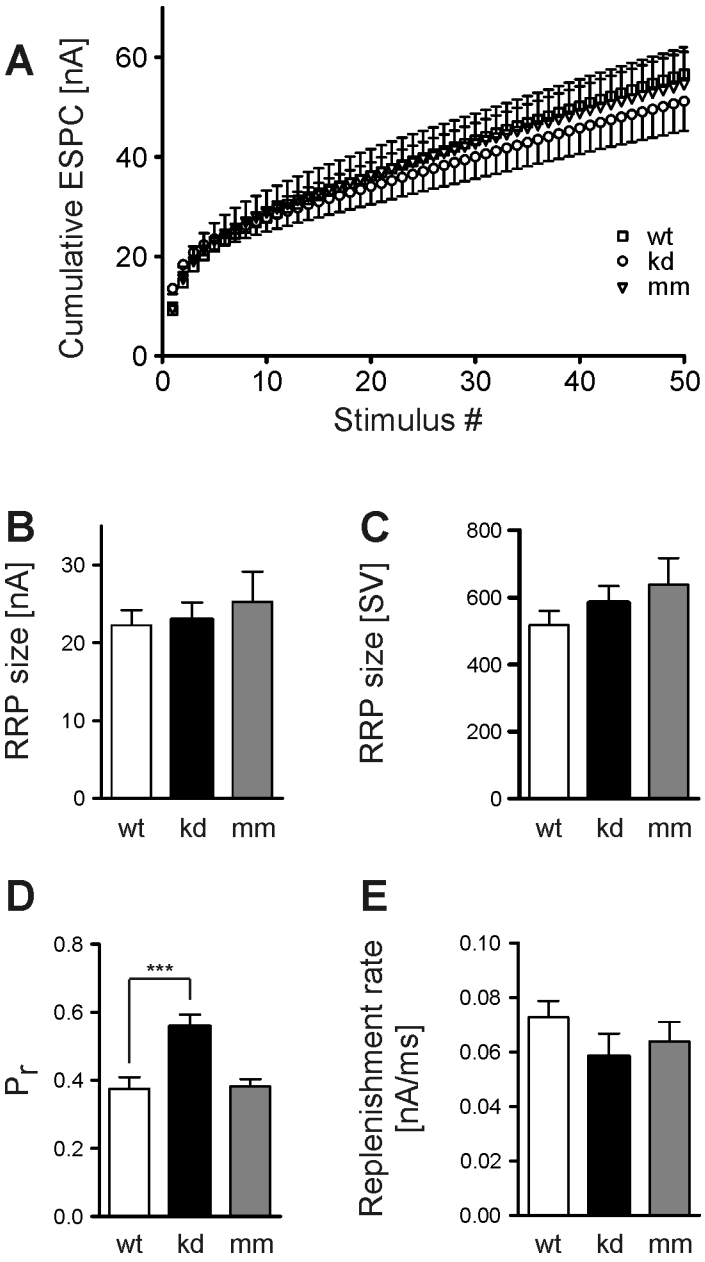

Figure 3.14: Mover knock-down increases the vesicular Pr whereas RRP size and SV replenishment are not altered.
A: Averaged cumulative EPSCs amplitudes during 100 Hz trains. **B, C:** Quantification RRP size by means of current and of SVs. **D, E:** Quantification of replenishment rate and compound Pr (n = 12-20).

Calculation of the cumulative EPSC during 100 Hz stimulation and line fitting through the linear part allows the calculation of the RRP size and the replenishment rate of SVs at the release sites (Schneggenburger et al., 1999). The intersection of the line fit with the Y-axis determines the RRP size and the slope the replenishment rate. When we compared the cumulative EPSCs recorded from Mover knock-down calyces with those obtained from wild type and mismatched controls (Fig. 3.14A), a slight reduction in the slope of the line fit and thereby a reduction in replenishment rate was evident in Mover knock-down calyces. However, this reduction did not reach significance (Fig. 3.14E). The size of the RRP was not affected by the knock-down of Mover, regardless whether it was directly determined by the line fit as the total current amplitude of the RRP (Fig. 3.14B) or as the number of SVs in the RRP (calculated by division of the total current amplitude by the average amplitude of spontaneous EPSCs in the same cell) (Fig. 3.14C).

Now, that we had determined both, the size of RRP and the quantal contend of an EPSC evoked at resting conditions, we could calculate the compound probability of release (P_r) of a SV (EPSC amplitude divided by RRP size of the respective synapse). Knock-down of Mover increased the vesicular P_r from 0.37 ± 0.03 in wild type calyces to 0.56 ± 0.04 while expression of the mismatched control shRNA had no effect (0.038 ± 0.02) (Fig. 3.14D). This increase in P_r is consisted with the accelerated STD and decreased PPR.

3.5.4 Recovery from depression

STD always requires a recovery from depression during periods of rest, during which the RRP is refilled, preparing the synapse for the next period of activity. We were wondering whether Mover, despite its influence on STD also plays a role in the refilling of the RRP in the absence of synaptic activity. Therefore we examined the time course of recovery after STD induced

by a pool-depleting stimulus train (20 stimuli at 100 Hz). Pool refilling can be monitored by application of test stimuli at increasing time intervals after the end of the depleting train. The amplitude of the EPSC elicited by the test pulse is normalized to the first EPSC of the depleting train, plotted against the time interval between the train and the test stimulus and fitted with a mono-exponential equation. The time constant of this fit determines the time course of RRP refilling (Fig. 3.15).

Knock-down of Mover resulted in an accelerated recovery from depression as indicated by the reduction in recovery time constants compared to wild type and mismatch control synapses (2.97 ± 0.44 s compared to 4.6 ± 0.73 s and 5.47 ± 0.56 s, respectively, Fig. 3.15D and E). The accelerated recovery from depression upon Mover knock-down is in line with an increased P_r. It supports a scenario in which the RRP is refilled with SVs of uniform, high P_r at a refilling speed that is independent of the presence of Mover at the synapse.

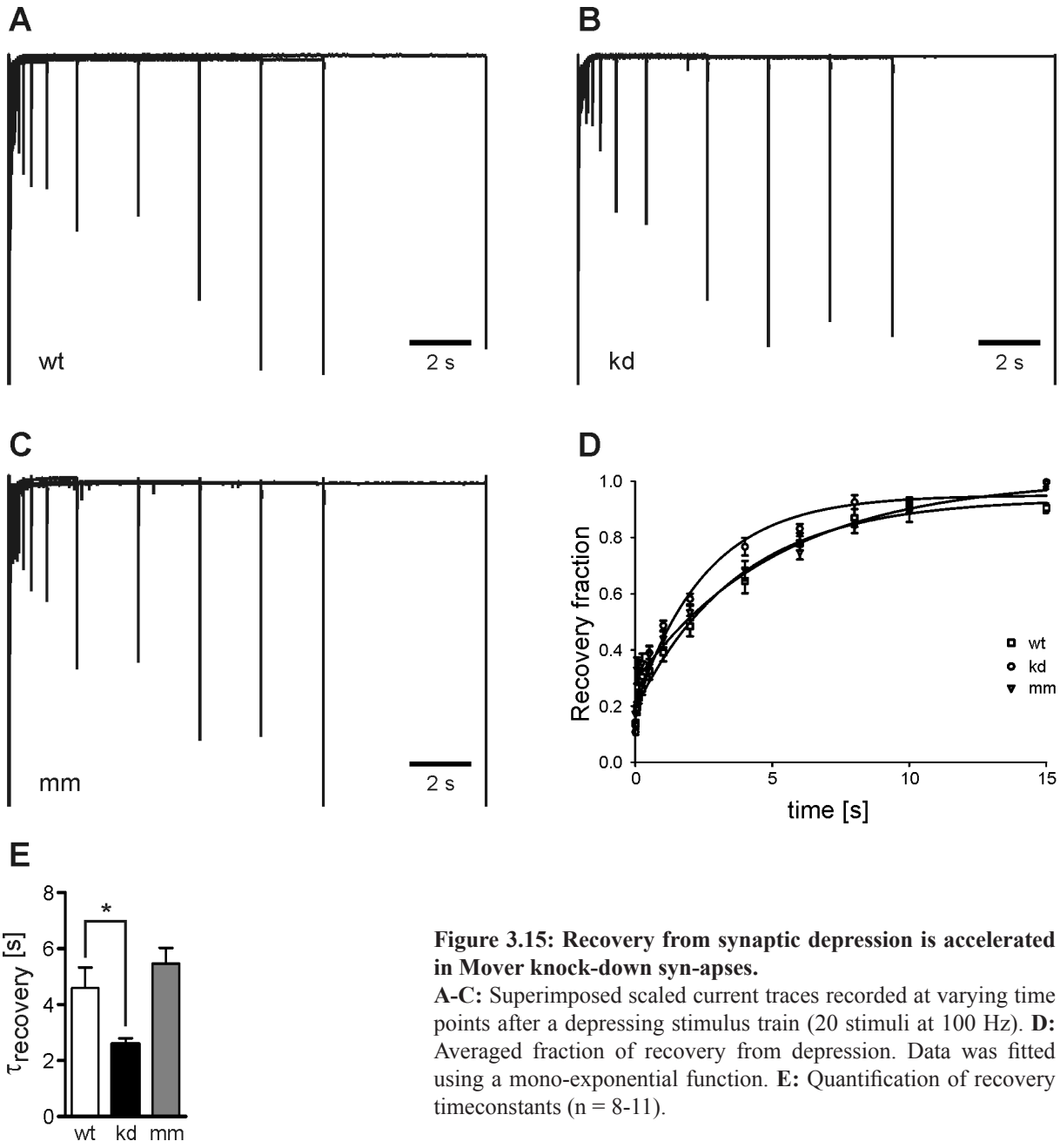

Figure 3.15: Recovery from synaptic depression is accelerated in Mover knock-down syn-apses.
A-C: Superimposed scaled current traces recorded at varying time points after a depressing stimulus train (20 stimuli at 100 Hz). **D:** Averaged fraction of recovery from depression. Data was fitted using a mono-exponential function. **E:** Quantification of recovery timeconstants (n = 8-11).

3.5.6 Presynaptic capacitance recordings

The central finding explaining all effects of Mover knock-down described so far is an increase in P_r. Unfortunately, this important finding has only been shown indirectly. We therefore tempted to directly demonstrate the increased P_r by presynaptic capacitance recordings. Whole-cell patch-clamp recordings were established from identified presynaptic terminals and the increase in membrane capacitance (ΔC_m) in response to depolarizing stimuli of various durations was determined. The membrane capacitance of the calyx is, via the capacitor equation, proportionally related to its membrane surface. This surface area increases when SVs fuse with the plasma membrane resulting in an increase in membrane capacitance. The membrane added by the fusion of a single SV is only ~80 aF (He et al., 2009) and well below the detection limit of whole-cell capacitance recordings. However, during a single EPSC 200-300 SVs fuse with the plasma membrane causing a capacitance increase of 16-24 fF, which is well detectable under our recording conditions. We investigated the changes in membrane capacitance in response to stimuli of 1, 2, 5, 10 and 30 ms duration (Fig. 3.16A), at which the 1 ms stimulus would roughly correspond to the depolarization induced by a single action potential (Schneggenburger et al., 1999). Changes in ΔC_m were normalized to those obtained in response to 10 ms depolarization, which is thought to be sufficient, at least in P8-10 rats, to deplete the RRP (e.g. Sun and Wu, 2001) , and plotted against the stimulus duration (Fig. 3.16C). The data was fitted with a mono-exponential equation. As expected for an increased P_r, Mover knock-down calyces showed an accelerated increase of ΔC_m resulting in faster time constants (2.64 ± 0.44 ms) as compared

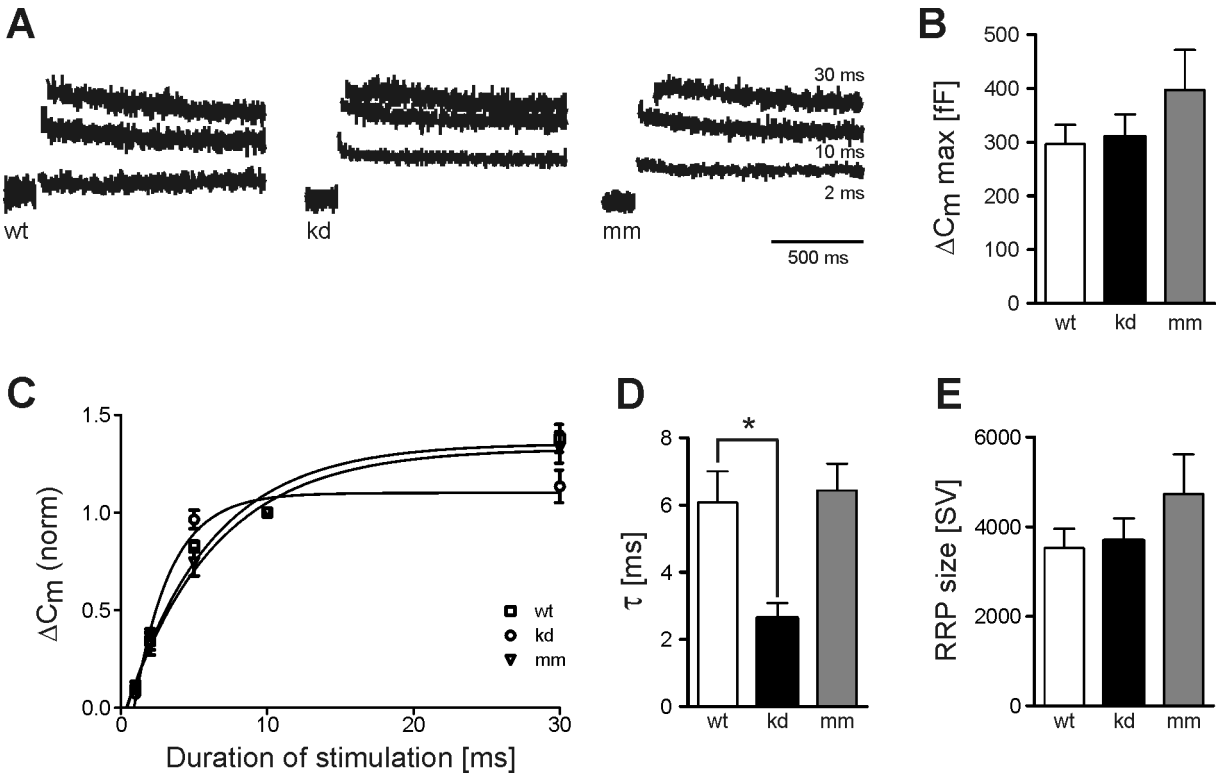

Figure 3.16: Presynaptic capacitance recordings confirm an increased vesicular P_r after knock-down of Mover.

A: Representative scaled capacitance jumps elicited by step depolarizations of 2, 10 and 30 ms duration. **B:** Maximal capacitance jump elicited by step depolarizations. **C:** Capacitance jumps induced by 1, 2, 5, 10 and 30 ms depolarization. Data was normalized to the 10 ms induced ΔC_m. Data was fitted using a mono-exponential equation. **D:** Timeconstants of the mono-exponential fits. **E:** RRP size as determined by the maximal capacitance jump (n = 8-13).

to wild type and mismatched controls (6.07 ± 0.92 ms and 6.43 ± 0.8 ms, respectively) (Fig. 3.16D). Thus, after knock-down of Mover the maximal SV release is achieved at shorter depolarizations (Fig. 3.16A and C), proving the increased P_r. However, the maximal change in membrane capacitance, induced by 30 ms depolarization, was unaffected by the knock-down of Mover (310 ± 42 fF (kd); 296 ± 36 fF (wt); 398 ± 74 fF (mm), $p > 0.3$, Fig. 3.16B) confirming that Mover has no effect on the size of the RRP (Fig. 3.16E). The fact that the increase in ΔC_m could be fitted well with a mono-exponential equation further supports a model of uniform vesicular P_r.

3.5.7 Presynaptic calcium currents

An increase in P_r could be explained by an increased calcium influx into the presynaptic terminal after Mover knock-down. To assess this question, we established presynaptic whole-cell recordings from identified calyces and recorded the pharmacologically isolated calcium currents in response to depolarizing stimuli of various durations. The calyces were depolarized for 1, 2, 5, 10, 30 and 50 ms (Fig. 3.17A) and the charge transfer through the calcium channels was calculated. As depicted in Figure 3.17B, Mover knock-down had no effect on the presynaptic calcium currents regardless of stimulus duration. Therefore, we can exclude alterations in calcium influx into the calyx as source of the increased P_r described above.

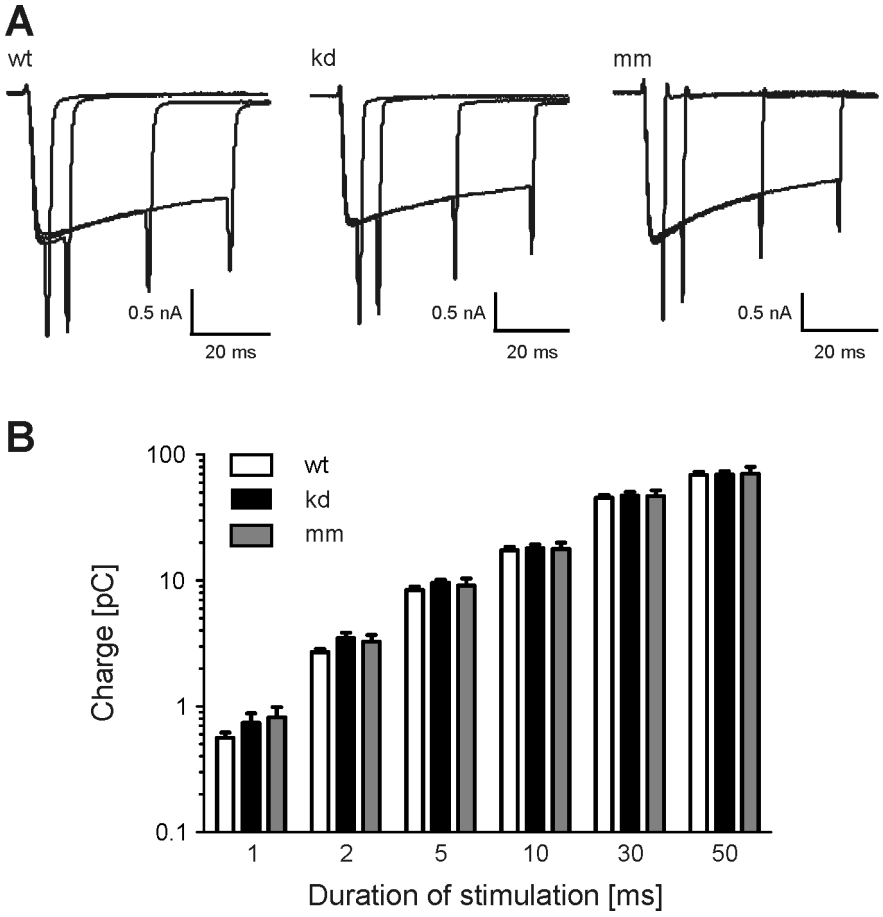

Figure 3.17: Presynaptic calcium currents are not affected by Mover knock-down.
A: Repre-sentative calcium currents induced by 5, 10, 30 and 50 ms step depolarizations. **B:** Quantification of charge transfer over the indicated stimulus durations (n = 6-20).

3.5.8 Calcium sensitivity of release

Alternatively, the increase in P_r upon Mover knock-down could be due to a knock-down induced increase in calcium sensitivity of the release machinery. Hence, we determined the dependence of SV release on the extracellular calcium concentration. Therefore, we monitored the postsynaptic EPSC elicited at 0.05 Hz, a frequency that does not induce STD at the calyx, in varying extracelluar calcium concentrations. After establishment of the recording, Ca^{2+}-influx into the calyx was reduced to a minimum by lowering the extracellular calcium concentration to 0.25 mM. The extracellular calcium concentration was then increased stepwise back to 2 mM, reaching new steady-state EPSC amplitudes within 3-5 min. Average EPSC amplitudes determined at each extracellular calcium concentration were normalized to the average amplitude obtained after restoration of the extracellular Ca^{2+}-concentration back to 2 mM to avoid errors introduced by rundown of the response or incomplete recovery. The dependence of the normalized EPSC amplitudes on the extracellular calcium concentration was fitted with an exponential growth function (Fig. 3.18A). The K-value of this fit was unaffected by Mover knock-down (Fig. 3.18B). Nevertheless, knock-down of Mover resulted in an increase in normalized amplitude at 1.5 mM extracellular calcium indicating an increased calcium sensitivity of release at this physiologically relevant calcium concentration range (Fig. 3.18A) (Lorteije et al., 2009).

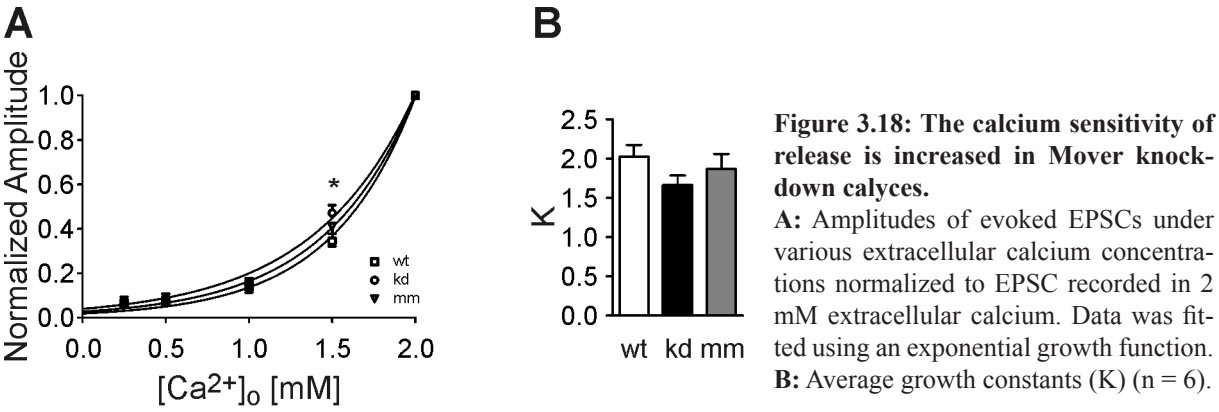

Figure 3.18: The calcium sensitivity of release is increased in Mover knock-down calyces.
A: Amplitudes of evoked EPSCs under various extracellular calcium concentrations normalized to EPSC recorded in 2 mM extracellular calcium. Data was fitted using an exponential growth function.
B: Average growth constants (K) (n = 6).

4 Discussion

In the present study, we investigated the functional role of the recently discovered vertebrat-specific presynaptic protein Mover (Kremer et al., 2007). Therefore, we established a LV mediated knock-down of Mover in hippocampal cultured neurons and examined the role of Mover during quantal synaptic transmission, unfortunately, without detecting any changes upon Mover knock-down. Since Mover is expressed heterogeneously in the hippocampus, we sought out to examine Mover function in a defined synapse population that had been shown to homogeneously express Mover, the calyx of Held (Kremer et al., 2007). Employing the calyx of Held as a model synapse required experiments in acute brain slices. This in turn made it necessary to use an AAV-mediated delivery system, since AAV particles spread much better in tissue than LV particles do (Fig. 3.3). About 75% knock-down efficiency was achieved in individual calyces after 10 days of *in vivo* incubation, at P12. This is the first time that a shRNA mediated knock-down has been established in the calyx *in vivo*. Till now, the calyx was only perturbed by using overexpression approaches of either wild type proteins (Wimmer et al., 2004) or dominant negative forms (Young and Neher, 2009, Schwenger and Kuner, 2010). The knock-down was synapse specific since the globular bushy cells that give rise to the calyx, project contralaterally (Kuwabara et al., 1991). This separates the injection site several millimetres from the target area, thereby leaving the target area largely unaffected by the virus injection.

The strong reduction in Mover protein led to a strong increase in P_r, which resulted in increased evoked EPSC amplitudes, accelerated and increased STD at moderate to high stimulus frequencies and a decrease in PPR. In line with the increase in P_r, a faster recovery from STD was observed after knock-down of Mover. Furthermore, the increased P_r caused by Mover knock-down could be confirmed by presynaptic capacitance recordings. Mover knock-down had no effect on spontaneous synaptic transmission at the calyx, confirming the results from hippocampal cultured neurons. Additionally, no effects of Mover on RRP size and replenishment rate under ongoing synaptic activity could be detected. Regarding the mechanisms that cause the increase in P_r upon Mover knock-down, we could exclude alterations in calcium influx into the calyx since presynaptic calcium currents were unaltered in Mover knock-down synapses. Conversely, we found the normalized EPSC amplitude at 1.5 mM extracellular calcium, a concentration well in the range found *in vivo* (Lorteije et al., 2009), to be increased in Mover knock-down synapses. This suggests that Mover decreases the calcium sensitivity of synaptic release.

4.1 Subcellular Localization of Mover

The data from cultured hippocampal neurons published so far suggests that Mover is a bassoon-interacting protein associated with SVs (Kremer et al., 2007). But since these experiments were carried out in small bouton-type synapses, it was not possible to determine the precise subsynaptic localization of Mover by conventional light microscopy. In the present study we assed this question by co-localization analyses of Mover and either bassoon or the SV marker

VGLUT1 in the much bigger calyx of Held terminal. 3D immunohistochemistry revealed a strong co-localization of Mover with both markers, confirming that Mover is in deed associated with SVs present at AZs in the calyx. The association of Mover with SVs was further confirmed by immuno-gold labelling of Mover which was found at the cytosolic membrane surface of SVs. Interestingly, the majority of Mover immuno-gold signal was found on SVs that were located about one to two SV-diameters away from the active zone. This is the same region in which the Mover interacting C-terminus of bassoon was found in a recent superresolution microscopy study (Dani et al., 2010).

4.2 The number of active zones

The number of active zones was approximated by the number of bassoon immunoreactive puncta in the calyx of Held. In this study, we detected ~300 bassoon clusters per calyx. This number is rather low when compared to electron microscopy (EM) studies that indicated 300-700 AZs, depending on the age examined (Sätzler et al., 2002, Taschenberger et al., 2002). The discrepancy in AZ numbers is likely due to AZs that are devoid of bassoon but are utilizing the closely related protein piccolo as described recently (Dondzillo et al., 2010). Thus, the number of bassoon positive clusters reported here severely underestimates the total number of AZs. Nevertheless, it is in good agreement with a recent study that examined both, piccolo and bassoon, clusters in the calyx (Dondzillo et al., 2010) and that came up with a total number of AZs comparable to EM studies (Taschenberger et al., 2002).

4.3 Synaptic transmission in the absence of Mover

Three modes of synaptic transmission have been examined in this study, spontaneous quantal release, evoked release in response to a single stimulus and release during trains of stimuli. Spontaneous quantal release was investigated in hippocampal cultured neurons and in the calyx, the latter two in the calyx only. At the calyx of Held, spontaneous events are equivalent to quantal events as they are insensitive to the addition of TTX (Ishikawa et al., 2002). Since quantal events were completely unaffected by Mover knock-down in both experimental systems, we focus on calyceal spontaneous synaptic transmission. Amplitudes and kinetics of spontaneous EPSCs obtained here are in good agreement with results from previous studies (Chuhma and Ohmori, 1998, Schneggenburger et al., 1999, Sahara and Takahashi, 2001, Taschenberger et al., 2005). The frequency of spontaneous EPSCs found in this study is within the range reported in earlier studies, although this parameter is rather variable (Taschenberger and von Gersdorff, 2000, Sahara and Takahashi, 2001, Ishikawa et al., 2002, Lou et al., 2005). Since spontaneous, quantal EPSC properties were not altered by knock-down of Mover we conclude that Mover neither changes the number of functional release sites, confirming results from hippocampal cultured neurons (Kremer, 2008), nor the vesicular content of neurotransmitter or the properties of the basic release machinery. Additionally, an indirect effect of Mover on postsynaptic AMPA receptors can be excluded since neither the quantal amplitude nor the decay kinetics of spontaneous EPSCs were affected by Mover knock-down.

Evoked EPSCs in response to single stimuli in Mover knock-down calyces showed an increased amplitude, when compared to controls, while the kinetics remained unchanged. The EPSC amplitude results from linear quantal summation (Meyer et al., 2001) and since the quantal amplitude was independent of Mover, the quantal content of the EPSC was increased

in Mover knock-down calyces. This indicates that more quanta (SVs) were synchronously released upon phasic calcium entry. Amplitudes, kinetics and quantal content of the EPSCs of Mover knock-down and control calyces were well in the range described in the literature (Barnes-Davies and Forsythe, 1995, Borst and Sakmann, 1996, Schneggenburger et al., 1999, Taschenberger and von Gersdorff, 2000, Bollmann et al., 2000). The increase in quantal content upon Mover knock-down could be explained by an increase in the number of SVs available for release or by an increase in P_r of a constant number of SVs (see below).

The properties of evoked synaptic release change during sustained synaptic activity (von Gersdorff and Borst, 2002). Thus we examined possible effects of Mover on release during trains of stimuli applied at moderate (10 Hz) and high frequencies (100 Hz). These stimulus protocols induce STD primarily due to RRP depletion (von Gersdorff and Borst, 2002) albeit inactivation of calcium channels may play a significant role at moderate stimulation frequencies (Xu and Wu, 2005). We described the properties of STD by quantifying extend and time course of EPSC depression and the PPR between the first two EPSCs (Taschenberger and von Gersdorff, 2000, Wong et al., 2003, Kushmerick et al., 2006, Schwenger and Kuner, 2010). Qualitatively similar results were obtained at both frequencies. STD was accelerated and more pronounced and the PPR was strongly decreased in Mover knock-down calyces as compared to controls. These alterations in STD, especially the decrease in PPR, suggest an effect of Mover on the synaptic release properties (see below) rather than on the number of available SVs. An increased number of SVs should not have affected STD properties but only increased EPSC amplitudes. Hence, Mover allows the synapse to better economize the release of SV, eventually preventing it from SV deprivation, by decreasing EPSC amplitudes and slowing STD.

4.4 Effects of Mover knock-down on the RRP

4.4.1 The RRP size

The size of the RRP was determined in two ways in this study, from the cumulative EPSC during 100 Hz trains and from ΔC_m measurements in response to prolonged presynaptic depolarization. The cumulative EPSC method assumes that during 100 Hz stimulation STD is exclusively due to RRP depletion with no contribution of AMPA receptor desensitization (Taschenberger et al., 2002, 2005). AMPA receptor desensitization leads to an underestimation of RRP size but is only prominent in immature calyces and diminishes after morphological changes during synaptic maturation (Kandler and Friauf, 1993, Scheuss et al., 2002, Wong et al., 2003, Taschenberger et al., 2002, 2005), probably due to faster neurotransmitter clearance (Renden et al., 2005). The RRP size determined here was not affected by knock-down of Mover and was comparable to previous estimates using this method (Schneggenburger et al., 1999, Bollmann et al., 2000, Taschenberger et al., 2002).

Alternatively, the RRP size can be determined by depleting the RRP with prolonged depolarizations of the calyx and analysing either the increase in C_m or the EPSC in the presence of the AMPA receptor desensitization blocker cyclothiazide (Partin et al., 1995). We analyzed the increase in C_m in response to 30 ms depolarization and found no difference in the RRP sizes of Mover knock-down and control synapses, confirming the results described above. The RRP sizes determined via ΔC_m analyses were much bigger (3500-4500 SVs) than those obtained from cumulative EPSCs (500-800 SVs), albeit in line with previous studies using this method (Sun and Wu, 2001, Wölfel and Schneggenburger, 2003, Wölfel et al., 2007, Wu and Wu, 2009).

Notably, a recent study using mature calyces reported extremely large RRP sizes in response to very long depolarizations (~7500 SVs, 90 ms depolarization, Leao and von Gersdorff, 2009). However, since the time course of the increase in ΔC_m apparently reached plateau at 30 ms stimulus duration, the depletion of the RRP was probably relatively complete arguing against a substantial underestimation of the RRP size.

It remains debatable which of the estimates reflects the actual RRP size. The ΔC_m approach may overestimate the RRP size due to messing up the calcium buffering properties which may result in artificially high release rates. SVs that were not part of the initial RRP may become mobilized and released during the sustained depolarizations employed. Therefore, the RRP size determined by the cumulative EPSC may represent a better estimate of the number of SVs accessible during sustained synaptic activity. Interestingly, assuming 400-600 active zones, the RRP size of 500-800 SV determined by the cumulative EPSC method, corresponds well to the 1-2 docked SVs per active zone detected by EM (Taschenberger et al., 2002). However, we could not detect differences in RRP size after knock-down of Mover by any of the two methods used. This implicates that Mover has no function in RRP size regulation.

4.4.2 RRP dynamics

Regarding the RRP dynamics, we examined depletion by sustained synaptic activity and refilling during periods of rest or during ongoing activity. Mover was found to alter both, depletion and refilling. Thus, even though Mover does not regulate the size of the RRP, it apparently affects the RRP dynamics profoundly.

Depletion of the RRP was assed in two ways, by application of trains of stimuli, and by prolonged direct depolarization of the terminal. The RRP depletion during application of 100 Hz trains was faster in Mover knock-down calyces. This was probably due to an increased P_r as suggested by accelerated EPSC amplitude decay and a decrease in PPR. Underlining this finding, in ΔC_m measurements we observed shorter depolarizations to be sufficient to evoke near maximal release in Mover knock-down calyces as compared to control synapses. Thus, in wild type synapses, Mover slows RRP depletion by decreasing the P_r.

The refilling of the RRP was approached in two ways, too. We examined RRP refilling under ongoing synaptic activity. Therefore, we analyzed the steady-state EPSC amplitude late in 100 Hz trains which is thought to represent SVs that got newly recruited to the release sites. The steady-state amplitude as well as the replenishment rate of SVs at the release sites were not affected by Mover, indicating that Mover has no effect on the mobilization of SVs during ongoing activity. On the contrary, Mover apparently accelerated the recovery from depression during periods of rest since the time course of RRP refilling during rest was faster in Mover knock-down calyces as compared to controls. However, taking into account that Mover is not involved in SV mobilization, the faster time course of refilling would also be in agreement with a scenario in which the RRP is refilled with SVs of increased P_r at a Mover independent rate. Thus, Mover apparently accelerates RRP depletion as well as refilling during rest. Both observations can be explained by an increase in P_r with no effect of Mover on the actual movements of SVs in the calyx.

4.4.3 Distinct subpools within the RRP?

In immature calyces, the refilling and depletion of the RRP have been shown to follow bi-exponential kinetics. This indicates the presence of two distinct RRP subpools with different P_r and recovery rates (e.g. Wu and Borst, 1999, Sakaba and Neher, 2001, Wu and Wu, 2009), the faster of which has been recently reported to be heterogeneous itself (Müller et al., 2010). In our hands, however, both depletion and refilling were well described by a single exponential, arguing against distinct subpools but rather suggesting homogeneous P_r among the SVs of the RRP.

The time constants obtained here for recovery from depression correspond to the slower of the two obtained from bi-exponential kinetics in immature animals (Sakaba and Neher, 2001) whereas the time constant of RRP depletion, as assed by ΔC_m measurements, is in the range of the faster one obtained from bi-exponential fitting (e.g. Wu and Wu, 2009). Thus, we could not detect the subpool of SVs that is supposed to be released late during stimulation but recovers fast (Wu and Borst, 1999, Sakaba and Neher, 2001). Instead, we observed uniform RRP depletion and refilling albeit slower than found in immature calyces. Since the present study was performed in more mature calyces, it seems plausible that a unification of P_r during synaptic maturation accounts for the apparent loss of RRP subpools. P_r unification has also been shown to be present during maturation of hippocampal synapses (Rosenmund et al., 1993, Chavis and Westbrook, 2001), but notably, a recent study reported RRP subpools with different P_r even in mature calyces (Kochubey et al., 2009). Hence, it remains elusive whether or not such subpools exist and what makes up their identity.

4.5 Mechanisms of P_r regulation by Mover

As already outlined in the previous paragraphs, the main effect of Mover in the calyx of Held is the negative regulation of P_r which manifests itself in larger EPSC amplitudes, accelerated STD, decreased PPR and a shortening in depolarization time needed to deplete the RRP upon knock-down of Mover. However, the mechanisms underlying the effect remain to be discussed.

An increased P_r can be due to three main causes: an increased number of SVs available for release, increased calcium influx into the terminal or alterations in calcium handling inside the terminal including changes in the calcium binding properties of the release sensor. The first possibility can be excluded (see above), since the RRP size is not regulated by Mover.

4.5.1 Calcium influx into the calyx

To distinguish between the latter two mechanisms, we recorded the presynaptic calcium currents in Mover knock-down and control calyces. The charge transfer in response to depolarizations of various duration was comparable to published data (Leao and von Gersdorff, 2009, Taschenberger et al., 2002), and independent of Mover knock-down. Furthermore, the calcium channel inactivation kinetics were not obviously changed in Mover knock-down calyces. This suggests that the calcium currents were carried by the same type of channel, most likely P/Q type calcium channels which almost exclusively mediate calcium currents at the age examined (Iwasaki and Takahashi, 1998, Fedchyshyn and Wang, 2005).We thus conclude that differences in calcium influx are not responsible for the increase in P_r after Mover knock-down. Since Mover has no effect on calcium influx, we can exclude the differential activation of presynaptic GPCRs and glycine receptores (Turecek and Trussel, 2001). Activation of GPCRs (metabotropic

glutamate receptors, $GABA_B$ receptors, A1 adenosine receptors, α2 noradrenergic receptors (Barnes-Davies and Forsythe, 1995, von Gersdorff et al., 1997, Elezgarai et al., 1999, Renden et al., 2005, Sakaba and Neher, 2003, Wong et al., 2006, Leao and von Gersdorff, 2002)) would result in a differential inactivation of calcium channels and therefore differences in calcium channel currents. Presynaptic glycine receptor activation on the contrary, would lead to an increase in calcium influx due to membrane depolarizations caused by the elevated chloride concentration inside the calyx (Price and Trussell, 2006).

4.5.2 Intracellular calcium handling

Taking into account the results described till here, the intra-terminal calcium handling seems to be responsible for the increased P_r observed after Mover knock-down. This suggestion was underlined by our estimation of the calcium sensitivity of release, which showed an increased efficacy of calcium in triggering synaptic release in the physiological calcium concentration range (1.5-2 mM, Lorteije et al., 2009, Borst, 2010). We examined the relation between the extracellular calcium concentration and the EPSC amplitude (Borst and Sakmann, 1996) which we call the apparent calcium sensitivity. The apparent calcium sensitivity was described best by an exponential growth function instead of the 4^{th} power equation that determines the relation between the intracellular calcium concentration and synaptic release (e.g. Schneggenburger and Neher, 2000, Bollmann et al., 2000, Lou et al., 2005, Müller et al., 2007). Since the K-value of the growth function was independent of Mover, we conclude that Mover affects intracellular calcium handling only in the physiologically relevant concentration range (1.5 - 2 mM).

The observed differences in the apparent calcium sensitivity of release upon knock-down of Mover could be caused by three distinct intracellular mechanisms that were not tested in this study. We therefore can not state which ones are regulated by Mover but nevertheless, will discuss the options in the following paragraphs. Mover could affect the intrinsic calcium sensitivity of the release machinery, meaning the number of calcium ions needed to trigger SV fusion, the coupling of SV to calcium channels or the local calcium buffering capacities.

4.5.3 The intrinsic calcium sensitivity

The intrinsic calcium sensitivity can be determined by simultaneous monitoring of changes in presynaptic calcium concentration and synaptic release (e.g. Schneggenburger and Neher, 2000, Bollmann et al., 2000, Lou et al., 2005, Müller et al., 2007). Presynaptic calcium concentration and synaptic release are normally connected via a 3^{rd} or 4^{th} power relationship, meaning that 3-4 calcium ions must bind to the presynaptic calcium sensor to trigger SV fusion. This corresponds well to the 4 calcium binding sites of synaptotagmin (Chapman, 2008). Mover does not interact directly with synaptotagmin (Kremer, 2008) but there are close to infinite possibilities, e.g. through protein phosphorylation, for indirect modulation of synaptotagmin function by Mover (Atwood and Karunanithi, 2002, Südhof, 2004, Chapman, 2008). The precise network of protein interactions in the presynaptic terminal is still not well understood and modulation of a single protein may alter the whole networks properties. Since any of those modulations may result in a change in P_r, we can not exclude that Mover may somehow influence the intrinsic calcium sensitivity of release.

4.5.4 Coupling between SVs and calcium channels

Alternatively, the increased apparent calcium sensitivity upon Mover knock-down could be caused by a tighter coupling of SVs to calcium channels. Coupling tightens during synaptic maturation and results in increased release in response to a given calcium influx, which is due to the higher local calcium concentration experienced by the calcium sensor on the SV (Meinrenken et al., 2002, Fedchyshyn and Wang, 2005, Wadel et al., 2007, Kochubey et al., 2009). Tighter coupling therefore enables mature calyces to release SVs in response to smaller calcium transients induced by shorter APs than immature calyces in which the coupling is more loosely (Fedchyshyn and Wang, 2005). Since tightly coupled SVs sense the local calcium concentration threshold for membrane fusion faster than loosely coupled ones, tighter coupling may explain the maturational acceleration in EPSC rise time (Taschenberger and von Gersdorff, 2000). If this is indeed the underlying mechanism of rise time acceleration than effects of Mover on coupling should result in changes in EPSC rise time. Since this was not observed after Mover knock-down, the possibility that Mover interferes with SV-calcium channel coupling is rather unlikely.

4.5.5 Local calcium buffering

The third possibility in which Mover could alter intracellular calcium handling is the interaction with local calcium buffers of which parvalbumin and calretinin are present in a high percentage of mature calyces (Felmy and Schneggenburger, 2004). Notably, both proteins are upregulated during synaptic maturation (Felmy and Schneggenburger, 2004). Local calcium buffers critically determine the temporal and spatial dynamics of the calcium microdomains induced by calcium channel opening. They are thereby regulating the effective calcium concentration experienced by the calcium sensors of SVs positioned at varying distances from the calcium channel (Meinrenken et al., 2002, Müller et al., 2007). Parvalbumin has slow calcium binding kinetics and thus does not affect the intracellular peak calcium concentration which is responsible for fast synchronous release (Collin et al., 2005a). Nevertheless, it has been shown to efficiently regulate the local calcium dynamics underlying short-term facilitation in the calyx which is probably depending on the build up of residual calcium (Müller et al., 2007). Short-term facilitation has only been observed in rather mature calyces (Taschenberger and von Gersdorff, 2000) or under conditions of low P_r (Borst et al., 1995, Müller et al., 2007). In our hands, short-term facilitation was observed occasionally during the early phase of 100 Hz stimulus trains in control but never in Mover knock-down calyces. However, parvalbumin does not affect the release in response to single stimuli, and alterations in the interaction with Mover should not change the quantal content of the EPSC as seen here upon knock-down of Mover. Calretinin on the other hand has fast calcium binding kinetics and can therefore interfere with release upon a single stimulus. Thus, we can not exclude that Mover interacts with calretinin and that knock-down of Mover results in changes in the buffering capacities of calretinin.

4.5.6 Does Mover influence P_r regulation during synaptic maturation?

The P_r determined here is in the range of what has been reported previously (e.g. Schneggenburger et al., 1999, Bollmann et al., 2000, Meyer et al., 2001), but interestingly, Mover knock-down calyces resemble, with regard to the elevated P_r, immature calyces. Nevertheless, the RRP in Mover knock-down calyces is similar to what has been reported for mature calyces

(Taschenberger et al., 2002). Thus, since Mover is upregulated during synaptic maturation in hippocampal cultured neurons (Kremer, 2008), it can be speculated that Mover may act as a crucial determinant for the decrease in P_r during synaptic maturation.

4.6 Possible molecular mechanisms of Mover action

Since Mover was discovered via a yeast-two-hybrid screen with the C-terminus of bassoon (Kremer et al., 2007), a bassoon related mechanism seems attractive. Studies in the hippocampus of bassoon knock-out mice revealed only a mild synaptic phenotype that could be explained by silencing of a fraction of synaptic release sites (Altrock et al., 2003). Even cultured neurons deficient in both, bassoon and the closely related protein piccolo, failed to show an electrophysiological phenotype, although the total number of SV clusters was reduced in these synapses as revealed by EM studies (Mukherjee et al., 2010). However, a recent study showed that bassoon is responsible for fast replenishment of SVs at the cerebellar mossy fiber to granule cell synapse (MF-GC) (Hallermann et al., 2010). Bassoon was also shown to regulate RRP size, Ca^{2+}-current amplitude and the occupancy of release sites at the ribbon synapse of the inner hair cell. These latter findings may be limited to ribbon synapses, since they seem to correlate with the detachment of the ribbon from the active zone (Frank et al., 2010). In our study, we could not detect any changes in RRP size or calcium current amplitude but we could detect a slight, non-significant reduction in the replenishment rate during high frequency trains. Contradictory, upon Mover knock-down, the recovery from depression was accelerated. However, the effect of bassoon on SV replenishment in MF-GC synapses may be a special feature of this synapse, since it has to relay very high firing frequencies with a limited number of release sites (Rancz et al., 2007). The calyx of Held in contrast, is equipped with a far higher number of release sites to achieve comparable firing frequencies (Taschenberger et al., 2002, Sätzler et al., 2002). Nevertheless, the slight reduction in the SV replenishment rate during high frequency trains could be attributable to a rather limited effect of Mover knock-down on bassoon function.

Taking into account the increased Ca^{2+}-sensitivity upon Mover knock-down, an interaction with Ca^{2+}-triggered SV release seems to be a possible mechanism. In this regard, three major Ca^{2+}-sensors have to be considered: Doc2b, synaptotagmin (syt) and calmodulin (CaM).

Doc2b is the major Ca^{2+}-sensor responsible for spontaneous release (Groffen et al., 2010), but since we could not detect changes in spontaneous release properties in this study, an interference of Mover with Doc2b-mediated release seems unlikely.

Phasic release upon Ca^{2+}-entry is mediated by synaptotagmin 2 (syt2) in the calyx of Held (Pang et al., 2006) and a modulatory effect of Mover is therefore expected to interfere with the synchronicity of release (Young and Neher, 2009). However, the rise times of evoked EPSCs are not changed in Mover knock-down synapses, arguing against interactions of Mover and syt2. Furthermore, alterations in the energy barrier of release as well as in SV docking and priming are usually connected to changes in spontaneous release as observed for Munc-13, Munc18 or complexin (Basu et al., 2007, Verhage et al., 2000, Brose, 2008, Maximov et al., 2009). Since this is not the case, we are confident to exclude direct effects of Mover on the basic release machinery and propose a role for Mover not associated with basic SNARE complex function.

The third high affinity Ca^{2+}-sensor present at synapses is CaM. CaM has been shown to interact with numerous proteins involved in all steps of SV release (Chin and Means, 2000, Junge et al., 2004, Dick et al., 2008, Di Giovanni et al., 2010). Knock-out studies of CaM are tedious because CaM is encoded by three distinct genes which have the same gene product. Nevertheless, a recent study managed to knock-down all three isoforms using a shRNA approach in cultured cortical neurons (Pang et al., 2010). Knock-down of CaM resulted in a decrease in P_r that manifested itself in decreased EPSC and IPSC amplitudes as well as in slowed and decreased STD. These are the very same parameters that were changed by the knock-down of Mover in our study, although the changes were directed to the opposite direction. Furthermore, similar to our results, CaM deficient neurons did not show any changes in EPSC kinetics, mEPSC properties or RRP size (Pang et al., 2010). In the calyx of Held, inhibition of CaM by peptides has been shown to slow recovery from synaptic depression (Sakaba and Neher, 2001), again a parameter that was changed to the opposite direction by knock-down of Mover. These findings suggest that Mover interacts - directly or indirectly - with CaM in an inhibitory manner, and that knock-down of Mover results in a disinhibition of CaM. Since the Ca^{2+}-sensitivity of release is affected by Mover knock-down, Mover may negatively regulate the Ca^{2+}-affinity of CaM. The phenotype of CaM knock-down could be fully rescued by overexpression of constitutively active CaMKIIα, suggesting CaMKIIα as the main regulatory target of CaM in synaptic terminals of cultured neurons (Pang et al., 2010). Therefore, an interaction of Mover with CaMKIIα resulting in modulation of its activity can not be excluded to be responsible for the phenotype observed in Mover knock-down calyces.

4.7 Implications of Mover for synaptic transmission

The localization of Mover at the outer membrane of SVs - although not detected in a previous study of the SV proteome (Takamori et al., 2006) - in combination with the results concerning Mover function presented above, strongly suggests a regulatory role of Mover within the synaptic vesicle cycle of synapses. This negative regulation of P_r may only be present in a distinct subset of synapses, as judged by the expression pattern of Mover (Kremer et al., 2007). Since Mover decreases the vesicular P_r, this could help to prevent synapses from RRP deprivation during high frequency firing. We thus speculate that neurons may dynamically regulate the expression levels of Mover to adjust for the momentary requirements of synaptic transmission. Higher levels of Mover would decrease P_r and therefore decrease the frequency response of the synapse while lower levels would increase P_r. Therefore, different expression levels of Mover could underly the highly heterogeneous P_r found in a large number of synapses (Branco and Staras, 2009). On the network level, this could affect homeostatic and activity-dependent forms of plasticity as well as information transfer in general. Underscoring these considerations, the human equivalent of Mover was found to be upregulated 2.5 fold in the anterior cingulate cortex of schizophrenic patients (Clark et al., 2006).

4.8 Future aspects

This study provides first insights into the function of the recently discovered presynaptic protein Mover, and although some progress has been made in understanding the functional role of Mover in SV release, many questions remain unanswered. First of all, future studies have to clarify the exact mechanisms by which Mover decreases the calcium sensitivity of

release. Therefore one may employ photolysis of caged calcium in paired recordings or load the calyx with calcium chelators of different binding kinetics to determine the intrinsic calcium sensitivity and the SV-calcium channel coupling, respectively.

Additional interaction partners of Mover, including the ones suggested above, could be identified by co-immunoprecipitation experiments. The phosphorylation site discovered in Mover raises the question whether phosphorylation is activity dependent or necessary for the attachment to SVs. Likewise, it would be interesting to investigate Mover function in other synaptic systems (e.g. hippocampal Mossy fibre terminals) and under different levels of synaptic activity to see whether Mover is involved in homeostatic or long-term plasticity. This could be especially interesting since a recent study suggested LTP to be due to changes in P_r, at least at the Schaffer collateral-CA1 synapse (Enoki et al., 2009).

Ultrastructural characterization of Mover knock-down synapses could shed light on potential effects of Mover on SV pools that were not detected by electrophysiology, as recently shown for synapses devoid of bassoon and piccolo (Mukherjee et al., 2010).

Lastly, it would be interesting, now that we have established a role for Mover in exocytosis, to investigate whether Mover is also involved in the regulation of synaptic endocytosis.

5 Acknowledgements

First of all I would like to thank Prof. Dr. Thomas Kuner for the opportunity to work in his lab and for giving me the freedom to explore a variety of interesting subjects while on the same time keeping me on track.

I thank Dr. Thomas Dresbach and Dr. Thomas Kremer for the fruitful collaboration on this project.

I am grateful to Dr. Darius Schwenger and Dr. Robert Renden for introducing me to the calyx of Held and for continuous support on all kinds of topics. Special thanks to Claudia Kocksch and Michaela Kaiser for the excellent support that made it possible for an electrophysiologist to survive. I thank Heinz Horstmann for the collaboration on various projects as well as for sharing ideas at early morning discussions and for constant coffee supply.

Many thanks to the past and present members of the Kuner lab and the rest of the department for useful advice, the great atmosphere and all the fun in the lab. I am also grateful for reliable lunch time hours and for bearing thousands of bad jokes.

Special thanks to John, Dorde, Manon, Raphael, Thomas, Julie, Olav, Isabel, Daniel, Ben, Mariya, Dorothee, Michael and Nina for beach volleyball, days in the sun, remarkable evenings and a life outside the lab.

I am very grateful to Dr. Markus Werner who introduced me to electrophysiology at what feels like an eternity ago. I am additionally thankful for his open ears, ongoing support and his opinions on all kinds of problems during the recent years.

I want to thank Thies, Alex, Lisa, Maria, Maze, Barbara, Jan and Sabrina for their incredible friendship during all the years and their wonderful way of dealing with science.

Last but not least, I would like to thank my family for the continuous unquestioned support in anything I did thus far.

6 Abbreviations

AAV	adeno-associated virus
ACSF	artificial cerebrospinal fluid
AMPA	2-amino-3-(5-methyl-3-oxo-1,2- oxazol-4-yl)propanoic acid
AP	action potential
APV	D-(-)-2-amino-5-phosphonopentanoic acid
ATP	adenosine-5'-triphosphate
AZ	active zone
CAZ	cytomatrix of the active zone
C_m	membrane capacitance
CNQX	6-cyano-7-nitroquinoxaline-2,3-dione
ΔC_m	change in membrane capacitance
DIV	days in vitro
DMEM	dulbecco's minimal essential medium
E	embryonic day
EGFP	enhanced green fluorescent protein
EGTA	ethylene glycol-bis(2-aminoethylether)-*N*,*N*,*N*′,*N*′-tetraacetic acid
EM	electron microscopy
EPSC	excitatory postsynaptic current
FCS	fetal calf serum
GABA	γ-aminobutyric acid
GFP	green fluorescent protein
GPCR	G-protein coupled receptor
GTP	guanosine-5'-triphosphate
HEK	human embryonic kidney
HBS	HEPES buffered solution
kd	knock-down
LV	Lenti virus
LTD	long-term depression
LTP	long-term potentiation
mEPSC	miniture excitatory postsynaptic current
mIPSC	miniture inhibitory postsynaptic current
mm	mismatch
MNTB	medial nucleus of the trapezoid body

mRNA	messenger ribonucleic acid
NA	numerical aperture
NGS	normal goat serum
NSF	N-ethylmaleimide-sensitive factor
P	postnatal day
PAGE	polyacrylamide gel-electrophoresis
PBS	phosphate buffered solution
PEI	polyethyleneimine
PFA	para-formaldehyde
PPR	paired-pulse ratio
P_r	probability of release
PSD	postsynaptic density
PVDF	polyvenyldifluorid
RRP	readily releasable pool
SDS	sodium dodecylsulfate
SEM	standard error of the mean
shRNA	small hairpin ribonucleic acid
SNARE	soluble NSF attachment protein receptor
STD	short-term depression
SV	synaptic vesicle
TEA	tetraethylammonium
TTX	tetrodotoxine
VCN	ventral choclear nucleus
VGLUT1	vesicular glutamate transporter 1
wt	wild type

7 References

Altrock W, tom Dieck S, Sokolov M, Meyer A, Sigler A, Brakebusch C, Fässler R, Richter K, Boeckers T, Potschka H, Brandt C, Lüscher W, Grimberg D, Dresbach T, Hempelmann A, Hassan H, Balschun D, Frey J, Brandstätter J, Garner C, Rosenmund C & Gundelfinger E. (2003). Functional inactivation of a fraction of excitatory synapses in mice deficient for the active zone protein bassoon. *Neuron* **37**, 787-800.

Antonini D, Dentice M, Mahtani P, De Rosa L, Della Gatta G, Mandinova A, Salvatore D, Stupka E & Missero C. (2008). Tprg, a gene predominantly expressed in skin, is a direct target of the transcription factor p63. *J Invest Dermatol* **128**, 1676-1678.

Araç D, Chen X, Khant H, Ubach J, Ludtke S, Kikkawa M, Johnson A, Chiu W, Südhof T & Rizo J. (2006). Close membrane-membrane proximity induced by Ca^{2+}-dependent multivalent binding of synaptotagmin-1 to phospholipids. *Nat Struct Mol Biol* **13**, 209-217.

Atwood H & Karunanithi S. (2002). Diversification of synaptic strength: presynaptic elements. *Nat Rev Neurosci* **3**, 497-516.

Augustin I, Rosenmund C, Südhof T & Brose N. (1999). Munc13-1 is essential for fusion competence of glutamatergic synaptic vesicles. *Nature* **400,** 457-461.

Barnes-Davies M & Forsythe I. (1995). Pre- and postsynaptic glutamate receptors at a giant excitatory synapse in rat auditory brainstem slices. *J Physiol* **488**, 387-406.

Basu J, Betz A, Brose N & Rosenmund C. (2007). Munc13-1 C1 domain activation lowers the energy barrier for synaptic vesicle fusion. *J Neurosci* **27**, 1200-1210.

Bennett M & Zukin R. (2004). Electrical coupling and neuronal synchronization in the Mammalian brain. *Neuron* **41**, 495-511.

Betz A, Ashery U, Rickmann M, Augustin I, Neher E, Südhof T, Rettig J & Brose N. (1998). Munc13-1 is a presynaptic phorbol ester receptor that enhances neurotransmitter release. *Neuron* **21**, 123-136.

Blatchley B, Cooper W & Coleman J. (1987). Development of auditory brainstem response to tone pip stimuli in the rat. *Brain Res* **429**, 75-84.

Blumer M, Gahleitner P, Narzt T, Handl C & Ruthensteiner B. (2002). Ribbons of semithin sections: an advanced method with a new type of diamond knife. *J Neurosci Methods* **120**, 11-16.

Bollmann J, Sakmann B & Borst J. (2000). Calcium sensitivity of glutamate release in a calyx-type terminal. *Science* **289**, 953-957.

Borst J, Helmchen F & Sakmann B. (1995). Pre- and postsynaptic whole-cell recordings in the medial nucleus of the trapezoid body of the rat. *J Physiol* **489**, 825-840.

Borst J & Sakmann B. (1996). Calcium influx and transmitter release in a fast CNS synapse. *Nature* **383**, 431-434.

Borst J. (2010). The low synaptic release probability in vivo. *Trends Neurosci* **33**, 259-266.

Branco T & Staras K. (2009). The probability of neurotransmitter release: variability and feedback control at single synapses. *Nat Rev Neurosci* **10**, 373-383.

Branco T, Clark B & Häusser M. (2010). Dendritic discrimination of temporal input sequences in cortical neurons. *Science* **329**, 1671-1675.

Bredt D & Nicoll R. (2003). AMPA receptor trafficking at excitatory synapses. *Neuron* **40**, 361-379.

Brose N. (2008). For better or for worse: complexins regulate SNARE function and vesicle fusion. *Traffic* **9**, 1403-1413.

Burré J, Beckhaus T, Corvey C, Karas M, Zimmermann H & Volknandt W. (2006). Synaptic vesicle proteins under conditions of rest and activation: analysis by 2-D difference gel electrophoresis. *Electrophoresis* **27**, 3488-3496.

Burré J, Sharma M, Tsetsenis T, Buchman V, Etherton M & Südhof T. (2010). α-Synuclein Promotes SNARE-Complex Assembly in Vivo and in Vitro. *Science* **329,** 1663-1667.

Cases-Langhoff C, Voss B, Garner A, Appeltauer U, Takei K, Kindler S, Veh R, De Camilli P, Gundelfinger E & Garner C. (1996). Piccolo, a novel 420 kDa protein associated with the presynaptic cytomatrix. *Eur J Cell Biol* **69**, 214-223.

Chapman E. (2008). How does synaptotagmin trigger neurotransmitter release? *Annu Rev Biochem* **77**, 615-641.

Chavis P & Westbrook G. (2001). Integrins mediate functional pre- and postsynaptic maturation at a hippocampal synapse. *Nature* **411**, 317-321.

Chin D & Means A. (2000). Calmodulin: a prototypical calcium sensor. *Trends Cell Biol* **10**, 322-328.

Chua J, Kindler S, Boyken J & Jahn R. (2010). The architecture of an excitatory synapse. *J Cell Sci* **123**, 819-823.

Chuhma N & Ohmori H. (1998). Postnatal development of phase-locked high-fidelity synaptic transmission in the medial nucleus of the trapezoid body of the rat. *J Neurosci* **18**, 512-520.

Clark D, Dedova I, Cordwell S & Matsumoto I. (2006). A proteome analysis of the anterior cingulate cortex gray matter in schizophrenia. *Mol Psychiatry* **11**, 459-470, 423.

Cohen F & Melikyan G. (2004). The energetics of membrane fusion from binding, through hemifusion, pore formation, and pore enlargement. *J Membr Biol* **199**, 1-14.

Collin T, Chat M, Lucas M, Moreno H, Racay P, Schwaller B, Marty A & Llano I. (2005a). Developmental changes in parvalbumin regulate presynaptic Ca^{2+} signaling. *J Neurosci* **25**, 96-107.

Collin T, Marty A & Llano I. (2005b). Presynaptic calcium stores and synaptic transmission. *Curr Opin Neurobiol* **15**, 275-281.

Colonnier M. (1968). Synaptic patterns on different cell types in the different laminae of the cat visual cortex. An electron microscope study. *Brain Res* **9**, 268-287.

Dani A, Huang B, Bergan J, Dulac C & Zhuang X. (2010). Superresolution imaging of chemical synapses in the brain. *Neuron* **68**, 843-856.

Dean C & Dresbach T. (2006). Neuroligins and neurexins: linking cell adhesion, synapse formation and cognitive function. *Trends Neurosci* **29**, 21-29.

del Castillo J & Katz B. (1954). Quantal components of the end-plate potential. *J Physiol* **124**, 560-573.

Deng L, Kaeser P, Xu W & Südhof T. (2011). RIM Proteins Activate Vesicle Priming by Reversing Autoinhibitory Homodimerization of Munc13. *Neuron* **69**, 317-331.

Di Giovanni J, Iborra C, Maulet Y, Lévêque C, El Far O & Seagar M. (2010). Calcium-dependent regulation of SNARE-mediated membrane fusion by calmodulin. *J Biol Chem* **285**, 23665-23675.

Dick I, Tadross M, Liang H, Tay L, Yang W & Yue D. (2008). A modular switch for spatial Ca^{2+} selectivity in the calmodulin regulation of CaV channels. *Nature* **451**, 830-834.

Dick O, tom Dieck S, Altrock W, Ammermüller J, Weiler R, Garner C, Gundelfinger E & Brandstätter J. (2003). The presynaptic active zone protein bassoon is essential for photoreceptor ribbon synapse formation in the retina. *Neuron* **37**, 775-786.

tom Dieck S, Sanmartí-Vila L, Langnaese K, Richter K, Kindler S, Soyke A, Wex H, Smalla K, Kämpf U, Fränzer J, Stumm M, Garner C & Gundelfinger E. (1998). Bassoon, a novel zinc-finger CAG/glutamine-repeat protein selectively localized at the active zone of presynaptic nerve terminals. *J Cell Biol* **142**, 499-509.

tom Dieck S, Altrock W, Kessels M, Qualmann B, Regus H, Brauner D, Fejtov· A, Bracko O, Gundelfinger E & Brandstätter J. (2005). Molecular dissection of the photoreceptor ribbon synapse: physical interaction of Bassoon and RIBEYE is essential for the assembly of the ribbon complex. *J Cell Biol* **168**, 825-836.

Dondzillo A, Sätzler K, Horstmann H, Altrock W, Gundelfinger E & Kuner T. (2010). Targeted three-dimensional immunohistochemistry reveals localization of presynaptic proteins Bassoon and Piccolo in the rat calyx of Held before and after the onset of hearing. *J Comp Neurol* **518**, 1008-1029.

Draguhn A, Traub R, Schmitz D & Jefferys J. (1998). Electrical coupling underlies high-frequency oscillations in the hippocampus in vitro. *Nature* **394**, 189-192.

Dresbach T, Hempelmann A, Spilker C, tom Dieck S, Altrock W, Zuschratter W, Garner C & Gundelfinger E. (2003). Functional regions of the presynaptic cytomatrix protein bassoon: significance for synaptic targeting and cytomatrix anchoring. *Mol Cell Neurosci* **23**, 279-291.

Dulubova I, Lou X, Lu J, Huryeva I, Alam A, Schneggenburger R, Südhof T & Rizo J. (2005). A Munc13/RIM/Rab3 tripartite complex: from priming to plasticity? *EMBO J* **24**, 2839-2850.

Dulubova I, Khvotchev M, Liu S, Huryeva I, Südhof T & Rizo J. (2007). Munc18-1 binds directly to the neuronal SNARE complex. *Proc Natl Acad Sci USA* **104**, 2697-2702.

Elezgarai I, Benítez R, Mateos J, Lázaro E, Osorio A, Azkue J, Bilbao A, Lingenhoehl K, Van Der Putten H, Hampson D, Kuhn R, Knöpfel T & Grandes P. (1999). Developmental expression of the group III metabotropic glutamate receptor mGluR4a in the medial nucleus of the trapezoid body of the rat. *J Comp Neurol* **411**, 431-440.

Enoki R, Hu Y, Hamilton D & Fine A. (2009). Expression of long-term plasticity at individual synapses in hippocampus is graded, bidirectional, and mainly presynaptic: optical quantal analysis. *Neuron* **62**, 242-253.

Fedchyshyn M & Wang L. (2005). Developmental transformation of the release modality at the calyx of Held synapse. *J Neurosci* **25**, 4131-4140.

Feldman D. (2009). Synaptic mechanisms for plasticity in neocortex. *Annu Rev Neurosci* **32**, 33-55.

Felmy F & Schneggenburger R. (2004). Developmental expression of the Ca^{2+}-binding proteins calretinin and parvalbumin at the calyx of held of rats and mice. *Eur J Neurosci* **20**, 1473-1482.

Fenster S, Chung W, Zhai R, Cases-Langhoff C, Voss B, Garner A, Kaempf U, Kindler S, Gundelfinger E & Garner C. (2000). Piccolo, a presynaptic zinc finger protein structurally related to bassoon. *Neuron* **25**, 203-214.

Frank T, Rutherford M, Strenzke N, Neef A, Pangrši T, Khimich D, Fetjova A, Gundelfinger E, Liberman M, Harke B, Bryan K, Lee A, Egner A, Riedel D & Moser T. (2010). Bassoon and the synaptic ribbon organize Ca^{2+} channels and vesicles to add release sites and promote refilling. *Neuron* **68**, 724-738.

von Gersdorff H, Schneggenburger R, Weis S & Neher E. (1997). Presynaptic depression at a calyx synapse: the small contribution of metabotropic glutamate receptors. *J Neurosci* **17**, 8137-8146.

von Gersdorff H & Borst J. (2002). Short-term plasticity at the calyx of held. *Nat Rev Neurosci* **3**, 53-64.

Giraudo C, Eng W, Melia T & Rothman J. (2006). A clamping mechanism involved in SNARE-dependent exocytosis. *Science* **313**, 676-680.

Groffen A, Martens S, Díez Arazola R, Cornelisse L, Lozovaya N, de Jong A, Goriounova N, Habets R, Takai Y, Borst J, Brose N, McMahon H & Verhage M. (2010). Doc2b is a high-affinity Ca^{2+} sensor for spontaneous neurotransmitter release. *Science* **327**, 1614-1618.

Grønborg M, Pavlos N, Brunk I, Chua J, Münster-Wandowski A, Riedel D, Ahnert-Hilger G, Urlaub H & Jahn R. (2010). Quantitative comparison of glutamatergic and GABAergic synaptic vesicles unveils selectivity for few proteins including MAL2, a novel synaptic vesicle protein. *J Neurosci* **30**, 2-12.

Hallermann S, Fejtova A, Schmidt H, Weyhersmüller A, Silver R, Gundelfinger E & Eilers J. (2010). Bassoon speeds vesicle reloading at a central excitatory synapse. *Neuron* **68**, 710-723.

Hamann M, Billups B & Forsythe I. (2003). Non-calyceal excitatory inputs mediate low fidelity synaptic transmission in rat auditory brainstem slices. *Eur J Neurosci* **18**, 2899-2902.

Han Y, Kaeser P, Südhof T & Schneggenburger R. (2011). RIM Determines Ca^{2+} Channel Density and Vesicle Docking at the Presynaptic Active Zone. *Neuron* **69**, 304-316.

Hauck B, Chen L & Xiao W. (2003). Generation and characterization of chimeric recombinant AAV vectors. *Mol Ther* **7**, 419-425.

He L, Xue L, Xu J, McNeil B, Bai L, Melicoff E, Adachi R & Wu L. (2009). Compound vesicle fusion increases quantal size and potentiates synaptic transmission. *Nature* **459**, 93-97.

Held H. (1893). Die centrale Gehörleitung. *Arch Anat Physiol Anat Abt* **17**, 201-248.

Hodgkin A & Huxley A. (1952). A quantitative description of membrane current and its application to conduction and excitation in nerve. *J Physiol* **117**, 500-544.

Hoffpauir B, Grimes J, Mathers P & Spirou G. (2006). Synaptogenesis of the calyx of Held: rapid onset of function and one-to-one morphological innervation. *J Neurosci* **26**, 5511-5523.

Hua Y, Sinha R, Martineau M, Kahms M & Klingauf J. (2010). A common origin of synaptic vesicles undergoing evoked and spontaneous fusion. *Nat Neurosci* **13**, 1451-1453.

Ishikawa T, Sahara Y & Takahashi T. (2002). A single packet of transmitter does not saturate postsynaptic glutamate receptors. *Neuron* **34**, 613-621.

Iwasaki S & Takahashi T. (1998). Developmental changes in calcium channel types mediating synaptic transmission in rat auditory brainstem. *J Physiol* **509**, 419-423.

Junge H, Rhee J, Jahn O, Varoqueaux F, Spiess J, Waxham M, Rosenmund C & Brose N. (2004). Calmodulin and Munc13 form a Ca^{2+} sensor/effector complex that controls short-term synaptic plasticity. *Cell* **118**, 389-401.

Kügler S, Lingor P, Schöll U, Zolotukhin S & Bähr M. (2003). Differential transgene expression in brain cells in vivo and in vitro from AAV-2 vectors with small transcriptional control units. *Virology* **311**, 89-95.

Kaeser P, Deng L, Wang Y, Dulubova I, Liu X, Rizo J & Südhof T. (2011). RIM proteins tether Ca^{2+} channels to presynaptic active zones via a direct PDZ-domain interaction. *Cell* **144**, 282-295.

Kandler K & Friauf E. (1993). Pre- and postnatal development of efferent connections of the cochlear nucleus in the rat. *J Comp Neurol* **328**, 161-184.

Khimich D, Nouvian R, Pujol R, tom Dieck S, Egner A, Gundelfinger E & Moser T. (2005). Hair cell synaptic ribbons are essential for synchronous auditory signalling. *Nature* **434**, 889-894.

Kim S & Ryan T. (2010) CDK5 serves as a major control point in neurotransmitter release. *Neuron* **67**, 797-809.

Klugmann M, Symes C, Leichtlein C, Klaussner B, Dunning J, Fong D, Young D & During M. (2005). AAV-mediated hippocampal expression of short and long Homer 1 proteins differentially affect cognition and seizure activity in adult rats. *Mol Cell Neurosci* **28**, 347-360.

Ko J, Na M, Kim S, Lee J & Kim E. (2003). Interaction of the ERC family of RIM-binding proteins with the liprin-alpha family of multidomain proteins. *J Biol Chem* **278**, 42377-42385.

Kochubey O, Han Y & Schneggenburger R. (2009). Developmental regulation of the intracellular Ca^{2+} sensitivity of vesicle fusion and Ca^{2+}-secretion coupling at the rat calyx of Held. *J Physiol* **587**, 3009-3023.

Kremer T, Kempf C, Wittenmayer N, Nawrotzki R, Kuner T, Kirsch J & Dresbach T. (2007). Mover is a novel vertebrate-specific presynaptic protein with differential distribution at subsets of CNS synapses. *FEBS Lett* **581**, 4727-4733.

Kremer T. (2008). Identification and characterisation of Mover as a novel vertebrate-specific presynaptic protein. Ruperto-Carola University of Heidelberg, Germany.

Kushmerick C, Renden R & von Gersdorff H. (2006). Physiological temperatures reduce the rate of vesicle pool depletion and short-term depression via an acceleration of vesicle recruitment. *J Neurosci* **26**, 1366-1377.

Kuwabara N, DiCaprio R & Zook J. (1991). Afferents to the medial nucleus of the trapezoid body and their collateral projections. *J Comp Neurol* **314**, 684-706.

Leão R & von Gersdorff H. (2002). Noradrenaline increases high-frequency firing at the calyx of held synapse during development by inhibiting glutamate release. *J Neurophysiol* **87**, 2297-2306.

Leão R & von Gersdorff H. (2009). Synaptic vesicle pool size, release probability and synaptic depression are sensitive to Ca^{2+} buffering capacity in the developing rat calyx of Held. *Braz J Med Biol Res* **42**, 94-104.

Li F, Pincet F, Perez E, Eng W, Melia T, Rothman J & Tareste D. (2007). Energetics and dynamics of SNAREpin folding across lipid bilayers. *Nat Struct Mol Biol* **14**, 890-896.

Lisman J, Raghavachari S & Tsien R. (2007). The sequence of events that underlie quantal transmission at central glutamatergic synapses. *Nat Rev Neurosci* **8**, 597-609.

Llano I, Gonz·lez J, Caputo C, Lai F, Blayney L, Tan Y & Marty A. (2000). Presynaptic calcium stores underlie large-amplitude miniature IPSCs and spontaneous calcium transients. *Nat Neurosci* **3**, 1256-1265.

Lorteije J, Rusu S, Kushmerick C & Borst J. (2009). Reliability and precision of the mouse calyx of Held synapse. *J Neurosci* **29**, 13770-13784.

Lou X, Scheuss V & Schneggenburger R. (2005). Allosteric modulation of the presynaptic Ca^{2+} sensor for vesicle fusion. *Nature* **435**, 497-501.

Müller M, Felmy F, Schwaller B & Schneggenburger R. (2007). Parvalbumin is a mobile presynaptic Ca^{2+} buffer in the calyx of held that accelerates the decay of Ca^{2+} and short-term facilitation. *J Neurosci* **27**, 2261-2271.

Müller M, Goutman J, Kochubey O & Schneggenburger R. (2010). Interaction between Facilitation and Depression at a Large CNS Synapse Reveals Mechanisms of Short-Term Plasticity. *J Neurosci* **30**, 2007-2016.

Maximov A, Shin O, Liu X & Südhof T. (2007). Synaptotagmin-12, a synaptic vesicle phosphoprotein that modulates spontaneous neurotransmitter release. *J Cell Biol* **176**, 113-124.

Maximov A, Tang J, Yang X, Pang Z & Südhof T. (2009). Complexin controls the force transfer from SNARE complexes to membranes in fusion. *Science* **323**, 516-521.

Meinrenken C, Borst J & Sakmann B. (2002). Calcium secretion coupling at calyx of held governed by nonuniform channel-vesicle topography. *J Neurosci* **22**, 1648-1667.

Meyer A, Neher E & Schneggenburger R. (2001). Estimation of quantal size and number of functional active zones at the calyx of held synapse by nonstationary EPSC variance analysis. *J Neurosci* **21**, 7889-7900.

Mohrmann R, de Wit H, Verhage M, Neher E & Sørensen J. (2010). Fast Vesicle Fusion in Living Cells Requires at Least Three SNARE Complexes. *Science* **330**, 502-505.

Mukherjee K, Yang X, Gerber S, Kwon H, Ho A, Castillo P, Liu X & Südhof T. (2010). Piccolo and bassoon maintain synaptic vesicle clustering without directly participating in vesicle exocytosis. *Proc Natl Acad Sci USA* **107**, 6504-6509.

Munton R, Tweedie-Cullen R, Livingstone-Zatchej M, Weinandy F, Waidelich M, Longo D, Gehrig P, Potthast F, Rutishauser D, Gerrits B, Panse C, Schlapbach R & Mansuy I. (2007). Qualitative and Quantitative Analyses of Protein Phosphorylation in Naive and Stimulated Mouse Synaptosomal Preparations. *Mol Cell Proteomics* **6**, 283-293.

Ohtsuka T, Takao-Rikitsu E, Inoue E, Inoue M, Takeuchi M, Matsubara K, Deguchi-Tawarada M, Satoh K, Morimoto K, Nakanishi H & Takai Y. (2002). Cast: a novel protein of the cytomatrix at the active zone of synapses that forms a ternary complex with RIM1 and munc13-1. *J Cell Biol* **158**, 577-590.

Olsen O, Moore K, Fukata M, Kazuta T, Trinidad J, Kauer F, Streuli M, Misawa H, Burlingame A, Nicoll R & Bredt D. (2005). Neurotransmitter release regulated by a MALS-liprin-alpha presynaptic complex. *J Cell Biol* **170**, 1127-1134.

Pang Z, Sun J, Rizo J, Maximov A & Südhof T. (2006). Genetic analysis of synaptotagmin 2 in spontaneous and Ca^{2+}-triggered neurotransmitter release. *EMBO J* **25**, 2039-2050.

Pang Z, Cao P, Xu W & Südhof T. (2010). Calmodulin controls synaptic strength via presynaptic activation of calmodulin kinase II. *J Neurosci* **30**, 4132-4142.

Partin K, Bowie D & Mayer M. (1995). Structural determinants of allosteric regulation in alternatively spliced AMPA receptors. *Neuron* **14**, 833-843.

Pobbati A, Stein A & Fasshauer D. (2006). N- to C-terminal SNARE complex assembly promotes rapid membrane fusion. *Science* **313**, 673-676.

Price G & Trussell L. (2006). Estimate of the chloride concentration in a central glutamatergic terminal: a gramicidin perforated-patch study on the calyx of Held. *J Neurosci* **26**, 11432-11436.

Rancz E, Ishikawa T, Duguid I, Chadderton P, Mahon S & Häusser M. (2007). High-fidelity transmission of sensory information by single cerebellar mossy fibre boutons. *Nature* **450**, 1245-1248.

Renden R, Taschenberger H, Puente N, Rusakov D, Duvoisin R, Wang L, Lehre K & von Gersdorff H. (2005). Glutamate transporter studies reveal the pruning of metabotropic glutamate receptors and absence of AMPA receptor desensitization at mature calyx of held synapses. *J Neurosci* **25**, 8482-8497.

Richmond J, Weimer R & Jorgensen E. (2001). An open form of syntaxin bypasses the requirement for UNC-13 in vesicle priming. *Nature* **412**, 338-341.

Rizo J & Rosenmund C. (2008). Synaptic vesicle fusion. *Nat Struct Mol Biol* **15**, 665-674.

Rizzoli S & Betz W. (2005). Synaptic vesicle pools. *Nat Rev Neurosci* **6**, 57-69.

Rosenmund C, Clements J & Westbrook G. (1993). Nonuniform probability of glutamate release at a hippocampal synapse. *Science* **262**, 754-757.

Rosenmund C, Sigler A, Augustin I, Reim K, Brose N & Rhee J. (2002). Differential control of vesicle priming and short-term plasticity by Munc13 isoforms. *Neuron* **33**, 411-424.

Sahara Y & Takahashi T. (2001). Quantal components of the excitatory postsynaptic currents at a rat central auditory synapse. *J Physiol* **536**, 189-197.

Sakaba T & Neher E. (2001). Calmodulin mediates rapid recruitment of fast-releasing synaptic vesicles at a calyx-type synapse. *Neuron* **32**, 1119-1131.

Sakaba T & Neher E. (2003). Direct modulation of synaptic vesicle priming by GABA(B) receptor activation at a glutamatergic synapse. *Nature* **424**, 775-778.

Sara Y, Virmani T, Deák F & Liu X, & Kavalali, ET. (2005). An isolated pool of vesicles recycles at rest and drives spontaneous neurotransmission. *Neuron* **45**, 563-573.

Sätzler K, Söhl L, Bollmann J, Borst J, Frotscher M, Sakmann B & Lübke J. (2002). Three-dimensional reconstruction of a calyx of Held and its postsynaptic principal neuron in the medial nucleus of the trapezoid body. *J Neurosci* **22**, 10567-10579.

Schaub J, Lu X, Doneske B, Shin Y & McNew J. (2006). Hemifusion arrest by complexin is relieved by Ca^{2+}-synaptotagmin I. *Nat Struct Mol Biol* **13**, 748-750.

Scheuss V, Schneggenburger R & Neher E. (2002). Separation of presynaptic and postsynaptic contributions to depression by covariance analysis of successive EPSCs at the calyx of held synapse. *J Neurosci* **22**, 728-739.

Schneggenburger R, Meyer A & Neher E. (1999). Released fraction and total size of a pool of immediately available transmitter quanta at a calyx synapse. *Neuron* **23**, 399-409.

Schneggenburger R & Neher E. (2000). Intracellular calcium dependence of transmitter release rates at a fast central synapse. *Nature* **406**, 889-893.

Schneggenburger R & Forsythe I. (2006). The calyx of Held. *Cell Tissue Res* **326**, 311-337.

Schoch S, Castillo P, Jo T, Mukherjee K, Geppert M, Wang Y, Schmitz F, Malenka R & Südhof T. (2002). RIM1alpha forms a protein scaffold for regulating neurotransmitter release at the active zone. *Nature* **415**, 321-326.

Schoch S & Gundelfinger E. (2006). Molecular organization of the presynaptic active zone. *Cell Tissue Res* **326**, 379-391.

Schwenger D & Kuner T. Acute genetic perturbation of exocyst function in the rat calyx of Held impedes structual maturation, but spares synaptic transmission. *Eur J Neurosci* **32**, 974-984.

Shen J, Tareste D, Paumet F, Rothman J & Melia T. (2007). Selective activation of cognate SNAREpins by Sec1/Munc18 proteins. *Cell* **128**, 183-195.

Südhof T. (2004). The synaptic vesicle cycle. *Annu Rev Neurosci* **27**, 509-547.

Südhof T & Rothman J. (2009). Membrane fusion: grappling with SNARE and SM proteins. *Science* **323**, 474-477.

Sun J & Wu L. (2001). Fast kinetics of exocytosis revealed by simultaneous measurements of presynaptic capacitance and postsynaptic currents at a central synapse. *Neuron* **30**, 171-182.

Sun J, Wu X, Wu W, Jin S, Dondzillo A & Wu L. (2004). Capacitance measurements at the calyx of Held in the medial nucleus of the trapezoid body. *J Neurosci Methods* **134**, 121-131.

Sun J, Pang Z, Qin D, Fahim A, Adachi R & Südhof T. (2007). A dual-Ca^{2+}-sensor model for neurotransmitter release in a central synapse. *Nature* **450**, 676-682.

Takamori S, Holt M, Stenius K, Lemke E, Grønborg M, Riedel D, Urlaub H, Schenck S, Brügger B, Ringler P, Müller S, Rammner B, Gräter F, Hub J, De Groot B, Mieskes G, Moriyama Y, Klingauf J, Grubmüller H, Heuser J, Wieland F & Jahn R. (2006). Molecular anatomy of a trafficking organelle. *Cell* **127**, 831-846.

Takao-Rikitsu E, Mochida S, Inoue E, Deguchi-Tawarada M, Inoue M, Ohtsuka T & Takai Y. (2004). Physical and functional interaction of the active zone proteins, CAST, RIM1, and Bassoon, in neurotransmitter release. *J Cell Biol* **164**, 301-311.

Taschenberger H & von Gersdorff H. (2000). Fine-tuning an auditory synapse for speed and fidelity: developmental changes in presynaptic waveform, EPSC kinetics, and synaptic plasticity. *J Neurosci* **20**, 9162-9173.

Taschenberger H, Le„o R, Rowland K, Spirou G & von Gersdorff H. (2002). Optimizing synaptic architecture and efficiency for high-frequency transmission. *Neuron* **36**, 1127-1143.

Taschenberger H, Scheuss V & Neher E. (2005). Release kinetics, quantal parameters and their modulation during short-term depression at a developing synapse in the rat CNS. *J Physiol* **568**, 513-537.

Turecek R & Trussell L. (2001). Presynaptic glycine receptors enhance transmitter release at a mammalian central synapse. *Nature* **411**, 587-590.

Varoqueaux F, Sigler A, Rhee J, Brose N, Enk C, Reim K & Rosenmund C. (2002). Total arrest of spontaneous and evoked synaptic transmission but normal synaptogenesis in the absence of Munc13-mediated vesicle priming. *Proc Natl Acad Sci USA* **99**, 9037-9042.

Verhage M, Maia A, Plomp J, Brussaard A, Heeroma J, Vermeer H, Toonen R, Hammer R, van den Berg Ta, M., Geuze H & Südhof T. (2000). Synaptic Assembly of the Brain in the Absence of Neurotransmitter Secretion. *Science* **287**, 864-869.

Virmani T, Ertunc M, Sara Y, Mozhayeva M & Kavalali E. (2005). Phorbol esters target the activity-dependent recycling pool and spare spontaneous vesicle recycling. *J Neurosci* **25**, 10922-10929.

Voglmaier S, Kam K, Yang H, Fortin D, Hua Z, Nicoll R & Edwards R. (2006). Distinct endocytic pathways control the rate and extent of synaptic vesicle protein recycling. *Neuron* **51**, 71-84.

Wadel K, Neher E & Sakaba T. (2007). The coupling between synaptic vesicles and Ca^{2+} channels determines fast neurotransmitter release. *Neuron* **53**, 563-575.

Wang X, Hu B, Zieba A, Neumann N, Kasper-Sonnenberg M, Honsbein A, Hultqvist G, Conze T, Witt W, Limbach C, Geitmann M, Danielson H, Kolarow R, Niemann G, Lessmann V & Kilimann M. (2009). A protein interaction node at the neurotransmitter release site: domains of Aczonin/Piccolo, Bassoon, CAST, and rim converge on the N-terminal domain of Munc13-1. *J Neurosci* **29**, 12584-12596.

Wang Y, Okamoto M, Schmitz F, Hofmann K & Südhof T. (1997). Rim is a putative Rab3 effector in regulating synaptic-vesicle fusion. *Nature* **388**, 593-598.

Wang Y, Liu X, Biederer T & Südhof T. (2002). A family of RIM-binding proteins regulated by alternative splicing: Implications for the genesis of synaptic active zones. *Proc Natl Acad Sci USA* **99**, 14464-14469.

Wang Y & Südhof T. (2003). Genomic definition of RIM proteins: evolutionary amplification of a family of synaptic regulatory proteins. *Genomics* **81**, 126-137.

Wilhelm B, Groemer T & Rizzoli S. (2010). The same synaptic vesicles drive active and spontaneous release. *Nat Neurosci* **13**, 1454-1456.

Wimmer V, Nevian T & Kuner T. (2004). Targeted in vivo expression of proteins in the calyx of Held. *Pflugers Arch* **449**, 319-333.

Wölfel M & Schneggenburger R. (2003). Presynaptic capacitance measurements and Ca^{2+} uncaging reveal submillisecond exocytosis kinetics and characterize the Ca^{2+} sensitivity of vesicle pool depletion at a fast CNS synapse. *J Neurosci* **23**, 7059-7068.

Wölfel M, Lou X & Schneggenburger R. (2007). A mechanism intrinsic to the vesicle fusion machinery determines fast and slow transmitter release at a large CNS synapse. *J Neurosci* **27**, 3198-3210.

Wong A, Graham B, Billups B & Forsythe I. (2003). Distinguishing between presynaptic and postsynaptic mechanisms of short-term depression during action potential trains. *J Neurosci* **23**, 4868-4877.

Wong A, Billups B, Johnston J, Evans R & Forsythe I. (2006). Endogenous activation of adenosine A1 receptors, but not P2X receptors, during high-frequency synaptic transmission at the calyx of Held. *J Neurophysiol* **95**, 3336-3342.

Wu L & Borst J. (1999). The reduced release probability of releasable vesicles during recovery from short-term synaptic depression. *Neuron* **23**, 821-832.

Wu L, Ryan T & Lagnado L. (2007). Modes of vesicle retrieval at ribbon synapses, calyx-type synapses, and small central synapses. *J Neurosci* **27**, 11793-11802.

Wu X & Wu L. (2009). Rapid endocytosis does not recycle vesicles within the readily releasable pool. *J Neurosci* **29**, 11038-11042.

Wyszynski M, Kim E, Dunah A, Passafaro M, Valtschanoff J, Serra-PagËs C, Streuli M, Weinberg R & Sheng M. (2002). Interaction between GRIP and liprin-alpha/SYD2 is required for AMPA receptor targeting. *Neuron* **34**, 39-52.

Xu J & Wu L. (2005). The decrease in the presynaptic calcium current is a major cause of short-term depression at a calyx-type synapse. *Neuron* **46**, 633-645.

Yamashita T, Hige T & Takahashi T. (2005). Vesicle endocytosis requires dynamin-dependent GTP hydrolysis at a fast CNS synapse. *Science* **307**, 124-127.

Young SJ & Neher E. (2009). Synaptotagmin has an essential function in synaptic vesicle positioning for synchronous release in addition to its role as a calcium sensor. *Neuron* **63**, 482-496.

Zhen M & Jin Y. (1999). The liprin protein SYD-2 regulates the differentiation of presynaptic termini in C. elegans. *Nature* **401**, 371-375.

Ziv N & Garner C. (2004). Cellular and molecular mechanisms of presynaptic assembly. *Nat Rev Neurosci* **5**, 385-399.

Zucker R & Regehr W. (2002). Short-term synaptic plasticity. *Annu Rev Physiol* **64**, 355-405.

Hiermit erkläre ich an Eides statt, dass ich die vorliegende Dissertation selbstständig und ohne unerlaubte Hilfsmittel durchgeführt habe.

Heidelberg, den 25.04.2011 .....

Christoph Körber